PACIFIC EARTHQUAKE ENGINEERING RESEARCH CENTER

# Assessment of Reinforced Concrete Building Exterior Joints with Substandard Details


**Chris P. Pantelides**

**Jon Hansen**

**Justin Nadauld**

and

**Lawrence D. Reaveley**
University of Utah



PEER 2002/18
MAY 2002

# Assessment of Reinforced Concrete Building Exterior Joints with Substandard Details

**Chris P. Pantelides**
Professor of Civil and Environmental Engineering
University of Utah

**Jon Hansen**
Research Assistant

**Justin Nadauld**
Research Assistant

**Lawrence D. Reaveley**
Professor of Civil and Environmental Engineering

PEER Report 2002/18
Pacific Earthquake Engineering Research Center
College of Engineering
University of California, Berkeley

May 2002

# ABSTRACT

Reinforced concrete (RC) buildings designed before the mid-1970s may have serious structural deficiencies and are considered substandard according to current seismic design criteria. Specifically, the failure of the beam-column joints has been the cause of building collapse in many recent earthquakes worldwide. This report evaluates the seismic performance of beam-column joints with three different details of beam and beam-column joint reinforcement. A total of six full-scale RC exterior joints were tested and their performance was examined in terms of lateral load capacity, drift, plastic rotation, joint shear strength, ductility, residual strength, and other PEER-established performance criteria. Two levels of axial compression load in the columns were investigated, and their influence on the performance of the joint is discussed. Performance levels for two types of failure mechanisms are established and comparisons are made to FEMA 273, FEMA 356, and ACI 352. In addition, the bond-slip behavior of the bottom beam bars is discussed. Limit states models are created and new modeling criteria for exterior joints with substandard details are proposed. Finally, a strut-and-tie model is developed for verifying the experimental results.

# ACKNOWLEDGMENTS

This work was supported by the Pacific Earthquake Engineering Research Center through the Earthquake Engineering Research Centers Program of the National Science Foundation under Award number EEC-9701568.

The in-kind contribution made by Gerber Construction is greatly appreciated.

The research presented in this report was performed at the University of Utah. The authors would like to thank the following students from the Department of Civil and Environmental Engineering for their assistance: Danny Alire, B.Sc., Chandra Clyde, M.Sc., and Yasuteru Okahashi, Ph.D. candidate.

# CONTENTS

# LIST OF FIGURES

# LIST OF TABLES

# 1 Introduction

Distress in beam-column joints leading to building collapse has been observed in past earthquakes (Moehle and Mahin 1991); the cause of collapse has been attributed to inadequate joint confinement. Observations of damage after the 1995 Hyogo-ken Nanbu, Japan, earthquake indicated that some reinforced concrete (RC) buildings designed before the mid-1970s may have serious structural deficiencies; these deficiencies are a consequence of a lack of capacity design approach and/or poor detailing of reinforcement (Park et al. 1995). In more recent earthquakes, the inadequacy of building joints designed according to earlier rather than more current standards was cause for severe damage or collapse. Characteristically, in 1999 reconnaissance reports from the Tehuacan, Mexico, earthquake of June 15, 1999 (EERI 1999a), the Izmit, Turkey, earthquake of August 17, 1999 (Sezen et al. 2000), the Athens, Greece, earthquake of September 7, 1999 (EERI 1999b), and the Chi-Chi Taiwan, earthquake of September 21, 1999 (Uang et al. 1999, EERI 1999c) show that all four earthquakes involved seismic damage to RC building joints with substandard details.

Figure 1.1 shows the inadequate detailing of a joint of an RC frame in the Tehuacan, Mexico, earthquake; notice the presence of splices and the lack of hoops. In the Izmit, Turkey, earthquake of August 17, 1999 (Sezen et al. 2000), several RC moment frame buildings experienced damage at beam-column joints (Fig. 1.2); it is apparent that no transverse hoops are present in the joint. In one case, the collapse of an RC building was attributed to the failure of the beam-column joints (Fig. 1.3). Although the framing is mostly intact, many of the beam-column joints are severely damaged; no transverse hoops are present in the joint, and the beam bar anchorage in the joint is apparently inadequate. In the Athens, Greece, earthquake of September 7, 1999 (EERI 1999b), the beam-column joints of RC frames had no joint steel hoops, as shown in Figure 1.4.

**Fig. 1.1 Inadequate detailing of joint in the Tehuacan, Mexico, earthquake of June 15, 1999 (EERI 1999)**

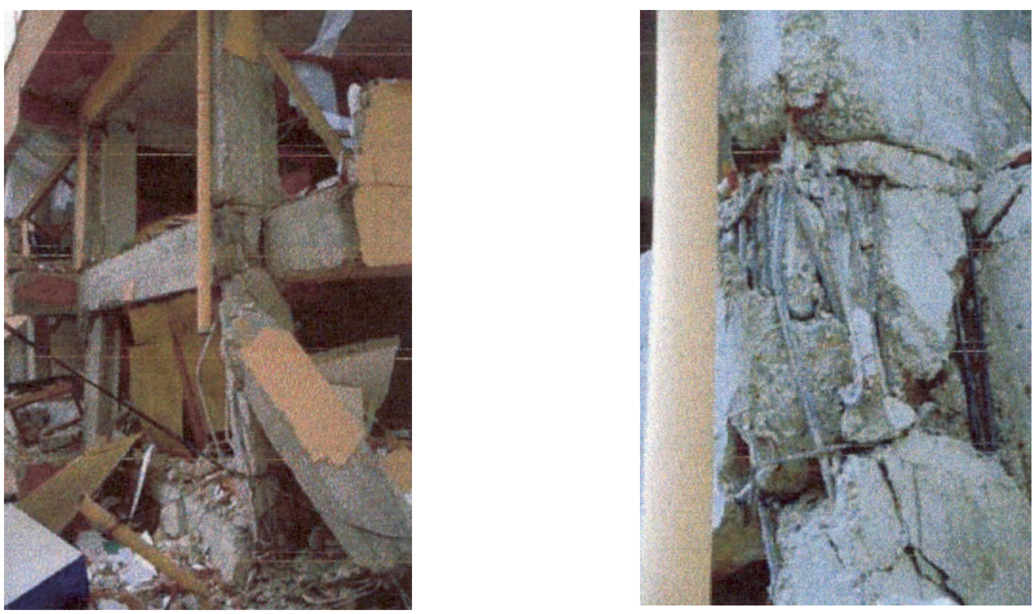

**Fig. 1.2 Severe damage to moment frame beam-column joints in the Izmit, Turkey, earthquake of August 17, 1999 (Sezen et al. 2000)**

**Fig. 1.3 Collapse of building due to failure of beam-column joints in the Izmit, Turkey, earthquake of August 17, 1999 (Sezen et al. 2000)**

**Fig. 1.4 Failure of beam-column joint in the Athens, Greece, earthquake of September 7, 1999 (EERI 1999b)**

The failure of beam-column joints was the cause for the partial collapse of the stories of a 15-story building (Fig. 1.5) in the 1999 Chi-Chi, Taiwan, earthquake (Uang et al. 1999, EERI 1999c); poor transverse reinforcement in the beam-column joint region was the major reason for the collapse. In another instance, inadequate beam-column joint confinement caused a 22-story building to tilt 4°, as shown in Fig. 1.6, and the building had to be demolished (Uang et al. 1999); buckling of the longitudinal column bars is evident.

**Fig. 1.5 Damage to partially collapsed 15-story building: beam-column failure at façade in the Chi-Chi, Taiwan, earthquake of September 21, 1999 (Uang et al. 1999, EERI 1999c)**

**Fig. 1.6 Damage to 22-story building beam-column joints in the Chi-Chi, Taiwan, earthquake of September 21, 1999 (Uang et al. 1999)**

A significant amount of research on the seismic performance of RC building beam-column joints has been carried out in the last four decades. The majority of the research literature has emphasized the improvement of the performance of these RC building beam-column joints through new design concepts and improved details such as joint hoops and improved anchorage. Several researchers have focused on an array of different variables, including the effect of column axial load, which is of interest in the present study.

A single-strut model for evaluating the shear strength of exterior joints was proposed by Meinheit and Jirsa (1977). The predictive relationship for joint shear strength was divided according to two categories of joints: (a) joints for which no beam hinge occurs at the face of the column, and (b) joints for which a beam hinge does occur at the face of the column. The parameters identified as affecting the monotonic shear strength of the joint are concrete strength, column axial load, geometric parameters, transverse reinforcement, and presence of lateral beams.

Of the eight specimens tested in another investigation (Uzumeri 1977), three exterior RC beam-column joints were tested under constant axial compressive load equal to $0.42f'_cA_g$. The presence of this axial load was found to be beneficial at the early stages of loading; however, at the latter stages when the concrete joint core acts as a series of struts, it was postulated that the large axial load might be detrimental rather than helpful. The three specimens were not reinforced in the joint area; two of the specimens contained a transverse stub beam on one side of the column, whereas the third specimen had no transverse beams. Load reversals after bond loss caused large deformations in the concrete, which resulted in splitting along column bars and anchorage failure of the beam steel. In all three cases, the beam remained intact while the joint rapidly deteriorated with increasing imposed displacements. The joints without transverse reinforcement were able to provide anchorage for the beam steel to the extent that between 92% and 98% of the theoretical ultimate moment capacity of the beams was reached. The joint was unable, however, to sustain the anchorage of the beam steel in cycles subsequent to this load level.

An experimental study of three exterior beam-column joints indicates that horizontal joint shear reinforcement may be reduced considerably (Paulay and Scarpas 1981). The amount of shear reinforcement varied between units; however, the vertical shear reinforcement (i.e., intermediate column bars) was the same in all units. The effect of the axial load was studied in one of the units when it was reduced from $0.15f'_cA_g$ to $0.075f'_cA_g$; this resulted in a dramatic reduction of the stiffness, strength, and energy dissipation of the specimen in the subsequent loading cycle.

Ehsani and Wight presented the results of six exterior RC beam-column subassemblages that were tested in cyclic loading (1985). It was determined that in order to avoid the formation of plastic hinges in the joint, the flexural strength ratio should be no less than 1.4. The maximum joint shear stress in exterior connections should be limited to $12\sqrt{f'_c}$ (psi) to reduce excessive joint damage, column bar slippage, and beam bar pullout. It was found that in cases where the flexural strength ratio, the joint shear stress, or the anchorage requirements are significantly more conservative than the limits of the recommendations, the amount of joint transverse reinforcement could be safely reduced.

Limited experimental evidence suggests that increasing the column axial load tends to reduce the total lateral drift at yield (Kurose 1987). Although some researchers report that increased column axial load results in increased shear strength of joints without reinforcement, the data do not show a significant trend (Beres et al. 1992).

Bond and anchorage of bars in RC beam-column joints was studied by Kaku and Asakusa (1991). It was shown that the consequences of bond deterioration included pinching of the force story-drift hysteresis curves, increasing the slip deformation at the beam-column interface, changing the shear transfer mechanism in the joint core, and decreasing the flexural strength of the adjoining members.

Pantazapoulou and Bonacci investigated the mechanics of beam-column joints in laterally loaded frames (1992). Their formulation established the compatibility of the strain and stress equilibrium. It was shown that the shear strength of a joint depends on the usable compressive strength of concrete. It was concluded that joint shear strength could decrease with increasing column axial load, and that in addition to bond failure, joint capacity could be limited by crushing along the principal diagonal or by yielding of the vertical reinforcement after hoop reinforcement yielding.

The effect of the column axial load was also investigated in an analytical study of 57 exterior beam-column joint tests (Pantazapoulou and Bonacci 1994). The relationship between maximum joint shear stress and nominal column axial stress (normalized by $f'_c$) was sought with respect to hinging and shear failures. For the limited amount of available experimental data, no discernible correlation was established between the two variables. It was concluded that deformability, rather than strength, would be affected by axial load. In the same study, a finite element model was developed to study the effect of several parameters on the shear behavior of interior and exterior joints.

In a recent study by Clyde et al. (2000), four half-scale RC exterior joints were tested to investigate their behavior in a shear-critical failure mode. The joints were typical of building frames with nonductile details in the beam-column joints. The joints were subjected to quasi-static cyclic loading, and their performance was examined in terms of lateral load capacity, drift ratio, axial load reduction in the column at high drift ratios, joint shear strength, ductility, shear deformation angle of the joint, and residual strength. Two levels of axial compressive column load were investigated to determine how this variable might influence the performance of the joint. Specific performance levels for this type of RC joint were established and a comparison was made to current design and rehabilitation standards. A limit states model was established, which could be used for performance evaluation or seismic rehabilitation.

More recently, Hakuto et al. (2000) performed simulated seismic load tests on RC one-way interior and exterior beam-column joints with substandard reinforcing details typical of buildings constructed before the 1970s. The exterior beam-column joints contained very little transverse reinforcement in the members and the joint core. In one beam-column joint unit the hooks at the end of the beam top bars were bent up and the hooks at the ends of the bottom bars were bent down. In the other beam-column joint unit the hooks at the ends of the bars were bent into the joint as in current practice. The improvement in performance of the joint with beam bars anchored according to current practice was demonstrated.

The emphasis of the present study was the evaluation of the seismic performance of exterior joints in existing nonductile one-way RC building frames with three different details of beam and beam-column joint reinforcement. These reinforcement details were selected to satisfy the 1963 ACI Code (ACI 1963), but do not satisfy current provisions such as the ACI 352 Committee Report (ACI 1991). A total of six test units were tested. All of the test units had top bars bent into the joints with a 180° hook; two of the test units had bottom bars extending only 6 in. into the joint, two test units had the bottom bars extending all the way into the joint, and the remaining two test units had bottom bars bent up into the joint with a 180° hook. The details of the reinforcement are somewhat typical of buildings built before the 1970s and are substandard according to current codes. These details can also be found in areas of the world where seismic forces are not the governing load condition. In the present study, two levels of axial compression load were investigated for each of the three details: 10% and 25% of the axial column capacity in compression.

# 2 Test Units

## 2.1 DESCRIPTION OF TEST UNITS

The six test units were full-scale models of typical exterior beam-column joints in RC buildings found in the United States before 1970. The longitudinal and transverse reinforcement in the beam and the column transverse steel was increased to prevent early degradation of the beam and column, forcing a shear mode of failure in the joint. There is no transverse reinforcement within the joint core, and the beam longitudinal bottom bars did not have adequate embedment into the joint. In addition, the confining reinforcement details are inadequate according to current criteria (ACI 352, 1991).

## 2.2 MATERIAL PROPERTIES

### 2.2.1 Concrete

The original design of the test units called for a concrete compressive strength of 4000 psi (27.6 MPa). Test units with identical reinforcement were cast from the same batch to eliminate variations between them. Care was taken to ensure that each batch met the mix design such that all six test units had comparable strengths. Table 2.1 shows the concrete compressive strength of each test unit obtained from the average of three 6x12 in. cylinders; in addition, the test units are identified according to the level of axial compressive load, $P$, in the columns, expressed as a fraction of the axial load capacity, $f'_c A_g$.

**Table 2.1 Concrete compressive strength of test units and level of axial load**

| Test Unit | $F'_c$ psi (Mpa) | $\frac{P}{f'_c A_g}$ |
|---|---|---|
| 1 | 4794 (33.1) | 0.10 |
| 2 | 4794 (30.2) | 0.25 |
| 3 | 4934 (34.0) | 0.10 |
| 4 | 4934 (31.6) | 0.25 |
| 5 | 4596 (31.7) | 0.10 |
| 6 | 4596 (31.0) | 0.25 |

### 2.2.2 Steel Reinforcement

Three sizes of deformed steel rebar were used for reinforcement in the test units. The column steel included #8 bars as longitudinal reinforcement with #3 hoops. The beam used #9 longitudinal bars as well as #3 bars for stirrups. The ultimate ($F_u$) and yield ($F_y$) strengths of reinforcement used in the tests are shown in Table 2.2 below.

**Table 2.2 Steel reinforcement strength**

| Reinforcement Type | Bar Size | $F_u$ (ksi) | $F_y$ (ksi) |
|---|---|---|---|
| Beam longitudinal | 9 | 110.4 | 66.5 |
| Column longitudinal | 8 | 107.6 | 68.1 |
| Stirrups/ties | 3 | 94.9 | 62.0 |

## 2.3 CONSTRUCTION OF TEST UNITS

All six of the test units were constructed with identical dimensions and similar detailing. The dimensions and reinforcement details for test units 1 and 2 are shown in Figure 2.1. Note that the bottom bars have only a 6 in. embedment into the column, a typical detail for 1970s' construction.

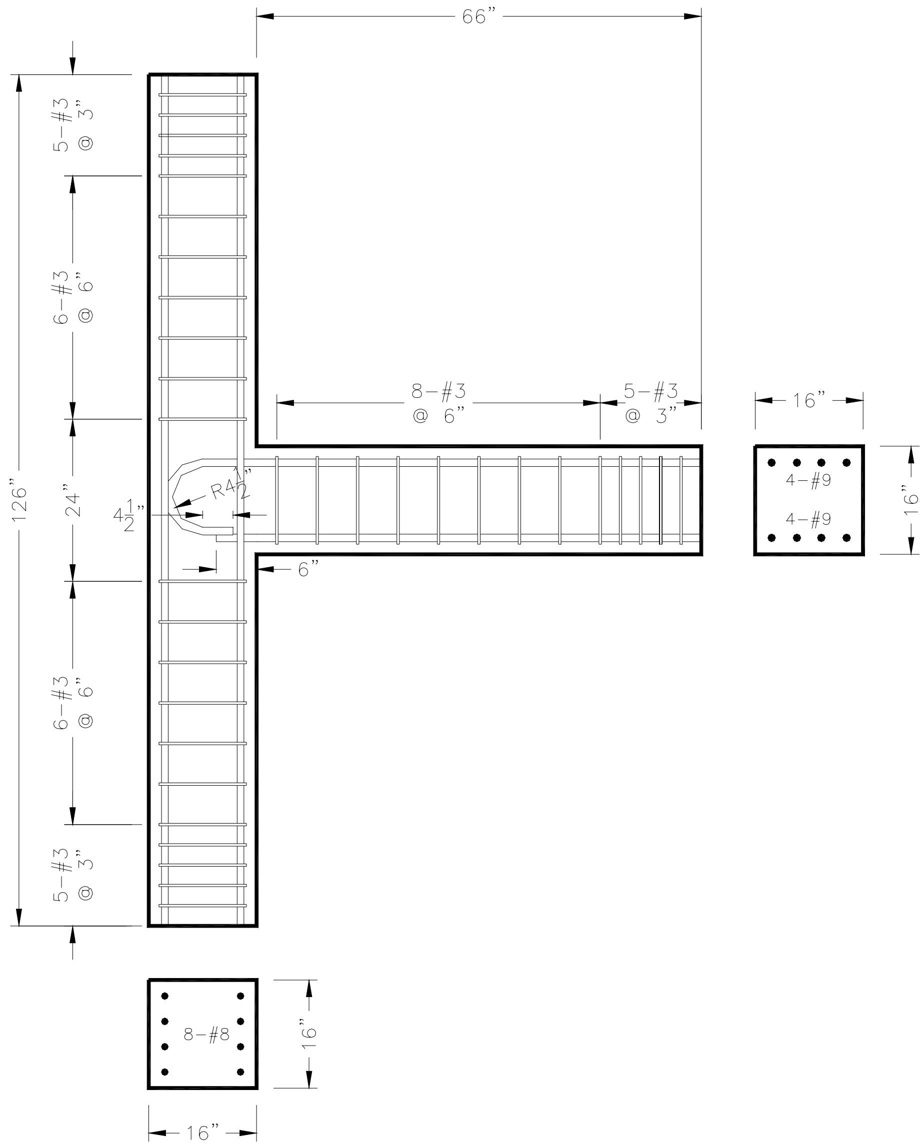


**Fig. 2.1 Test units 1 and 2: dimensions and reinforcement details**

Similarly, Figures 2.2 and 2.3 show the dimensions and reinforcement details for test units 3 and 4, and 5 and 6, respectively. Note that the bottom bars for test units 3 and 4 have a 14 in. embedment into the column, a typical detail for 1970s' construction. Test units 5 and 6 have the top and bottom bars ending in hooks, as shown in Figure 2.3.

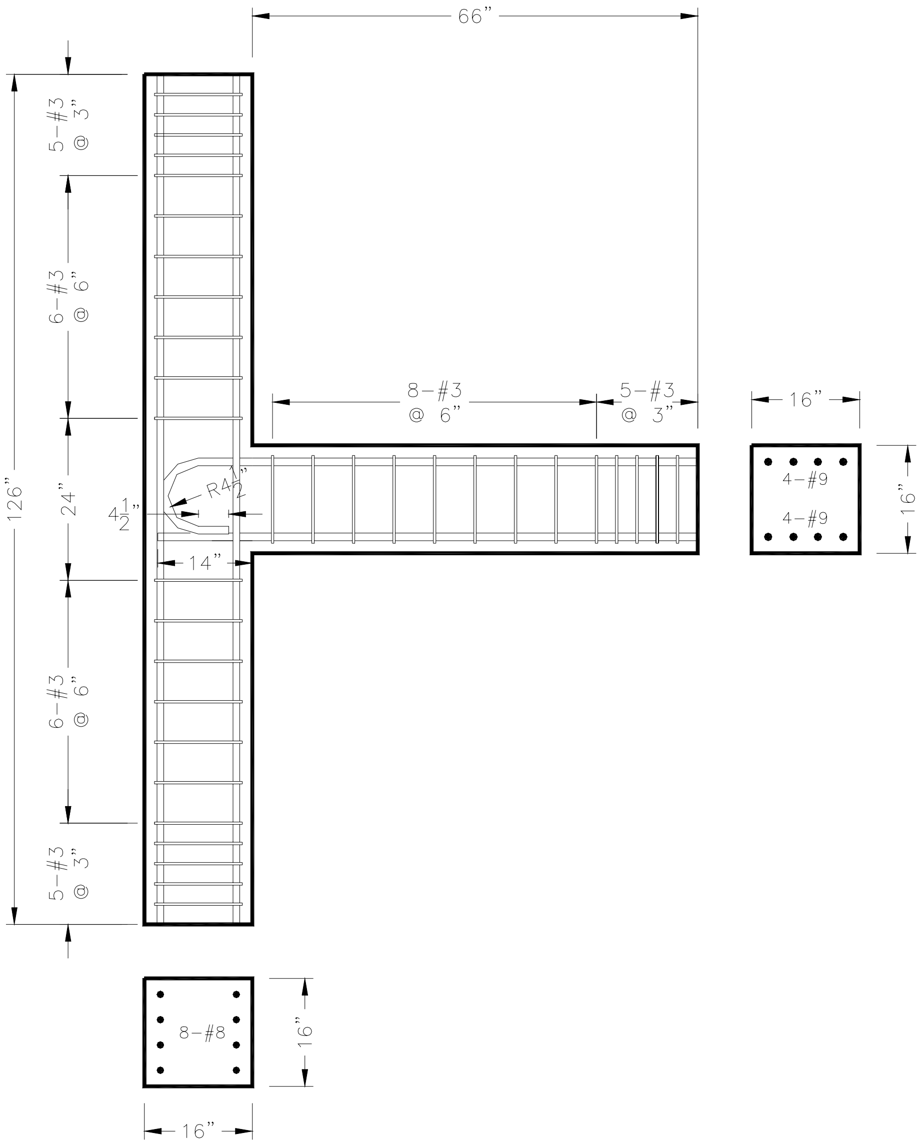


**Fig. 2.2 Test units 3 and 4: dimensions and reinforcement details**

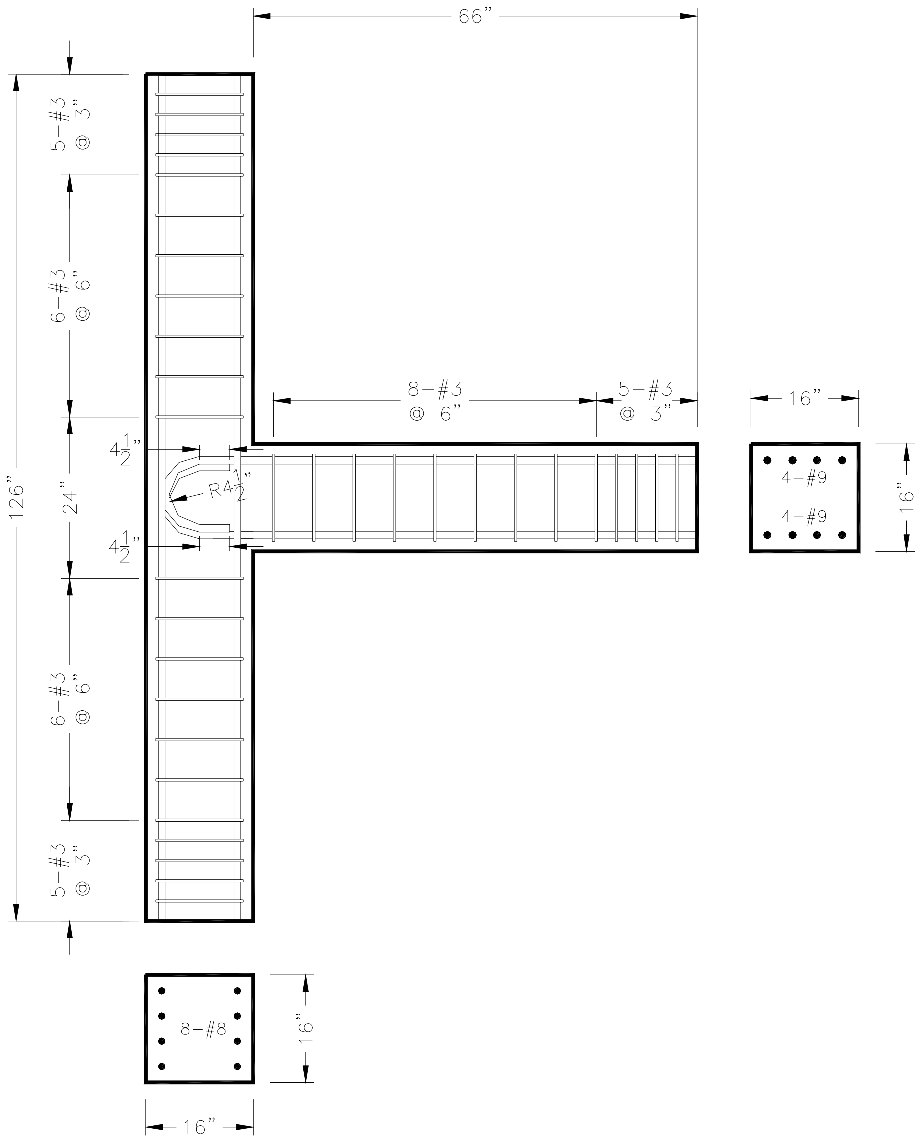


**Fig. 2.3 Test units 5 and 6: dimensions and reinforcement details**

For the six test units, the beam is 16 in. (40.60 cm) wide and 16 in. (40.60 cm) deep. It is symmetrically reinforced with 4-#9 bars for both the positive and negative reinforcement; the steel ratio is 1.86% at both top and bottom. Each top longitudinal beam bar ends with a 180° hook bent down into the joint with an extension of $4d_b$ back toward the beam. Each bottom longitudinal bar in test units 1 and 2 extends straight into the joint area 6 in. beyond the face of the column. Top and bottom steel overlap 2.5 in. (6.35 cm) inside the joint. The bottom longitudinal bars for test units 3 and 4 are similar to those of test units 1 and 2 but extend completely into the joint a distance of 14 in. (35.56 cm) causing approximately 5 in. (12.70 cm) of overlap. The bottom longitudinal bars in test units 5 and 6 end with a 180° hook bent up into the joint with an extension of $4d_b$ back toward the beam. This allows complete overlapping of hooks and extensions inside the joint. The transverse reinforcement in the beam consists of two stirrups. A #3 bar closed stirrup encloses the four corner bars and ends with a 145° bend and a 2.5 in. (6.35 cm) extension for both ends. A #3 bar open stirrup wraps around the four inside bars and ends with a 180° bend and a 2.5 in. (6.35 cm) extension for both ends as shown in Figure 2.4. These two stirrups are tied together and are spaced at 6 in. (15.24 cm) along the beam except within 15 in. (38.10 cm) of the beam end where the spacing is reduced by half to 3 in. (7.62 cm). The closer spacing is intended to give adequate strength at the location where the force is applied during the test.

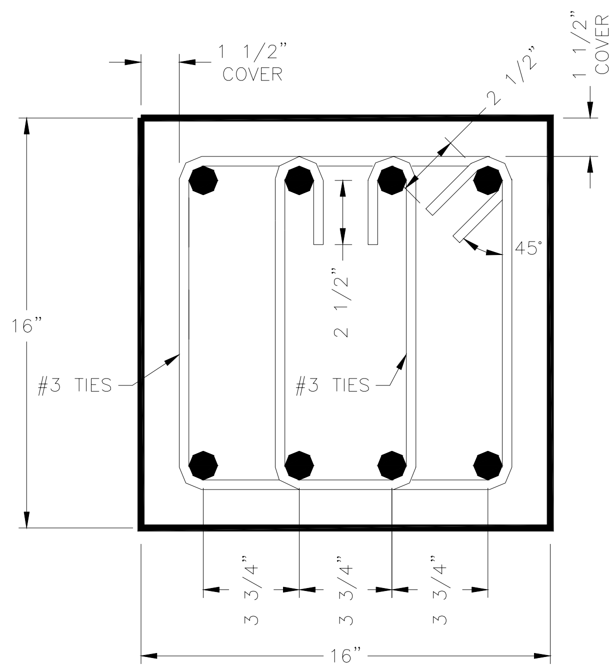


**Fig. 2.4 Beam cross section**

For the six test units, the column is 16 in. (40.60 cm) wide and 16 in. (40.60 cm) deep. It is reinforced with 4-#8 longitudinal bars on the beam-column face and another 4-#8 bars on the opposite face, giving a steel ratio of 2.47%. The longitudinal steel extends continuously from bottom to top of column. The transverse reinforcement in the column consists of 2-#3 bar closed stirrups each ending with 145° bends and 2.5 in. (6.35 cm) extensions for both ends, as shown in Figure 2.5. The stirrups are spaced at 6 in. (15.24 cm) along the height of the column except within the joint region where no transverse steel is present. Spacing of the transverse steel is reduced to 3 in. (7.62 cm) at the top and bottom ends of the column, where the column was supported during the test.

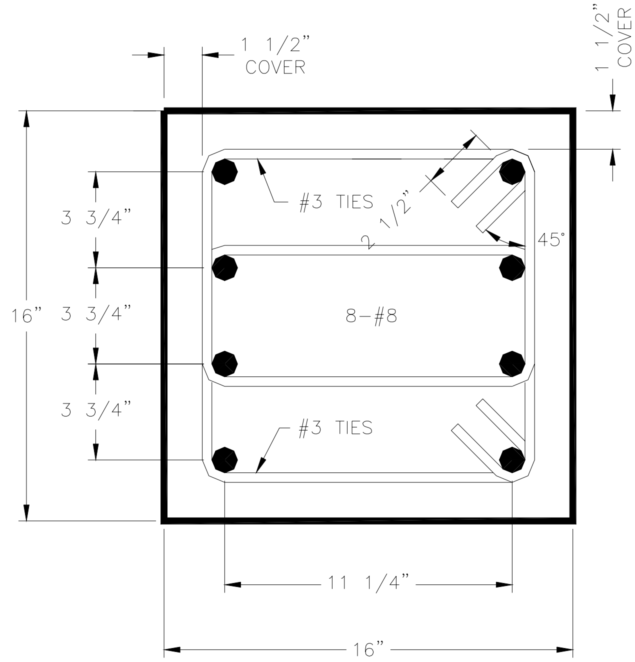


**Fig. 2.5 Column cross section**

Table 2.3 compares the design requirements of ACI 318-63, which the test units were built to meet, with current design requirements.

**Table 2.3 Comparison of steel details to current ACI code**

| Parameter | As-built (ACI 318-63) | Type 1 (ACI 352-91) | Type 2 (ACI 352-91) |
|---|---|---|---|
| Column long. bars passing through joint | $0.01A_g<A_s<0.08A_g$ Min. (4) #5 bars | $0.01A_g<A_s<0.08A_g$ Min. (4) bars | Dist. around perimeter s<8″,1/3w |
| Standard Hook | 180° turn + extension > $4d_b$, 2.5″ | 180° turn + extension > $4d_b$, 2.5″ | 180° turn + extension > $4d_b$, 2.5″ |
| Stirrup/Tie Anchorage | 135° turn + extension > $6d_b$, 2.5″ | 180° turn + extension > $6d_b$, 2.5" | 180° turn + extension > $6d_b$, 2.5" |
| Min. inside rad. of bend | For #9 = $4d_b$ | For #9 = $4d_b$ | For #9 = $4d_b$ |
| Transverse Joint Reinforcement | Not Required | Not Satisfied | Not Satisfied |
| Beam depth to Column Bar Ratio | Not Required | 16<20 | 16<20 |
| Bottom Bar Embedment | 6 in. | Not Satisfied: min 49 in. per ACI 318 Sec. 12.2.3 | Not Satisfied: 90° hook required |

The standard 180° hooks in the 1963 code currently have identical requirements. The joints have no transverse hoop reinforcement, which was not required according to the 1963 ACI Code, but which violates recommendations according to the 1991 ACI 352 recommendations. In addition, the beam depth to column bar ratio is substandard according to the 1991 ACI 352 recommendation of being at least equal to 20. It should also be noted from Figure 2.5 that the column has inferior detailing regarding the distribution of the column bars, since two of the faces of the joint do not contain any column bars. This affects the confinement of the joint concrete in an adverse manner.

The test unit reinforcement cages were constructed according to Figures 2.1 through 2.5 over a period of several weeks and cast in place in pairs within two weeks. A high-frequency vibrator was used to consolidate the concrete, and trowels were used to finish the concrete allowing a smooth surface for crack mapping. Each test unit was allowed to cure for at least 72 hours before they were removed from the forms.

# 3 Test Setup

## 3.1 INSTRUMENTATION

### 3.1.1 Strain Gages

Strain gages were placed on both the longitudinal and transverse reinforcement at selected locations within and around the concrete beam-column joints. Wires were attached to each strain gage. In order for the concrete-rebar bond to be unaltered, these wires were gathered into bundles and run along the center of the reinforcing cage in the beam or column to the closest end where the wires exited the test unit. Precautions were taken to protect the strain gages during the casting process.

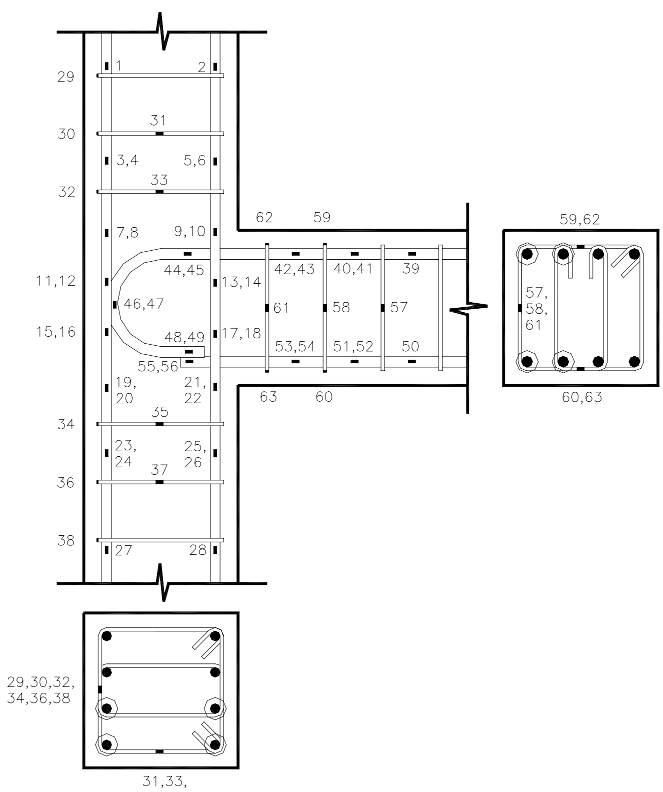


**Fig. 3.1 Test units 1 and 2: strain gage locations**

Figure 3.1 shows the locations of the strain gages for test units 1 and 2. A total of 63 strain gages were applied to each of these test units. Most of the strain gages were applied on the longitudinal bars closest to the front face of the test unit. A few were applied on the second set of longitudinal bars to add redundancy. The numbering pattern for all test units begins on the top of the column on the longitudinal bars and works its way down to the bottom of the column. It then starts again from the top of the column on the horizontal hoops and continues to the bottom of the column. Next, the numbering goes to the top longitudinal beam bars, from outside the joint toward the end of the bar inside the joint.

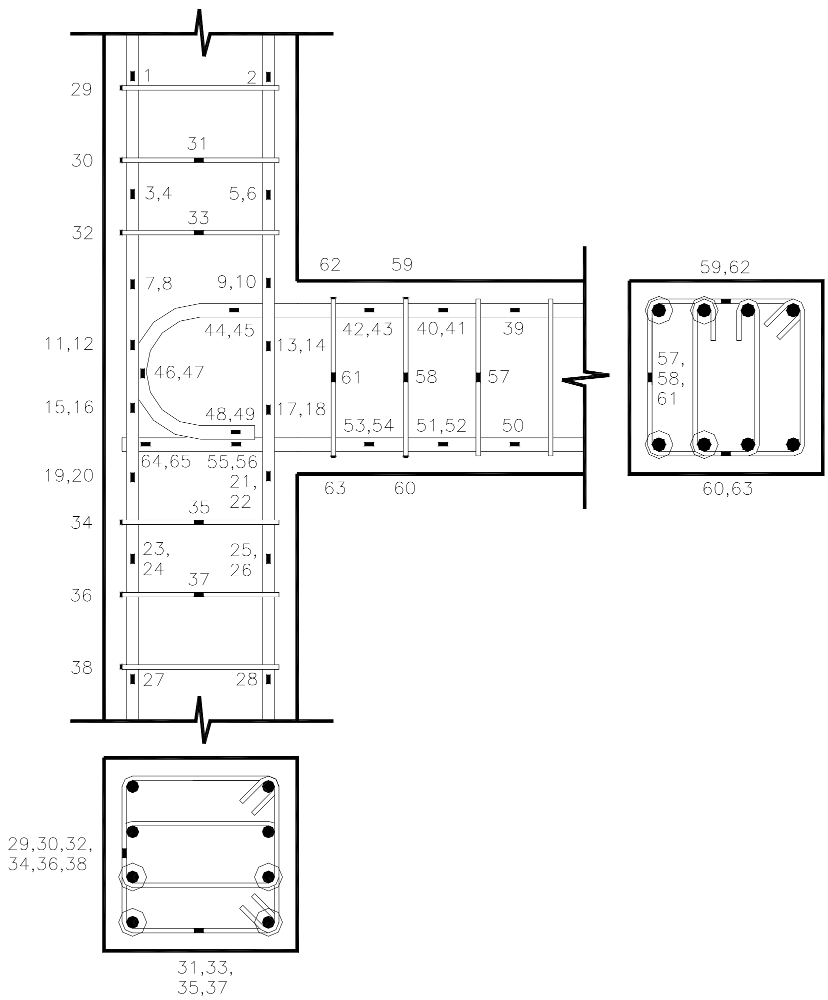


**Fig. 3.2 Test units 3 and 4: strain gage locations**

This same pattern is repeated for the bottom longitudinal beam bars. Finally, the strain gages on the vertical beam stirrups are numbered from outside the joint toward the joint. Figure 3.2 shows the placement of strain gages for test units 3 and 4. This is identical to test units 1 and 2 with the exception of two extra strain gages, 64 and 65, at the end of the bottom beam bars.

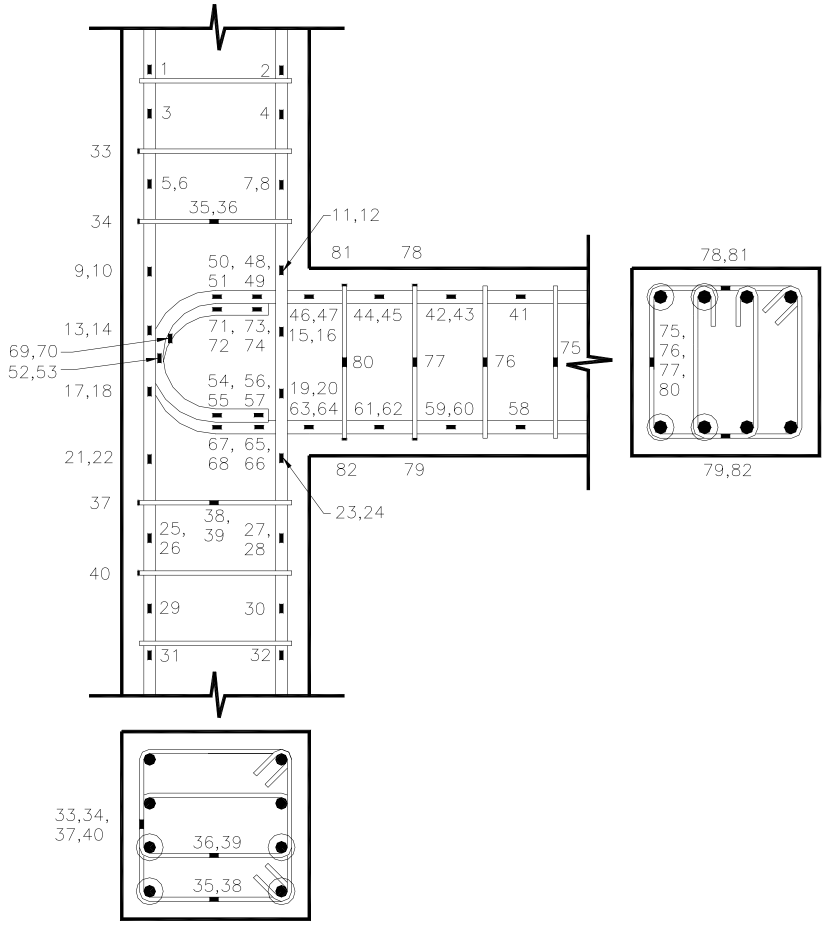


**Fig 3.3 Test units 5 and 6: strain gage locations**

Figure 3.3 represents the strain gage placement for test units 5 and 6. A total of 82 strain gages were placed on each of these test units. These were the first two test units to be instrumented with strain gages and were afterward considered too redundant. Test units 1 through 4 reflect the revised amount omitting 17 to 19 strain gages.

### 3.1.2 LVDTs

A configuration of 14 linear variable differential transducers (LVDTs) was mounted unobtrusively on the column at the front face of the joint, perpendicular to the joint at the four corners, and along the top and bottom of the beam near the joint. Figure 3.4 shows this LVDT configuration. The data from these LVDTs were used to calculate shear strain.

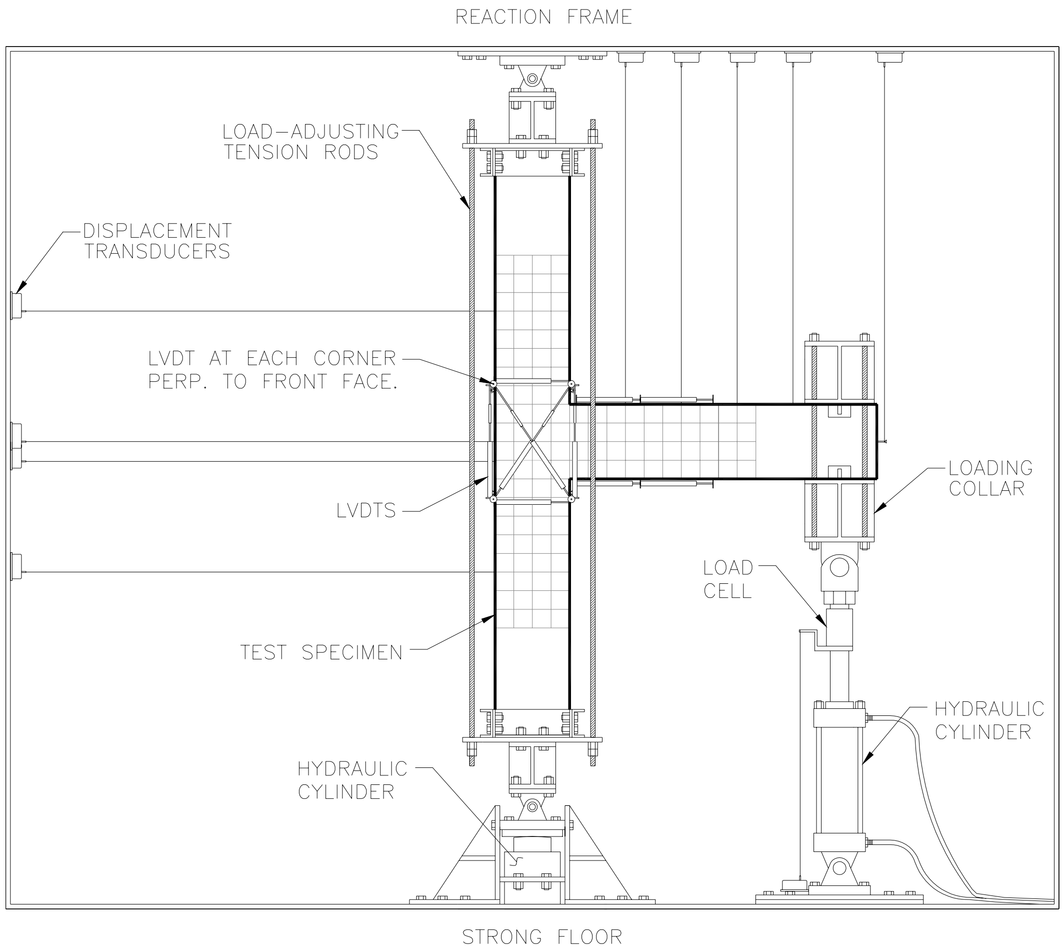


**Fig. 3.4 Test setup**

### 3.1.3 Displacement Transducers

Displacement transducers were attached to each test unit to measure deflection at the end of the beam, deflection at the point of lateral loading, curvature along the beam, rotation of the joint, and rigid body movement of the specimen. Additional displacement transducers were attached to test units 1 through 4 to measure bottom beam bar pullout. This was accomplished by attaching a stiff, thin wire to the end of one of the bottom beam bars prior to casting. A small groove was cut approximately ¼″ away from the end of the bar around its perimeter so that the wire could loop around the bar. Another groove was cut to lead the wire to the end of the bar near the bar's center. Strain gage glue was applied to the wire inside the groove and a small carbon-fiber straw was placed around the wire to protect it as it exited the test unit. During the test setup, the displacement transducer was attached to the wire.

## 3.2 LOADING APPARATUS

A schematic of the loading apparatus is shown in Figure 3.4. The column was mounted vertically with pinned supports at both ends. The axial load was applied using a small hydraulic cylinder and transferred to the column from the reaction against the loading frame and floor. Eight strain gages, one on each face of the column both top and bottom, were used to measure the axial load. Four threaded rods at each corner around the test unit were used to balance the applied axial load. The average of the eight strain gages was used as the axial load. The lateral load was applied at the end of the beam through a loading collar. A load cell situated between the hydraulic actuator and the loading collar measured the quasi-static cyclic load applied to the beam. The actuator was pinned at the end to allow rotation during the test. This loading device was manually operated.

## 3.3 TEST PROCEDURE

Before beginning each test, the axial load was slowly applied to the column and balanced in steps until the appropriate level was achieved. An axial compressive load equal to $0.1f'_c$ was applied to test units 1, 3, and 5. Test units 2, 4, and 6 received an axial compressive load equal to $0.25f'_c$. During each test, the appropriate level of axial compression was maintained by manually adjusting the small hydraulic cylinder after each load step. The lateral load was applied cyclically through the loading collar, in a quasi-static fashion, at the end of the beam, as shown in Figure 3.4. The loading procedure outlined by PEER was followed. This consisted of displacement-controlled steps beginning at a 0.1% drift followed by steps of 0.25%, 0.50%, 0.75%, 1.0%, 1.5%, 2.0%, 3.0%, 5.0%, 7.0%, and 10.0% drift. Owing to the limits of stroke in the actuator, 10.0% drift was not achievable. An alternate step of approximately 9.0% was used instead of 10.0%. Each drift step consisted of 3 cycles of push and pull, or up and down, respectively. The test concluded when the 9.0% drift step was completed, or the column was unable to maintain the axial load. The loading procedure for test 4, shown in Figure 3.5, is typical of all six tests.

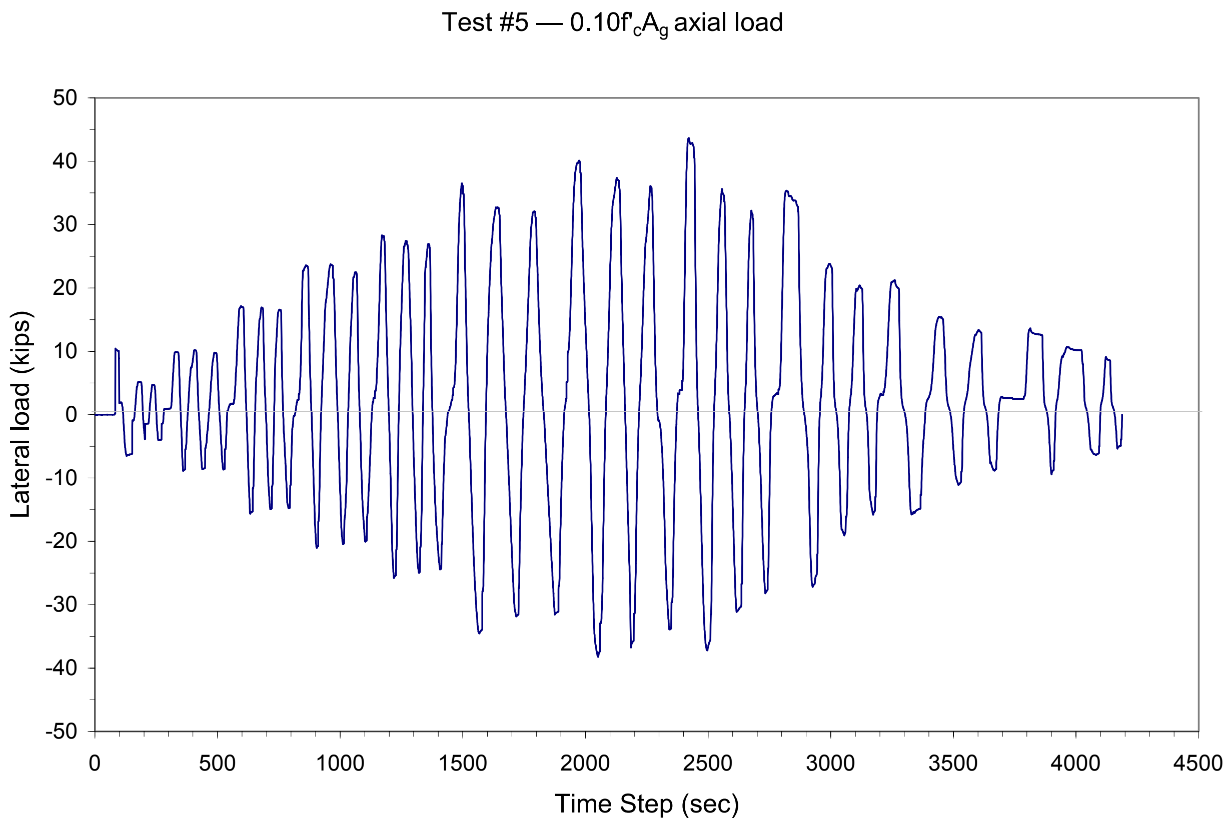


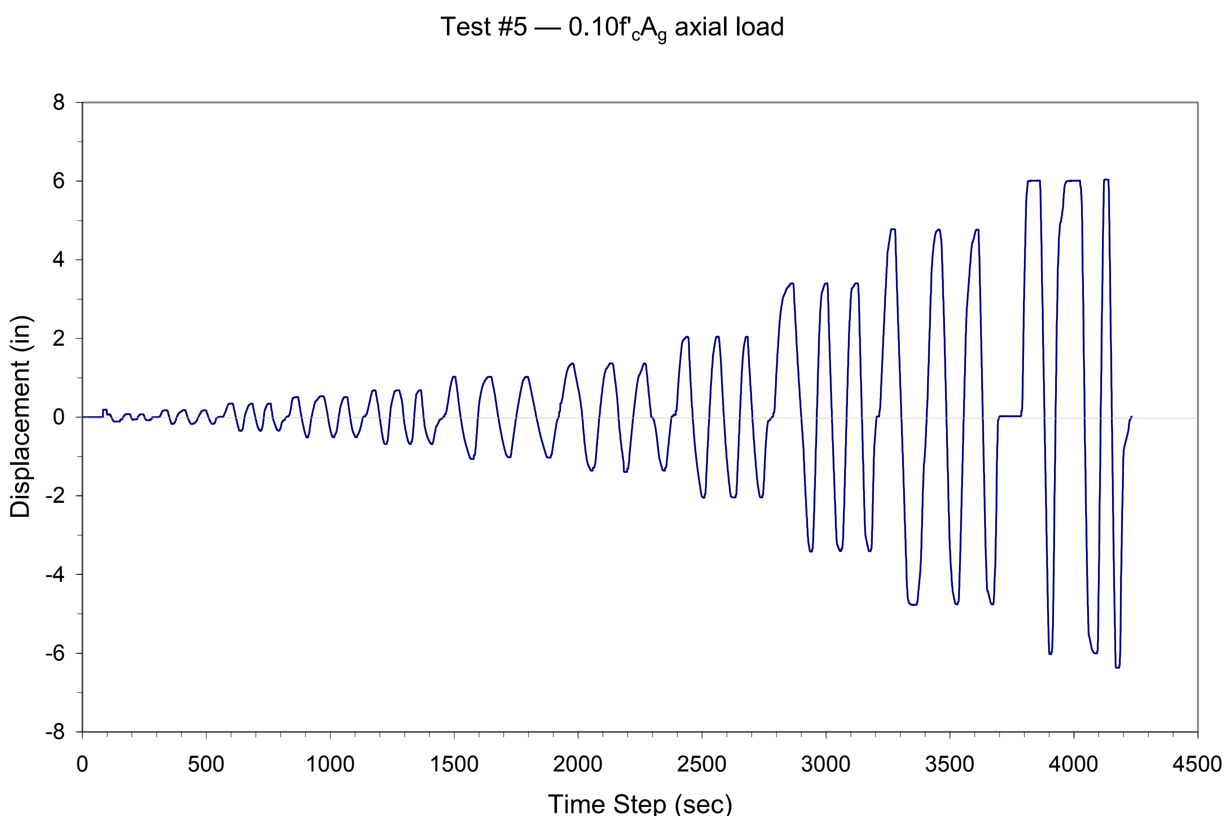


**Fig. 3.5 Typical loading pattern**

# 4 Test Results and Discussion

## 4.1 THEORETICAL PREDICTIONS

The test units had the material properties described in Chapter 2. Based on the compressive concrete strength of each unit, the actual value of the axial compressive load applied during the tests is shown in Table 4.1; the table also provides a brief description of each unit in terms of the bottom bar embedment details. The theoretical beam moment capacity was calculated by using the actual material properties of the units at the face of the column assuming that the beam reinforcement yields with $f_y$ = 66.5 ksi. Table 4.1 shows the theoretical beam and column flexural capacity and the flexural strength ratio. The column flexural capacity was calculated for the specific axial compressive load applied during the test of each unit, by using the specific column interaction diagram, and $f_y$ = 68.1 ksi. Table 4.1 also gives the flexural strength ratio of columns to beam; this ratio is specified as equal to 1.2 in the ACI 318 Code (1999) in order to satisfy the strong-column weak-beam design philosophy.

**Table 4.1 Beam and column theoretical flexural capacity and flexural strength ratio**

| Test Unit | Bottom Bar Embedment | $\frac{P}{f'_c A_g}$ | $P$ (kips) | Beam Moment, $M_b$ (kip-in.) | Column Moment, $M_c$ (kip-in.) | $\frac{\Sigma M_c}{M_b}$ |
|---|---|---|---|---|---|---|
| 1 | 6-in. | 0.10 | 123 | 3024 | 2832 | 1.87 |
| 2 | 6-in. | 0.25 | 307 | 3024 | 3120 | 2.06 |
| 3 | 14-in. | 0.10 | 126 | 3024 | 2880 | 1.90 |
| 4 | 14-in. | 0.25 | 316 | 3024 | 3168 | 2.09 |
| 5 | Hook | 0.10 | 118 | 3024 | 2796 | 1.85 |
| 6 | Hook | 0.25 | 294 | 3024 | 3084 | 2.04 |

As Table 4.1 shows, all test units satisfy the provision of the ACI Code regarding the flexural strength ratio.

## 4.2 EXPERIMENTAL RESULTS

### 4.2.1 Test Unit 1

The lateral load applied versus drift for unit 1 is shown in Figure 4.1. The horizontal axis shows the drift ratio for the unit. In addition the figure shows the step numbers near each load step. Note that a positive load indicates that the load was applied in the upward direction. It is clear that the upward direction resistance is deficient because of the inadequate anchorage of the bottom beam bars of only 6 in. into the joint, as shown in Figure 2.1. The maximum load in the upward direction occurred at a drift ratio of 1.5% and had a value of 20.7 kips; in the downward direction, the maximum load occurred at a drift of 1.5% and had a value of 43.8 kips. The ratio between the lateral load capacity in the strong and weak directions is thus equal to 2.12. This indicates early bond slip of the bottom reinforcement with inadequate embedment.

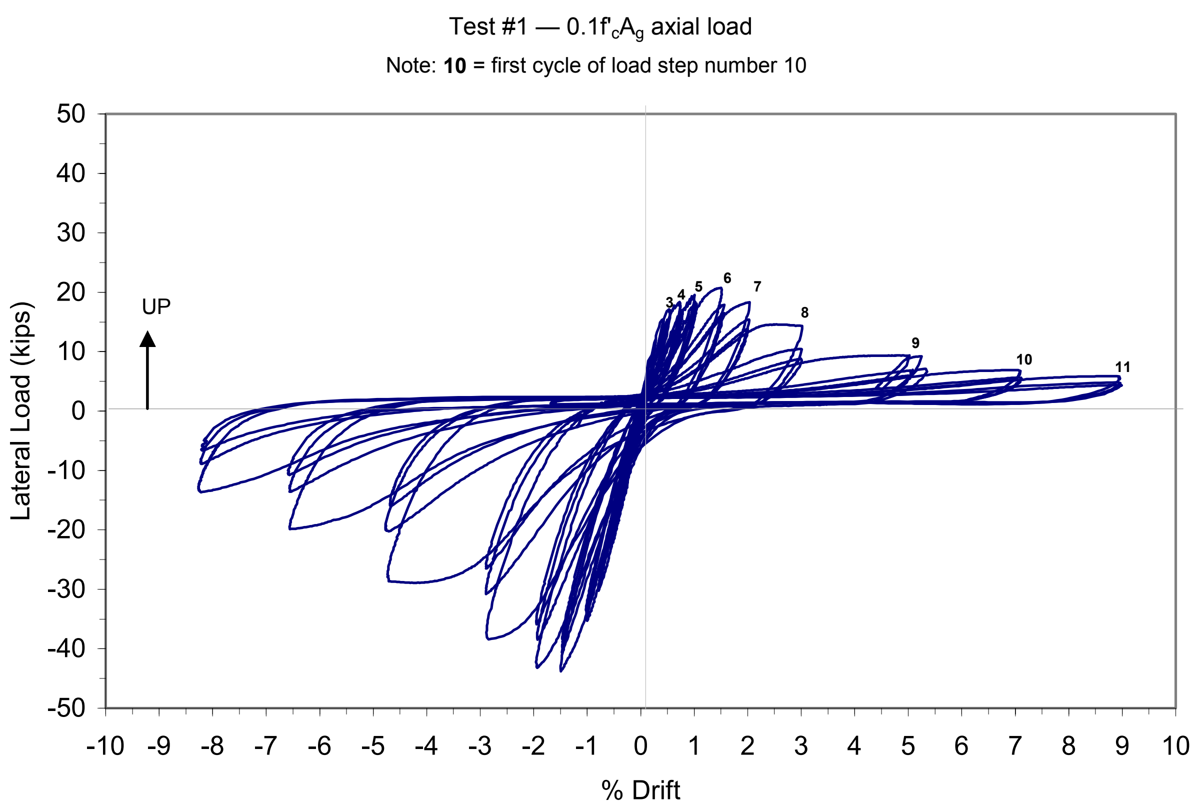


**Fig. 4.1 Unit 1: lateral load versus drift ratio**

The flexural moment applied is compared to the theoretical moment capacity in Table 4.2 for all test units. Test unit 1 had an actual beam moment capacity 41% of the theoretical in the upward direction and 86% in the downward direction. Figure 4.2 shows the moment-rotation and the moment-plastic-rotation curves. The plastic rotation at the peak moment in the upward direction was 0.005 radian, and at the peak moment in the downward direction it was 0.006 radian; the plastic rotation at 80% of the peak moment was 0.015 radian in the upward direction and 0.020 radian in the downward direction.

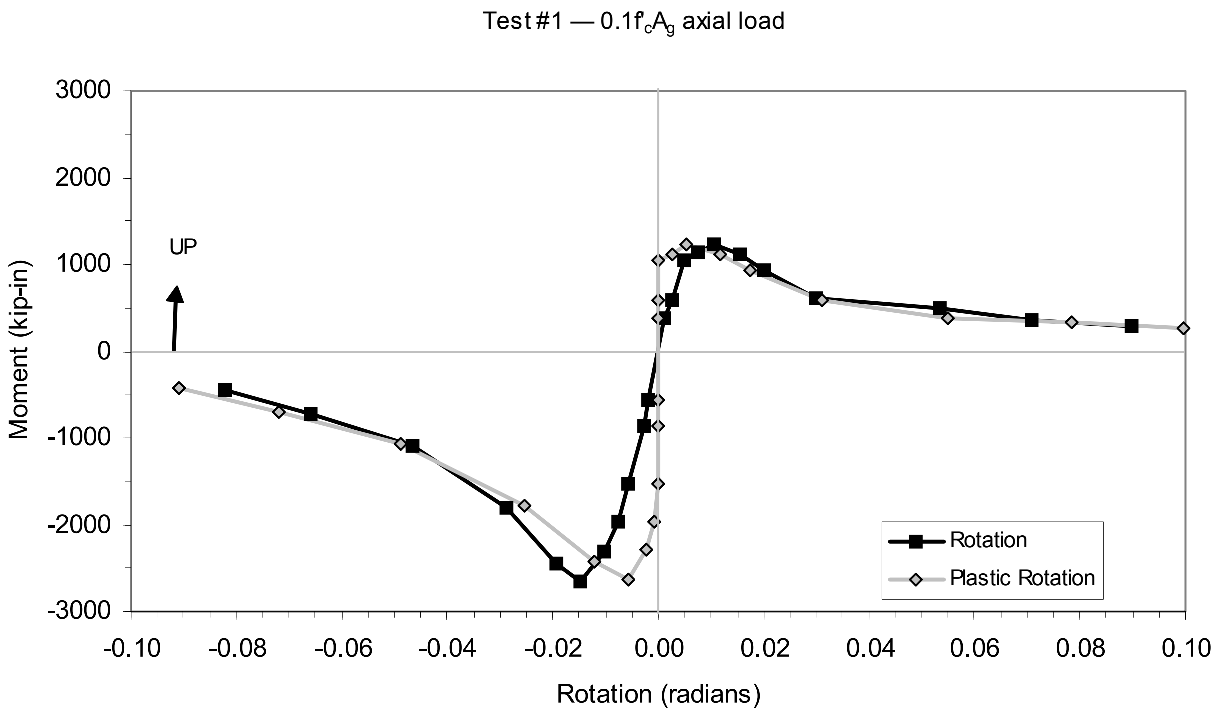


**Fig. 4.2 Unit 1: moment-rotation and moment-plastic-rotation envelopes**

The column axial load for test unit 1 was set at a level of 0.1 $f'_c A_g$, which corresponds to a 123 kips compression load. Although every effort was made to maintain the axial load at this level throughout the test, variations were unavoidable. As shown in Figure 4.3, the axial load varied from 106 to 144 kips, or a range of 86% to 117%. However, there was no indication that test unit 1 reached its capacity because it could not support the axial compression load.

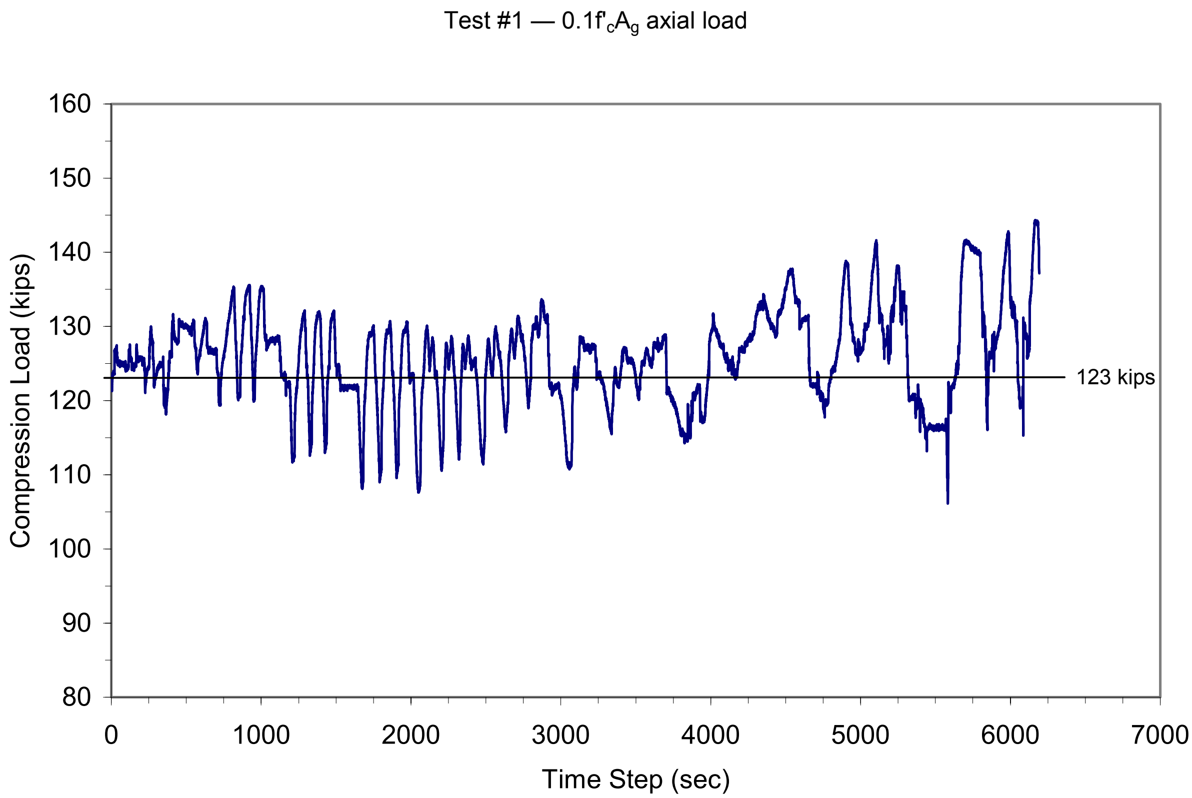


**Fig. 4.3 Unit 1: variation of axial compression column load**

The cumulative energy absorbed by test unit 1 is shown in Figure 4.4. The total energy absorbed was 558 kip-in. at a drift ratio of 9%. At a drift ratio of 1.5%, at which the maximum load occurred for both the upward and downward directions, the absorbed energy was only 15% of the total energy absorbed, and at a drift ratio of 4% it was 50% of the total energy absorbed.

The joint shear stress versus joint shear strain for test unit 1 is shown in Figure 4.5. The maximum joint shear stress was 372 psi in the upward direction, which corresponds to a $\gamma$=5.3 (psi). The downward maximum joint shear stress was 780 psi with a corresponding $\gamma$=11.1 (psi). The joint shear strain at the maximum shear stress was 3480 $\mu\varepsilon$ in the upward direction and 1960 $\mu\varepsilon$ in the downward direction.

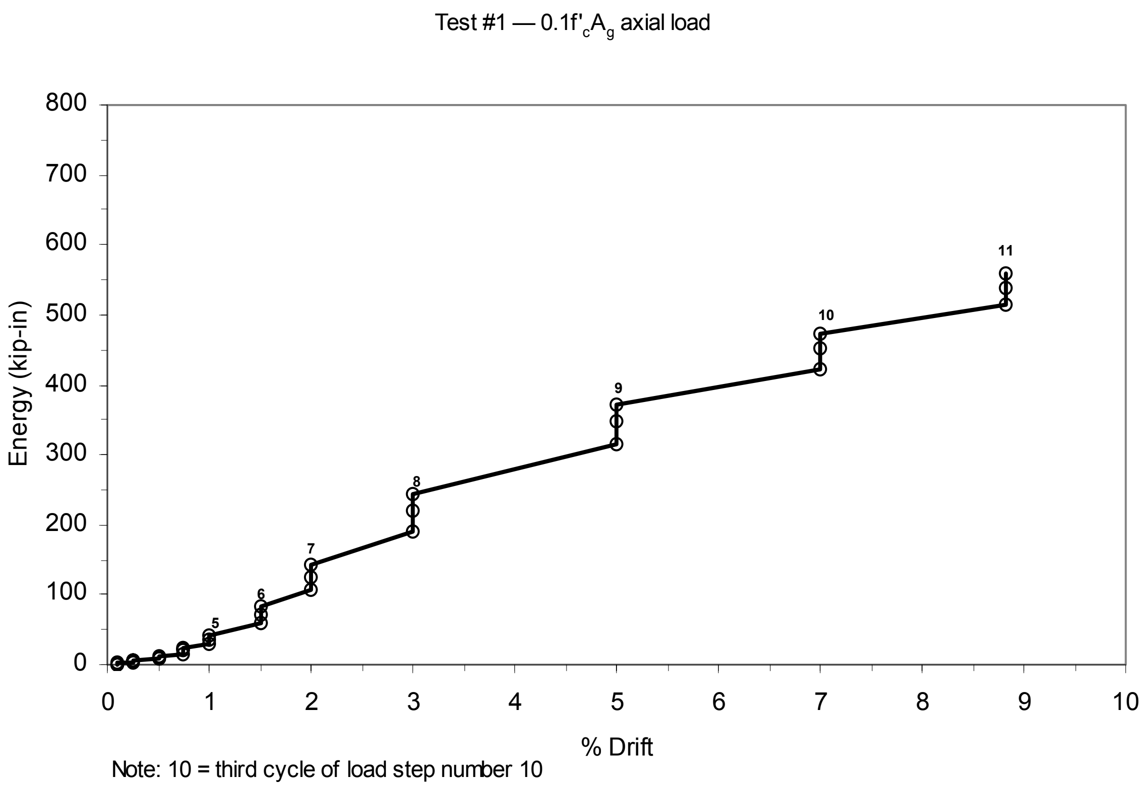


**Fig. 4.4 Unit 1: cumulative energy dissipation**

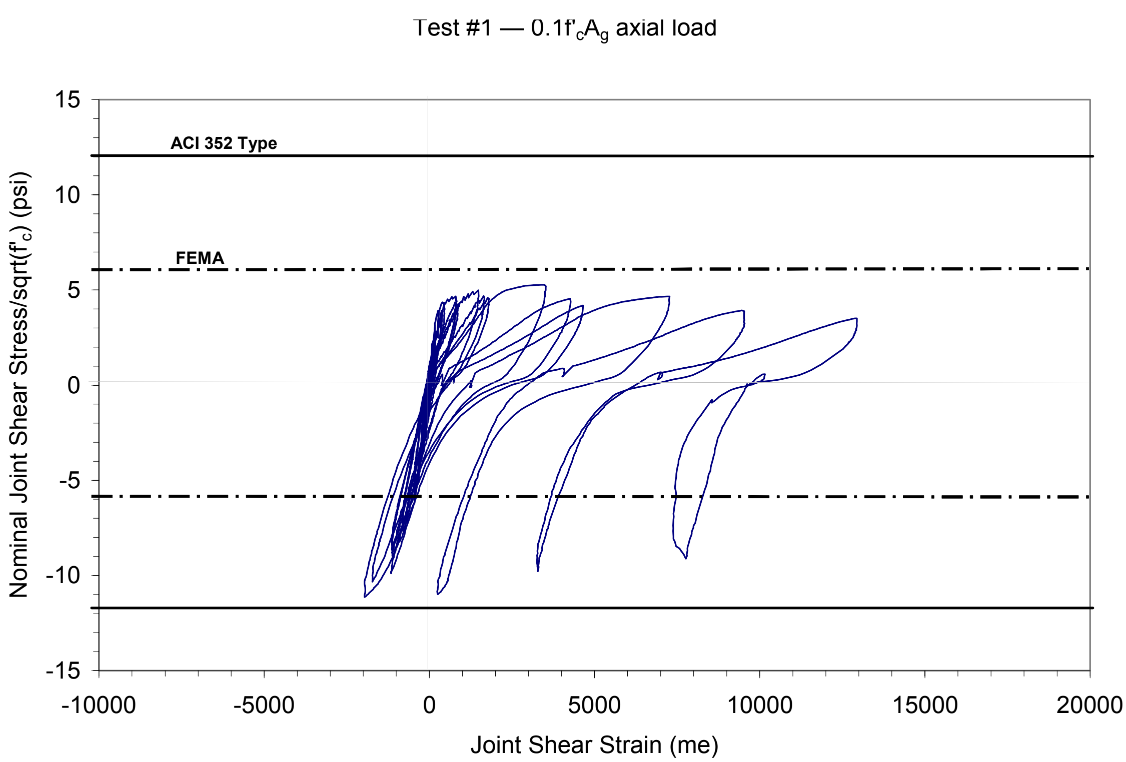


**Fig. 4.5 Unit 1: joint shear stress versus joint shear strain**

### 4.2.2 Test Unit 2

The lateral load applied versus drift for unit 2 is shown in Figure 4.6. The upward direction resistance is deficient because of the inadequate anchorage of the bottom beam bars of only 6 in. into the joint, as shown in Figure 2.1. The maximum load in the upward direction occurred at a drift ratio of 1.48% and had a value of 28.3 kips; in the downward direction, the maximum load occurred at a drift of 1.52% and had a value of 42.7 kips. The ratio between the lateral load capacity in the strong and weak directions is thus equal to 1.51, which is more favorable than the 2.12 ratio obtained for test unit 1. This indicates that the presence of the higher axial load was beneficial in preventing the early bond slip of the bottom reinforcement, even though the embedment was exactly the same for units 1 and 2, i.e., 6 in.

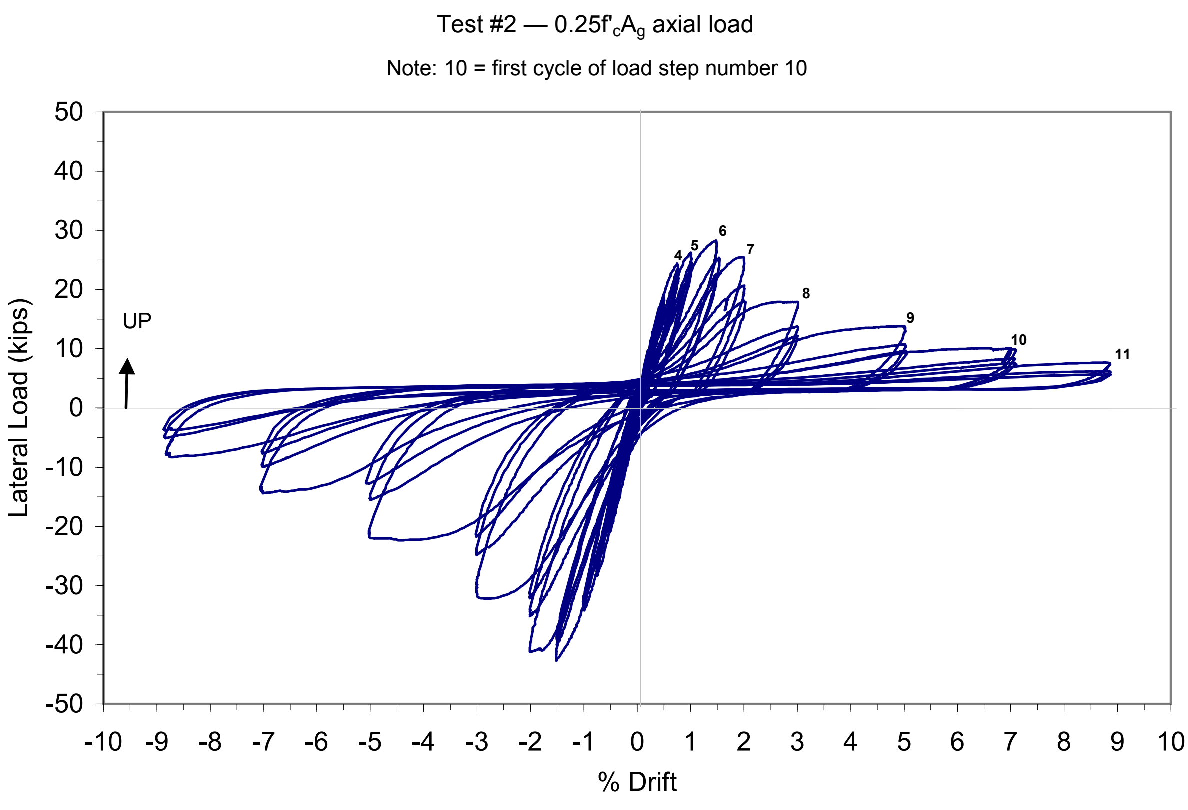


**Fig. 4.6 Unit 2: lateral load versus drift ratio**

The flexural moment applied is compared to the theoretical moment capacity in Table 4.2 for all test units. Test unit 2 had an actual beam moment capacity of 56% of the theoretical in the upward direction and 83% in the downward direction. Figure 4.7 shows the moment-rotation and the moment-plastic-rotation curves. The plastic rotation at the peak moment in the upward direction was 0.005 radian, and at the peak moment in the downward direction it was 0.006 radian; the plastic rotation at 80% of the peak moment was 0.016 radian in the upward direction and 0.015 radian in the downward direction.

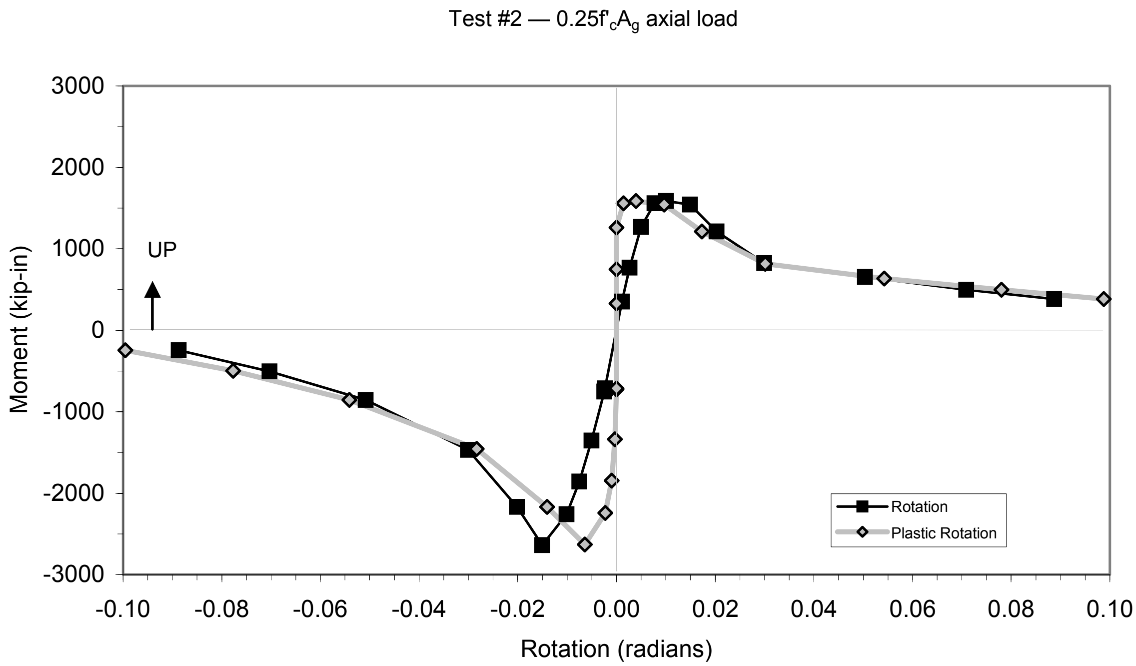


**Fig. 4.7 Unit 2: moment-rotation and moment-plastic-rotation envelopes**

The column axial load for test unit 2 was set at a level of 0.25 $f'_cA_g$, which corresponds to a 307 kips compression load. Variations in the level of axial load were unavoidable as shown in Figure 4.8; the axial load varied in the range of 97% to 110%. However, there was no indication that test unit 2 reached its capacity because it could not support the axial compression load. It is clear that the failure mode is again bond slip of the bottom bars; however, the presence of the increased axial load compression in the column brought the upward capacity close to the downward capacity.

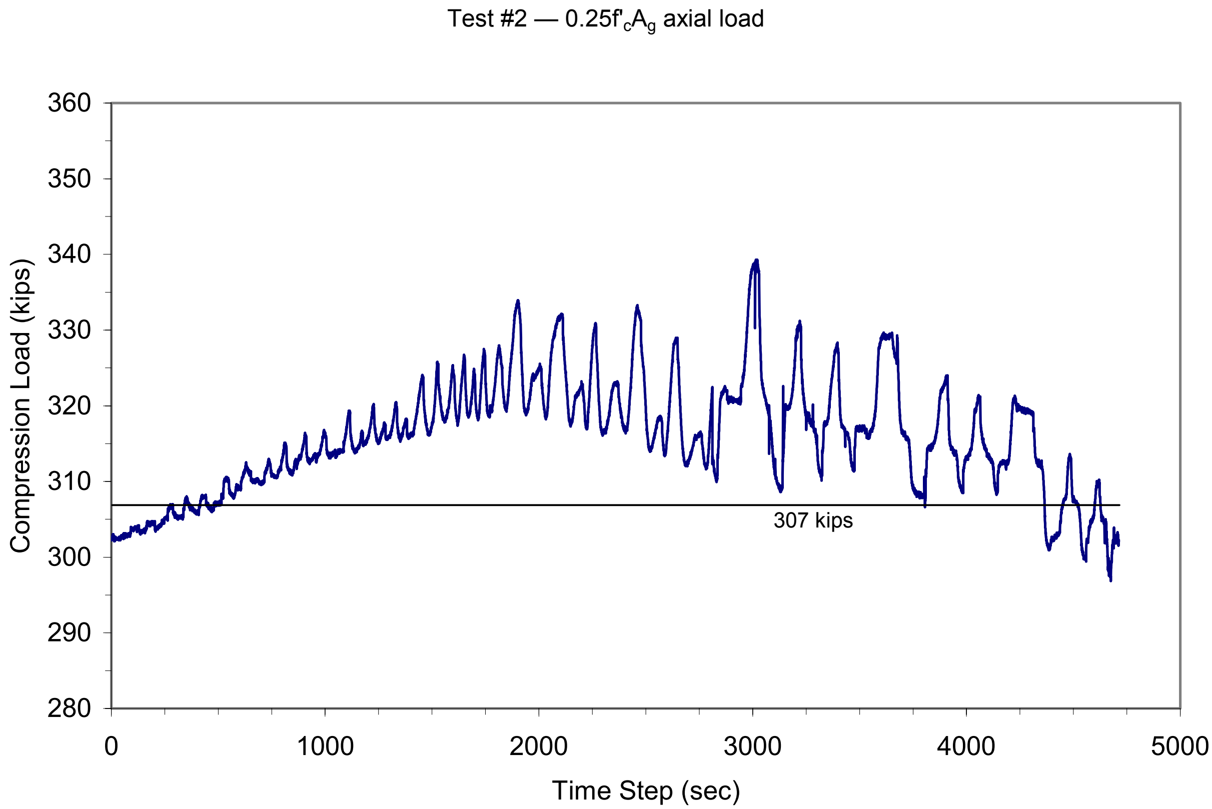


**Fig. 4.8 Unit 2: variation of axial compression column load**

The cumulative energy absorbed by test unit 2 is shown in Figure 4.9. The total energy absorbed was 563 kip-in. at a drift ratio of 9%. At a drift ratio of 1.5%, at which the maximum load occurred for both the upward and downward directions, the absorbed energy was only 14% of the total energy absorbed, and at a drift ratio of 4% it was 50% of the total energy absorbed. The energy absorption behavior is very similar to that of test unit 1.

The joint shear stress versus joint shear strain for test unit 2 was not able to be determined due to the LVDTs malfunctioning during the test.

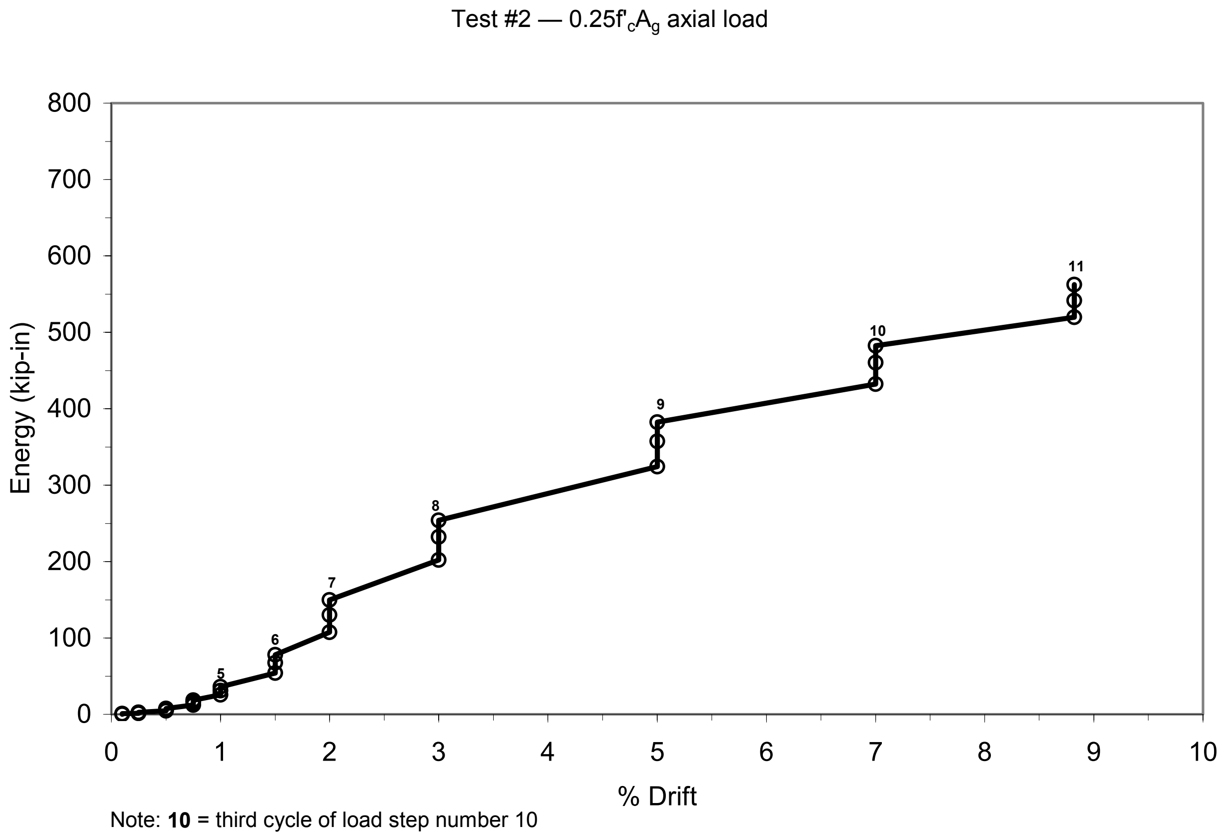


**Fig. 4.9 Unit 2: cumulative energy dissipation**

### 4.2.3 Test Unit 3

The lateral load applied versus drift for unit 3 is shown in Figure 4.10. The upward direction resistance is similar to the downward, since the anchorage of the bottom beam bars was 14 in. into the joint, as shown in Figure 2.2. The maximum load in the upward direction occurred at a drift ratio of 2.00% and had a value of 42.2 kips; in the downward direction, the maximum load occurred at a drift of 2.00% and had a value of 41.4 kips. The ratio between the lateral load capacity in the two directions is thus equal to 1.02, which shows that the capacity in the upward and downward directions is almost the same. This indicates that the 14 in. embedment with the 5 in. overlap with the hook from the top bars was effective in providing anchorage to the bottom bars and preventing a premature bond slip.

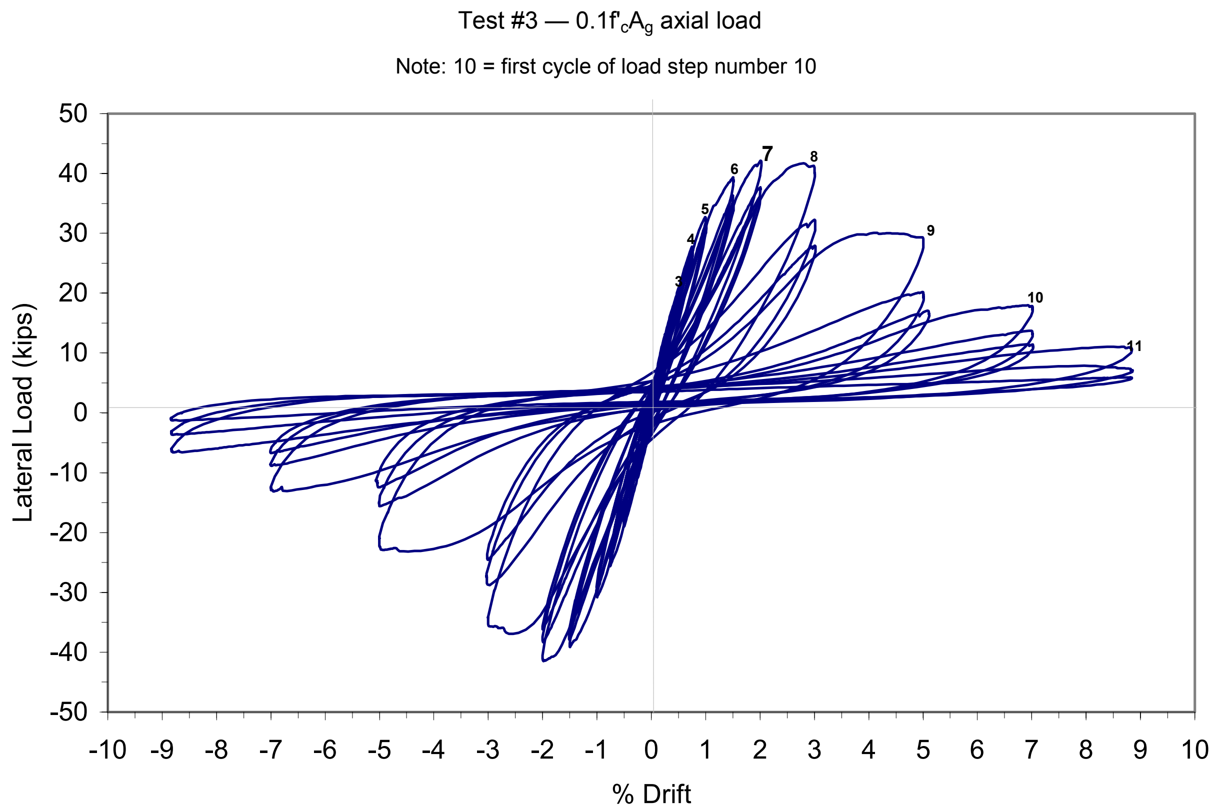


**Fig. 4.10 Unit 3: lateral load versus drift ratio**

The flexural moment applied is compared to the theoretical moment capacity in Table 4.2 for all test units. Test unit 3 had an actual beam moment capacity of 83% of the theoretical in the upward direction and 81% in the downward direction. Figure 4.11 shows the moment-rotation and the moment-plastic-rotation curves. The plastic rotation at the peak moment in the upward direction was 0.013 radian, and at the peak moment in the downward direction it was 0.006 radian; the plastic rotation at 80% of the peak moment was 0.025 radian in the upward direction and 0.020 radian in the downward direction.

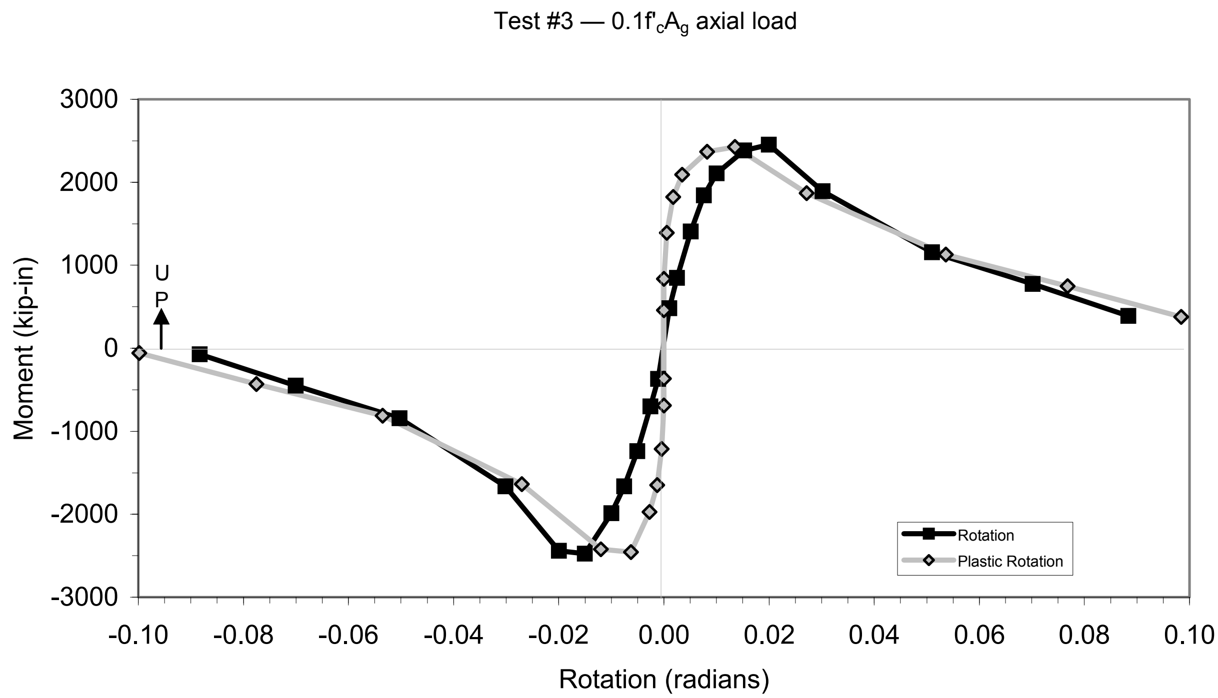


**Fig. 4.11 Unit 3: moment-rotation and moment-plastic-rotation envelopes**

The column axial load for test unit 3 was set at a level of 0.10 $f'_c A_g$, which corresponds to a 126 kips compression load. Variations in the level of axial load were substantial as shown in Figure 4.12; the axial load varied in the range of 65% to 140%. Shear failure of the joint was the primary failure mode. The drop in axial load was 35%, so it is clear that test unit 3 reached its ultimate capacity because it could not support the axial compression load once the shear mechanism occurred.

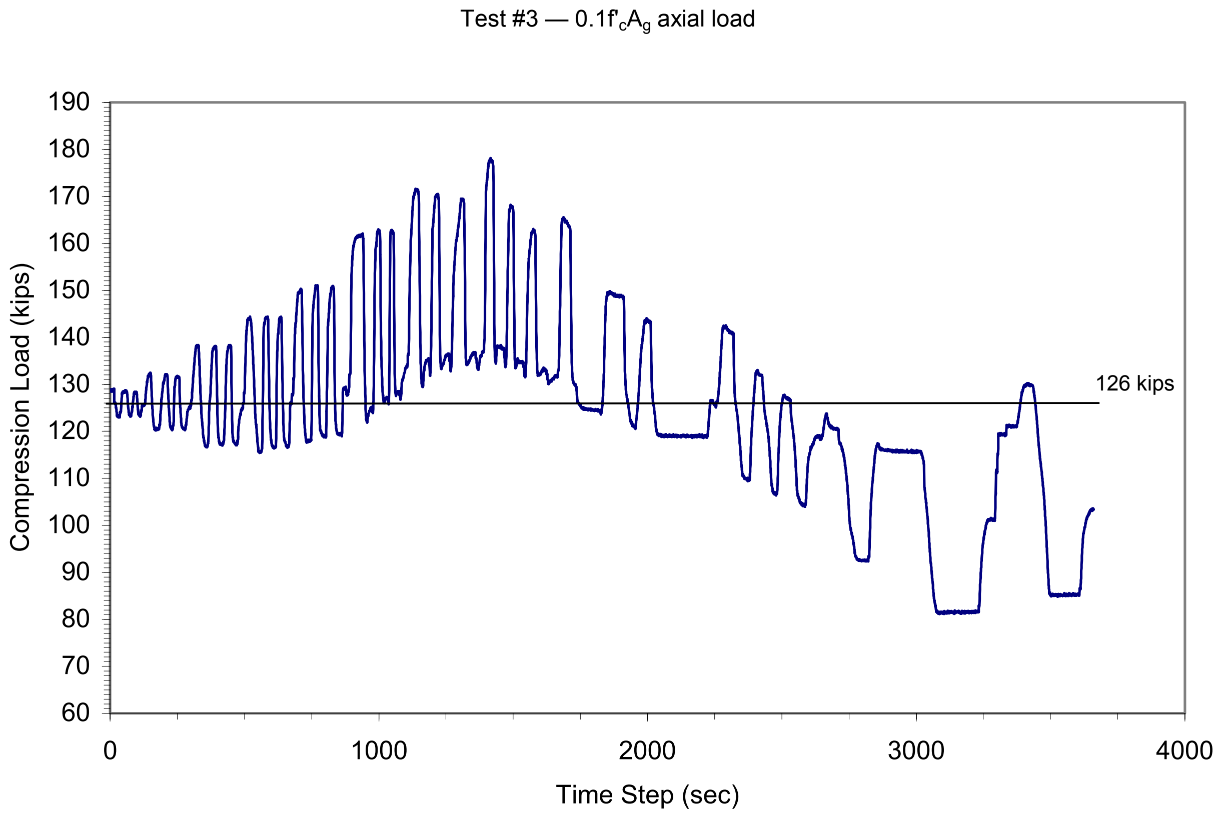


**Fig. 4.12 Unit 3: variation of axial compression column load**

The cumulative energy absorbed by test unit 3 is shown in Figure 4.13. The total energy absorbed was 683 kip-in. at a drift ratio of 9%. At a drift ratio of 2.0%, at which the maximum load occurred for both the upward and downward directions, the absorbed energy was 21% of the total energy absorbed, and at a drift ratio of 4.5% it was 50% of the total energy absorbed. The energy absorption is 22% higher compared to test unit 1.

The joint shear stress versus joint shear strain for test unit 3 is shown in Figure 4.14. The maximum joint shear stress was 734 psi in the upward direction, which corresponds to a $\gamma$=10.6 (psi). The downward maximum joint shear stress was 720 psi with a corresponding $\gamma$=10.4 (psi). The joint shear strain at the maximum shear stress was 3250 $\mu\varepsilon$ in the upward direction and 4270 $\mu\varepsilon$ in the downward direction.

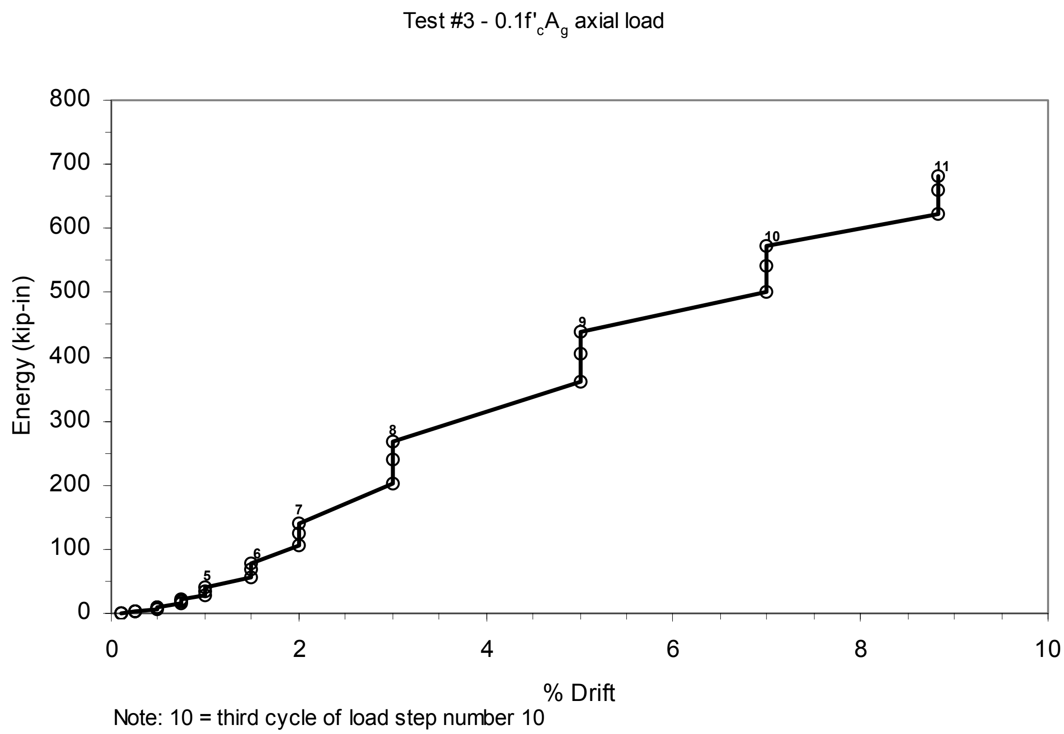


**Fig. 4.13 Unit 3: cumulative energy dissipation**

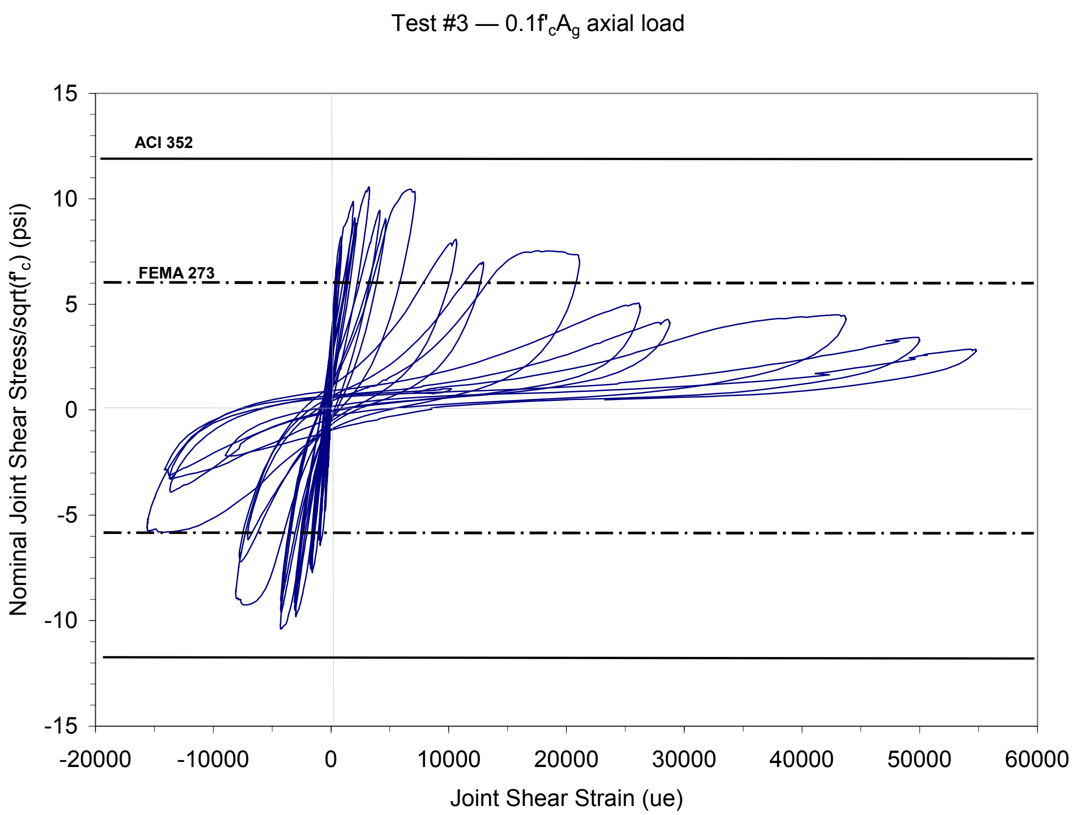


**Fig. 4.14 Unit 3: joint shear stress versus joint shear strain**

### 4.2.4 Test Unit 4

The lateral load applied versus drift for unit 4 is shown in Figure 4.15. The upward direction resistance is similar to the downward, since the anchorage of the bottom beam bars was 14 in. into the joint, as shown in Figure 2.2. The maximum load in the upward direction occurred at a drift ratio of 2.00% and had a value of 45.1 kips; in the downward direction, the maximum load occurred at a drift of 2.00% and had a value of 47.5 kips. The ratio between the lateral load capacity in the two directions is thus equal to 1.05, which shows that the capacity in the upward and downward directions is almost the same. This indicates that the 14 in. embedment with the 5 in. overlap with the hook from the top bars was effective in providing anchorage to the bottom bars and preventing a premature bond slip; this was also observed in test unit 3.

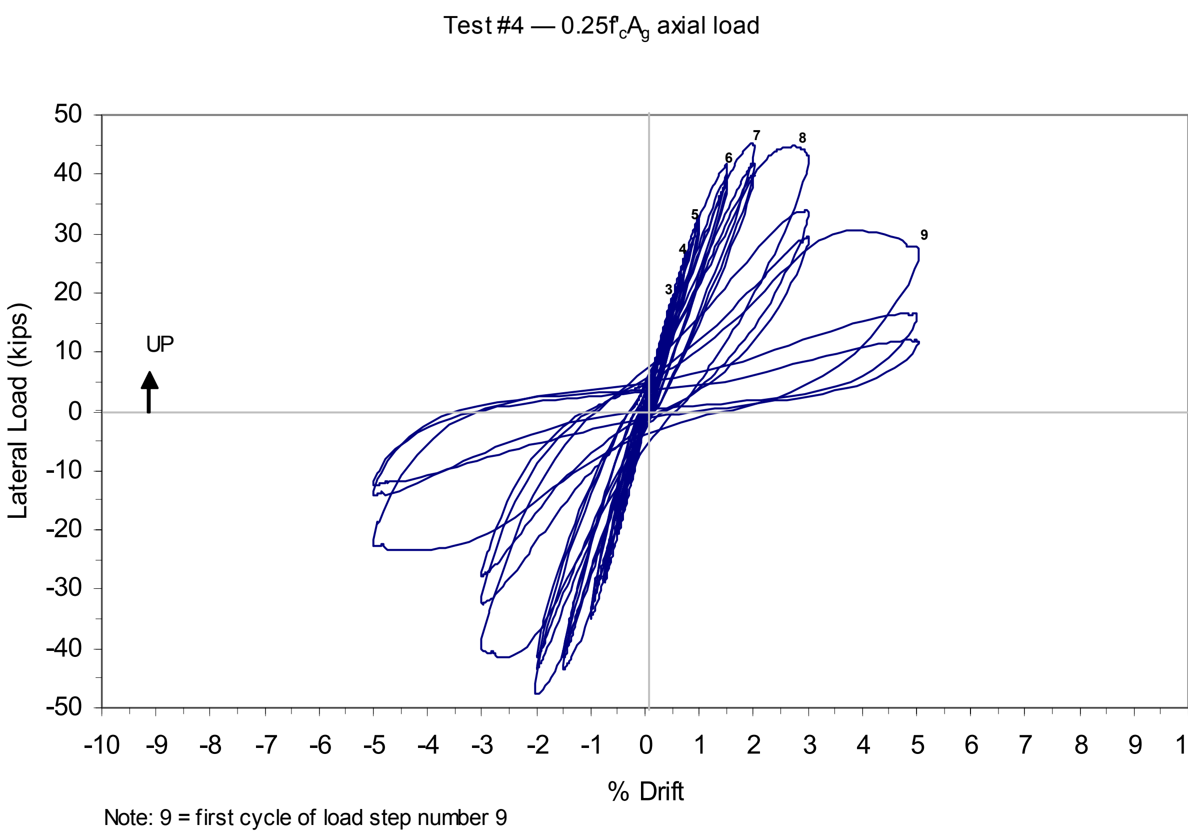


**Fig. 4.15 Unit 4: lateral load versus drift ratio**

The flexural moment applied is compared to the theoretical moment capacity in Table 4.2 for all test units. Test unit 4 had an actual beam moment capacity of 87% of the theoretical in the upward direction and 93% in the downward direction; this is a better performance than unit 3 and it shows the beneficial effect of the axial compression load in confining the joint concrete.

Figure 4.16 shows the moment-rotation and the moment-plastic-rotation curves. The plastic rotation at the peak moment in the upward direction was 0.011 radian, and at the peak moment in the downward direction it was 0.012 radian; the plastic rotation at 80% of the peak moment was 0.022 radian in the upward direction and 0.020 radian in the downward direction.

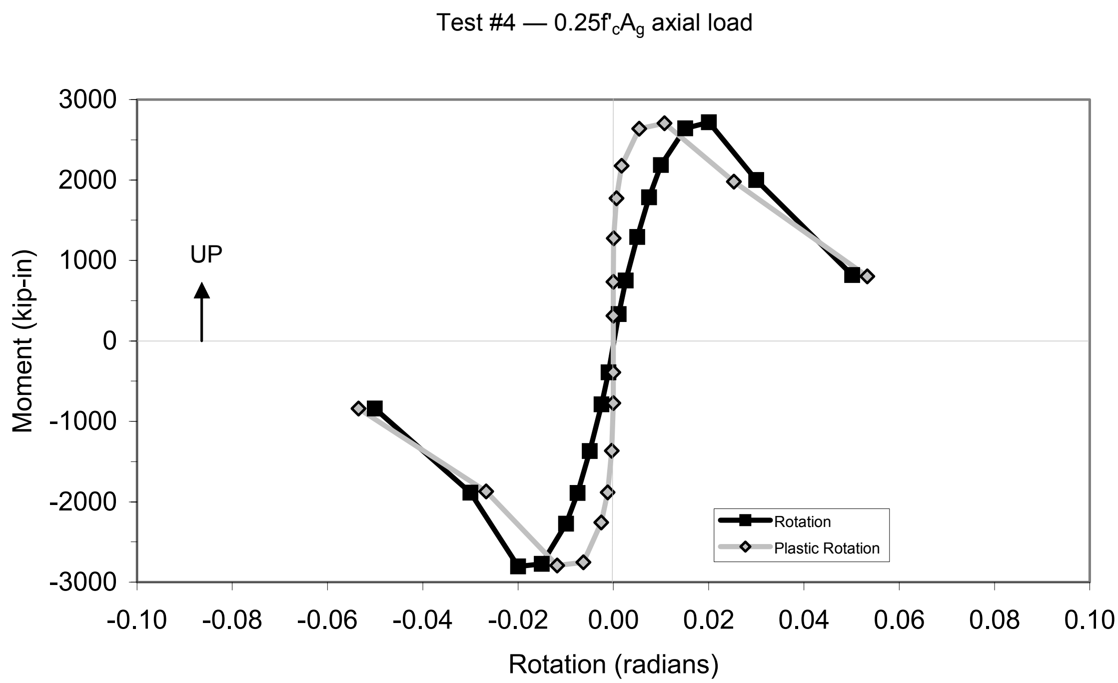


**Fig. 4.16 Unit 4: moment-rotation and moment-plastic-rotation envelopes**

The column axial load for test unit 4 was set at a level of 0.25 $f'_c A_g$, which corresponds to a 316 kips compression load. Every effort was made to maintain the axial load at this level throughout the test. Variations in the level of axial load were substantial, as shown in Figure 4.17; the axial load varied in the range of 76% to 113%. The previous failure mechanism is joint shear, followed by loss of axial load capacity. The drop in axial load was 24%, and it is clear that test unit 4 reached its ultimate capacity because it could not support the axial compression load.

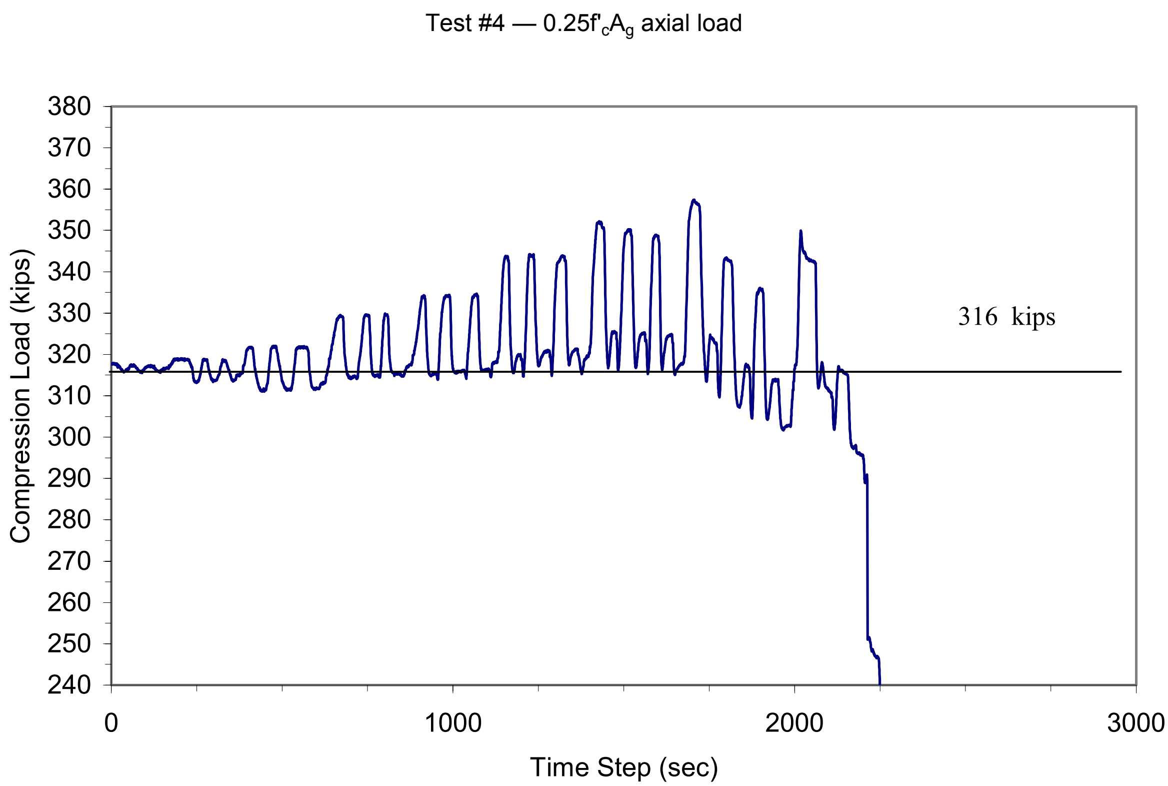


**Fig. 4.17 Unit 4: variation of axial compression column load**

The cumulative energy absorbed by test unit 4 is shown in Figure 4.18. The total energy absorbed was 470 kip-in. at a drift ratio of 5%. At a drift ratio of 2.0%, at which the maximum load occurred for both the upward and downward directions, the absorbed energy was 29% of the total energy absorbed, and at a drift ratio of 3% it was 50% of the total energy absorbed. It should be noted that test unit 4 shows that with the higher axial compression load, there was much less drift achieved in the test, approximately 56% that of unit 3.

The joint shear stress versus joint shear strain for test unit 1 is shown in Figure 4.19. The maximum joint shear stress was 794 psi in the upward direction, which corresponds to a $\gamma$=11.3 (psi). The downward maximum joint shear stress was 836 psi with a corresponding $\gamma$=11.9 (psi). The joint shear strain at the maximum shear stress was 2990 $\mu\varepsilon$ in the upward direction and 2220 $\mu\varepsilon$ in the downward direction.

Test #4 — 0.25f'$_c$A$_g$ axial load

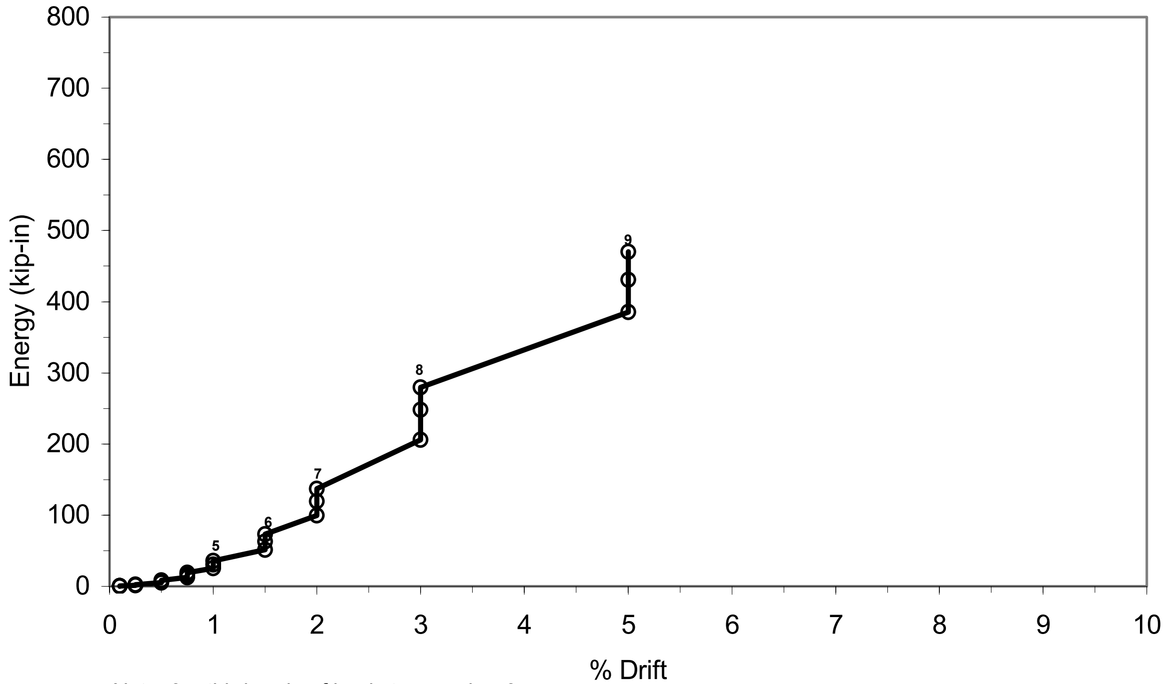


Note: 9 = third cycle of load step number 9

**Fig. 4.18 Unit 4: cumulative energy dissipation**

Test #4 — 0.25f'$_c$A$_g$ axial load

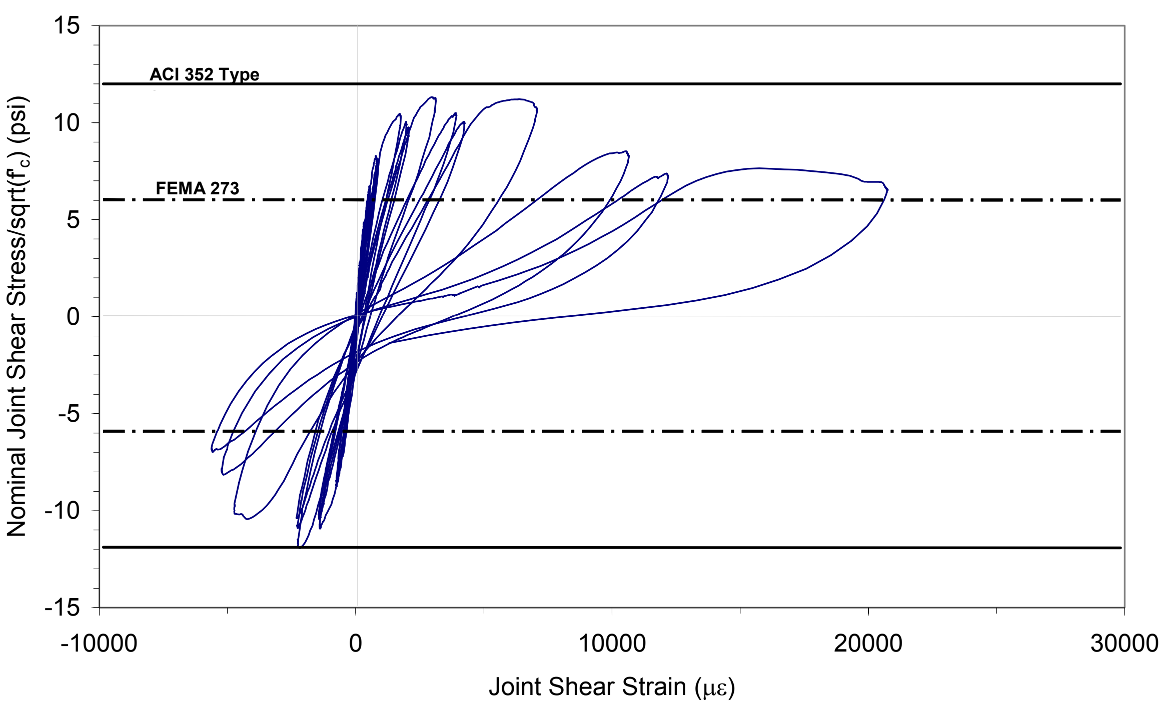


**Fig. 4.19 Unit 4: joint shear stress versus joint shear strain**

### 4.2.5 Test Unit 5

The lateral load applied versus drift for unit 5 is shown in Figure 4.20. The bottom beam bars have a hooked anchorage detail identical to the top bars in the joint, as shown in Figure 2.3. The maximum load in the upward direction occurred at a drift ratio of 2.8% and had a value of 43.6 kips; in the downward direction, the maximum load occurred at a drift of 2.0% and had a value of 38.2 kips. The ratio between the lateral load capacity in the upward and downward directions is thus equal to 1.14 due to manufacturing tolerances of the test unit.

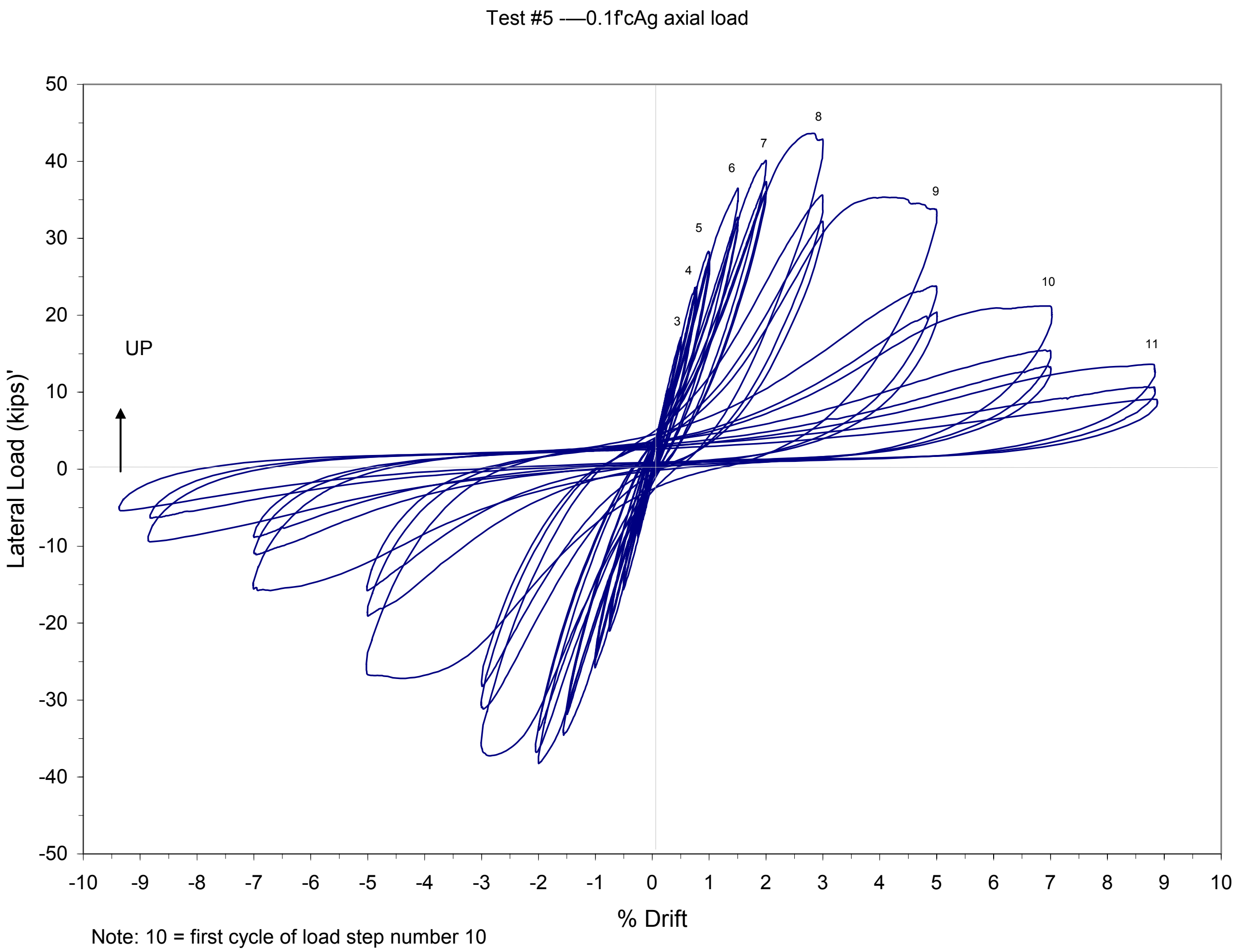


**Fig. 4.20 Unit 5: lateral load versus drift ratio**

The flexural moment applied is compared to the theoretical moment capacity in Table 4.2 for all test units. Test unit 5 had an actual beam moment capacity of 87% of the theoretical in the upward direction and 75% in the downward direction. Figure 4.21 shows the moment-rotation and the moment-plastic-rotation curves. The plastic rotation at the peak moment in the upward direction was 0.011 radian, and at the peak moment in the downward direction it was 0.010 radian; the plastic rotation at 80% of the peak moment was 0.030 radian in the upward direction and 0.024 radian in the downward direction.

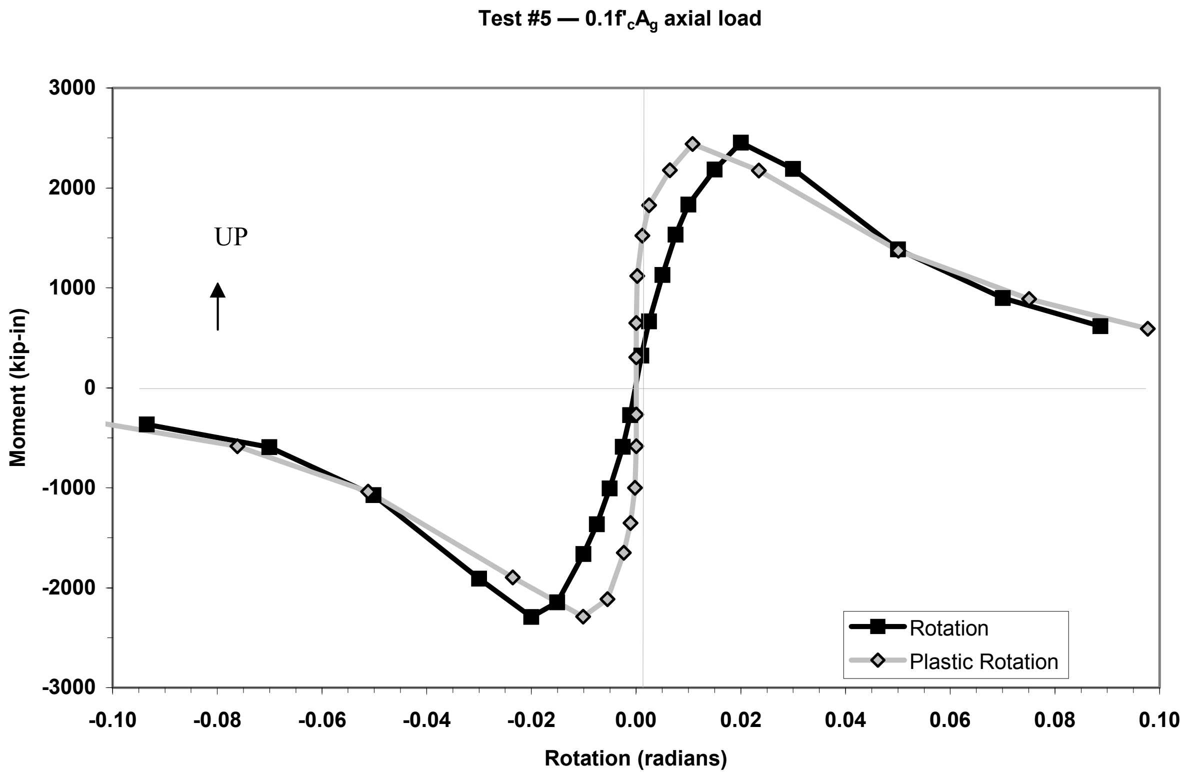


**Fig. 4.21 Unit 5: moment-rotation and moment-plastic-rotation envelopes**

The column axial load for test unit 5 was set at a level of 0.10 $f'_c A_g$, which corresponds to 118 kips compression load. Variations in the level of axial load were unavoidable as shown in Figure 4.22; the axial load varied in the range of 79% to 149%. The drop in axial load was 21% and unit 5 eventually lost its axial-load-carrying capacity. It is clear that the primary failure mode is joint shear.

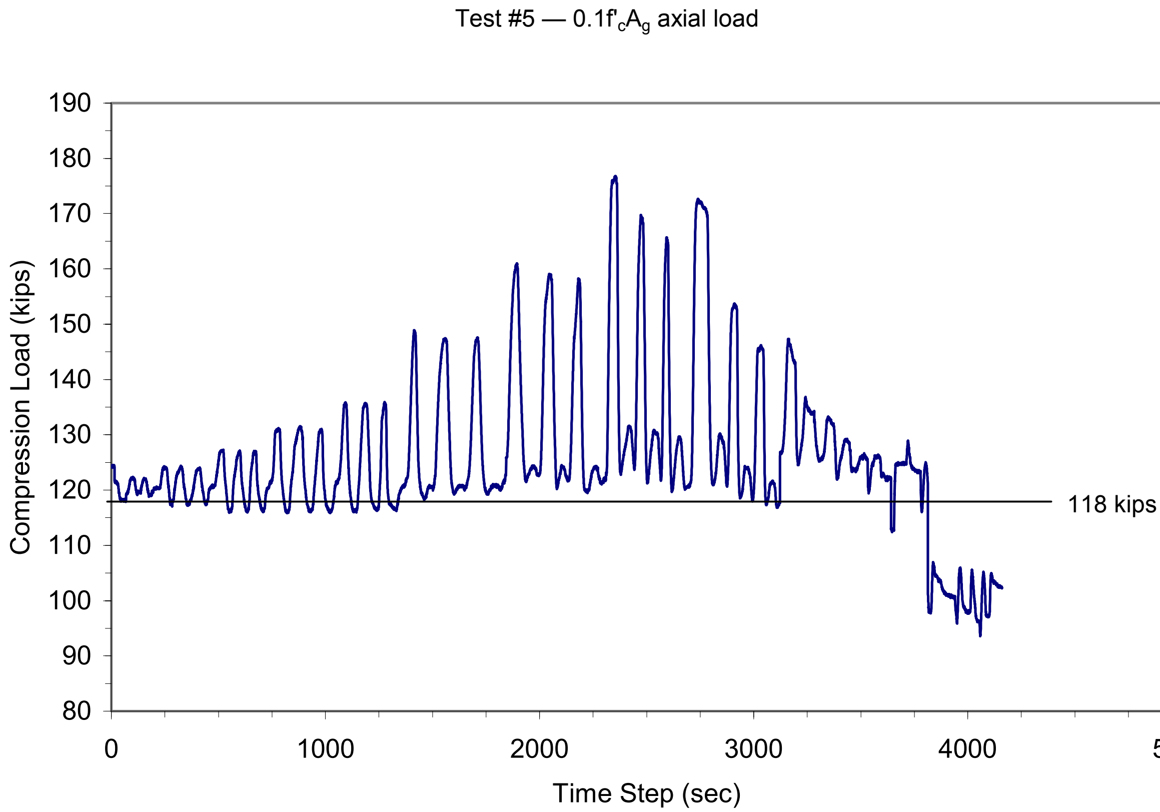


**Fig. 4.22 Unit 5: variation of axial compression column load**

The cumulative energy absorbed by test unit 5 is shown in Figure 4.23. The total energy absorbed was 707 kip-in. at a drift ratio of 9%. At a drift ratio of 2.5%, at which the maximum load occurred on average for the upward and downward directions, the absorbed energy was 20% of the total energy absorbed, and at a drift ratio of 5% it was 50% of the total energy absorbed. The energy absorption behavior of unit 5 was the highest of all six tests.

The joint shear stress versus joint shear strain for test unit 5 is shown in Figure 4.24. The maximum joint shear stress was 766 psi in the upward direction, which corresponds to a $\gamma$=11.3 (psi). The downward maximum joint shear stress was 671 psi with a corresponding $\gamma$=9.9 (psi). The joint shear strain at the maximum shear stress was 5840 $\mu\varepsilon$ in the upward direction and 2890 $\mu\varepsilon$ in the downward direction.

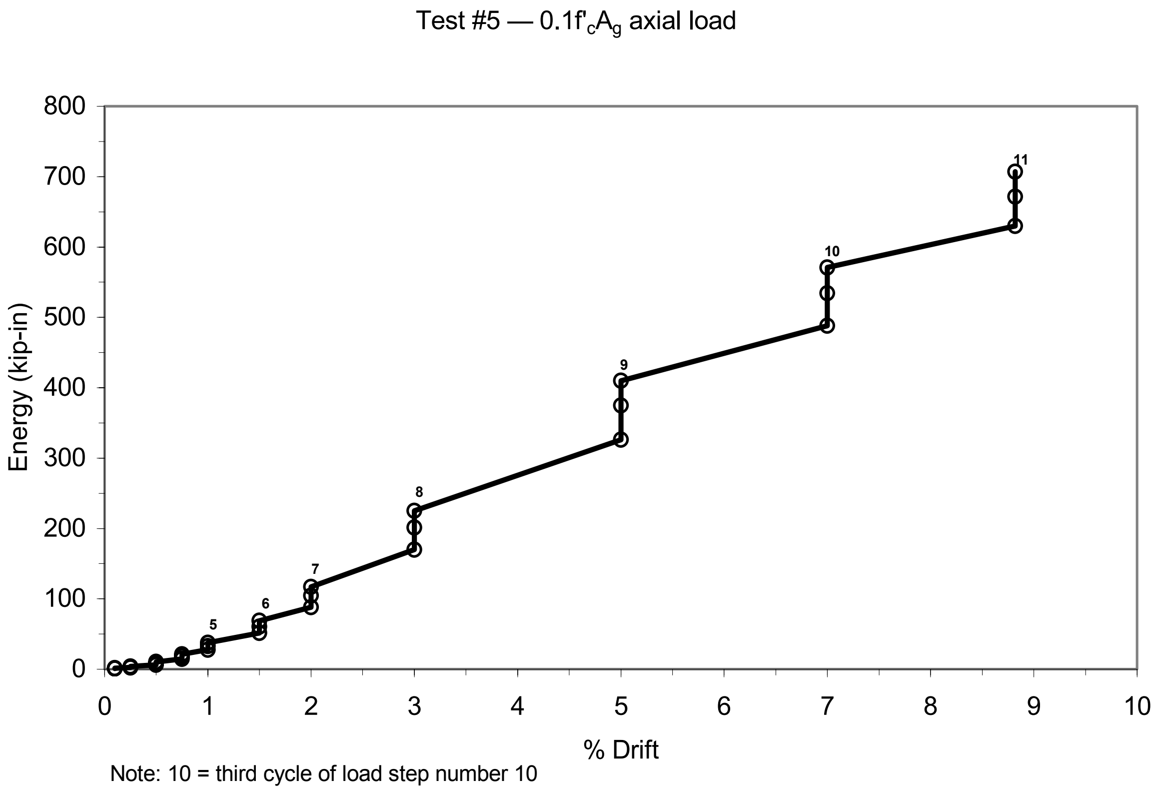


**Fig. 4.23 Unit 5: cumulative energy dissipation**

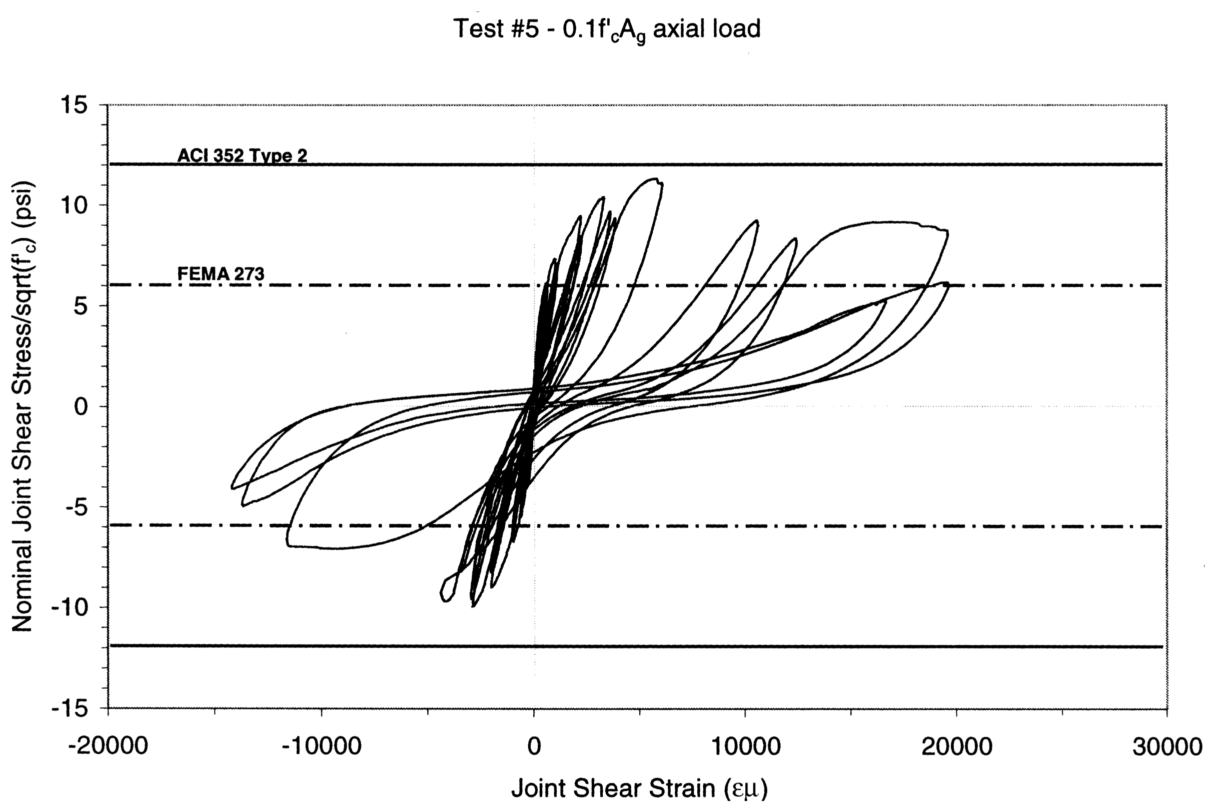


**Fig. 4.24 Unit 5: join stress versus joint shear strain**

### 4.2.6 Test Unit 6

The lateral load applied versus drift for unit 6 is shown in Figure 4.25. The upward direction resistance is similar to the downward, since the anchorage of the bottom beam bars was identical to that of the top bars in the joint, as shown in Figure 2.3. The maximum load in the upward direction occurred at a drift ratio of 3.00% and had a value of 44.4 kips; in the downward direction, the maximum load occurred at a drift of 2.00% and had a value of 43.1 kips. The ratio between the lateral load capacity in the two directions is thus equal to 1.03, which shows that the capacity in the upward and downward directions is almost the same.

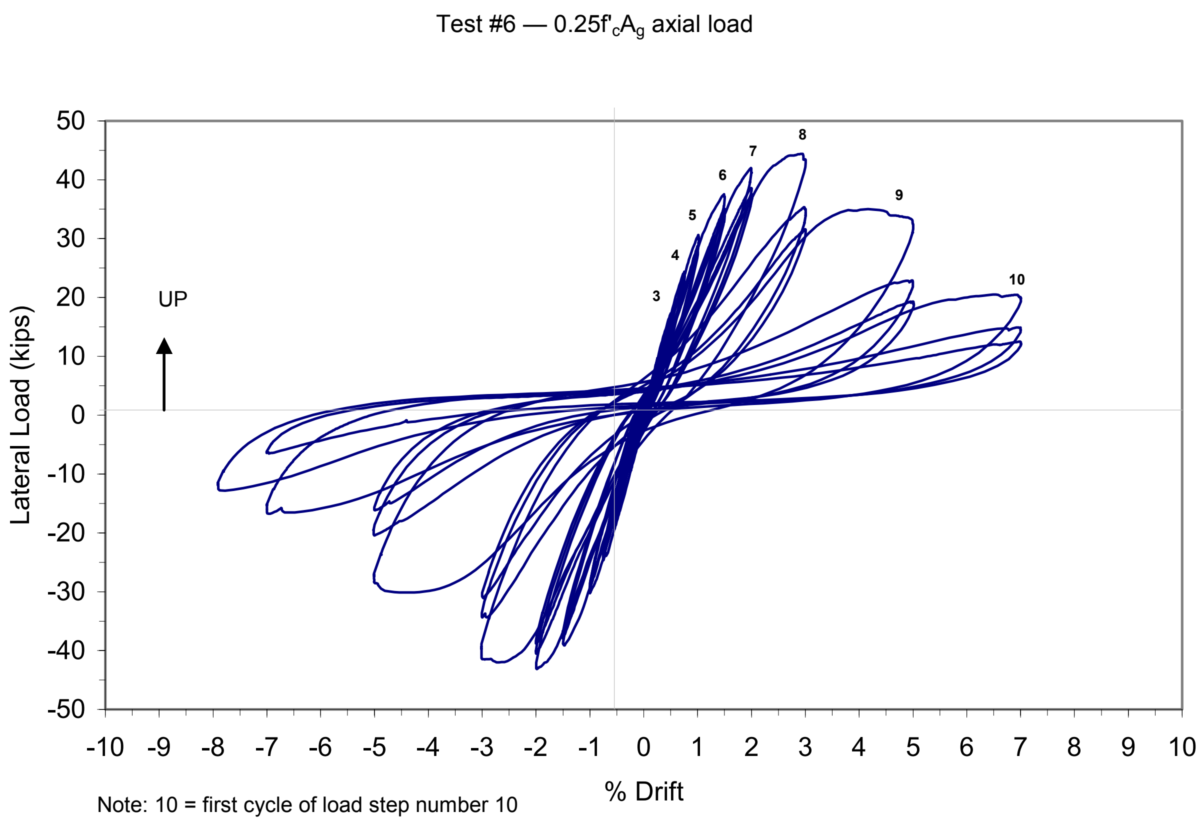


**Fig. 4.25 Unit 6: Lateral load versus drift ratio**

The flexural moment applied is compared to the theoretical moment capacity in Table 4.2 for all test units. Test unit 6 had an actual beam moment capacity of 87% of the theoretical in the upward direction and 84% in the downward direction. Figure 4.26 shows the moment-rotation and the moment-plastic-rotation curves. The plastic rotation at the peak moment in the upward direction was 0.010 radian, and at the peak moment in the downward direction was also 0.010 radian; the plastic rotation at 80% of the peak moment was 0.024 radian in the upward direction and 0.024 radian in the downward direction as well. Thus the upward and downward capacities and performance are very close.

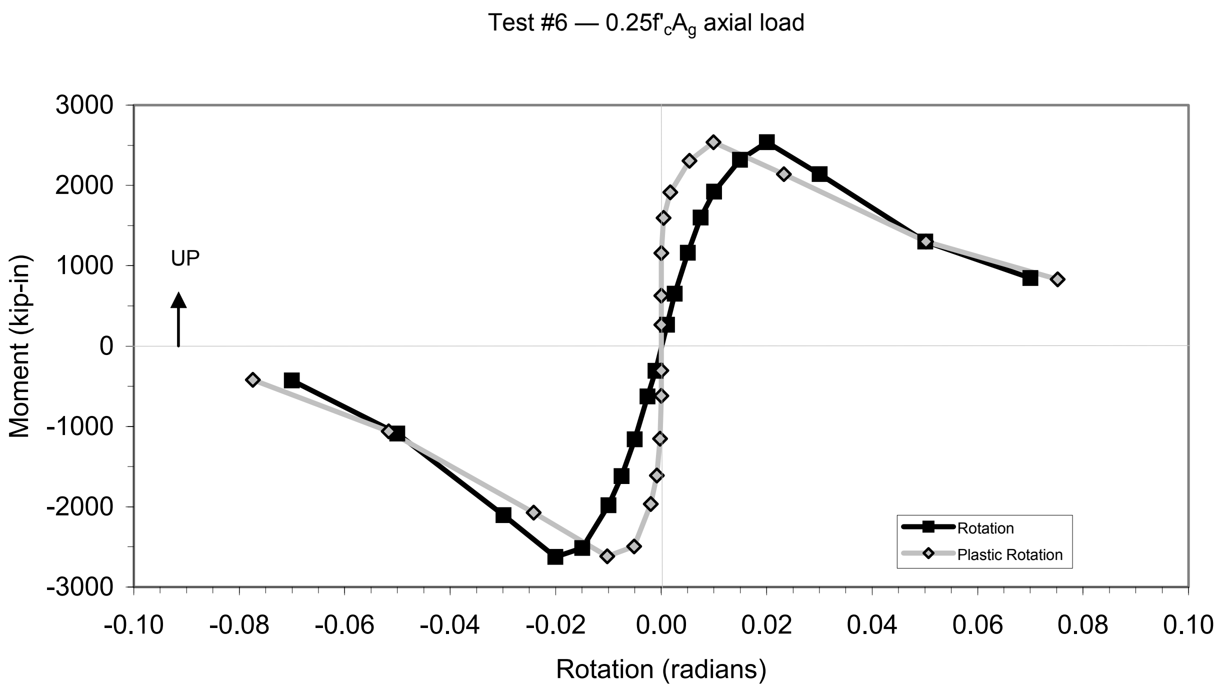


**Fig. 4.26 Unit 6: Moment-rotation and moment-plastic-rotation envelopes**

The column axial load for test unit 6 was set at a level of 0.25 $f'_cA_g$, which corresponds to a 294 kips compression load. Variations in the level of axial load were substantial as shown in Figure 4.27; the axial load varied in the range of 79% to 122%. The drop in axial load was 21%; unit 6 eventually lost its axial-load-carrying capacity. It is clear that the primary failure mode is joint shear.

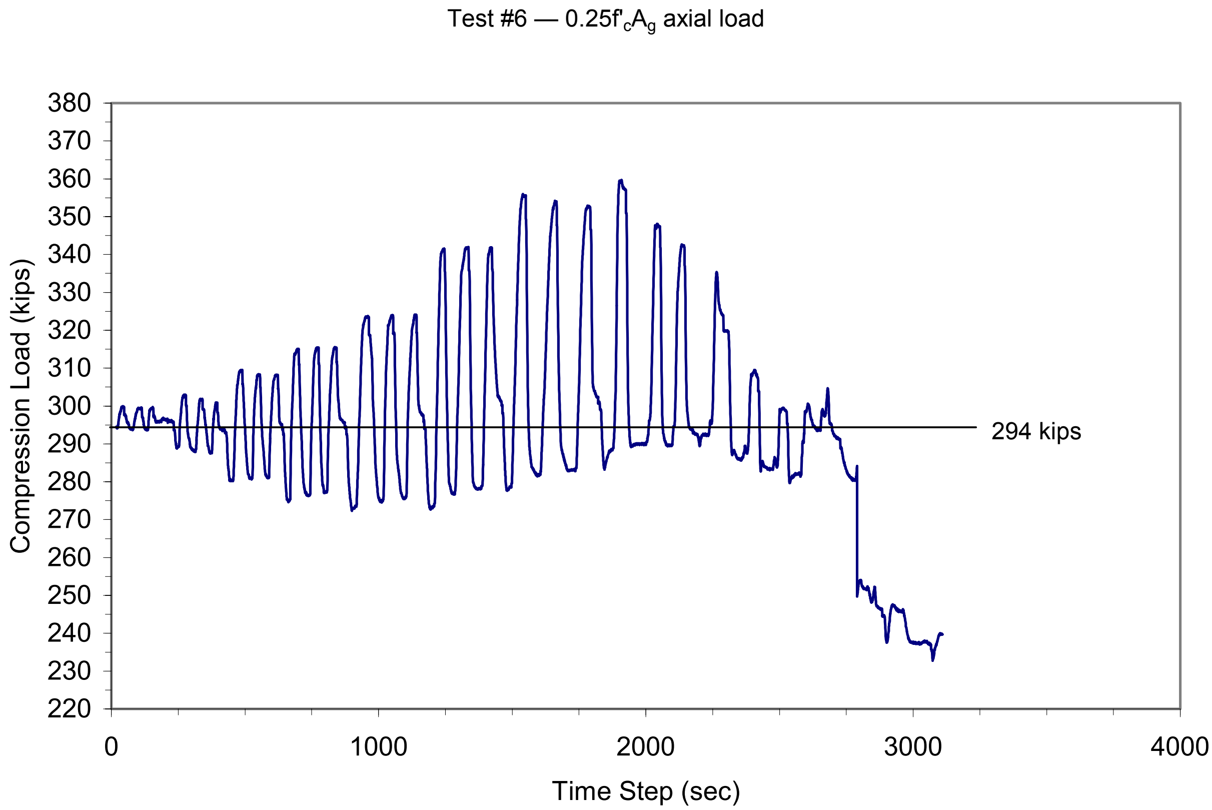


**Fig. 4.27 Unit 6: variation of axial compression column load**

The cumulative energy absorbed by test unit 6 is shown in Figure 4.28. The total energy absorbed was 597 kip-in. at a drift ratio of 7.6%, which was lower than that absorbed by unit 5; note also that the maximum drift reached was lower compared to unit 5 due to the higher axial load. At a drift ratio of 2.5%, at which the maximum load occurred on average for the upward and downward directions, the absorbed energy was 25% of the total energy absorbed, and at a drift ratio of 4.0% it was 50% of the total energy absorbed.

The joint shear stress versus joint shear strain for test unit 6 is shown in Figure 4.19. The maximum joint shear stress was 780 psi in the upward direction, which corresponds to a $\gamma$=11.5 (psi). The downward maximum joint shear stress was 759 psi with a corresponding $\gamma$=11.2 (psi). The joint shear strain at the maximum shear stress was 6270 $\mu\varepsilon$ in the upward direction and 6830 $\mu\varepsilon$ in the downward direction.

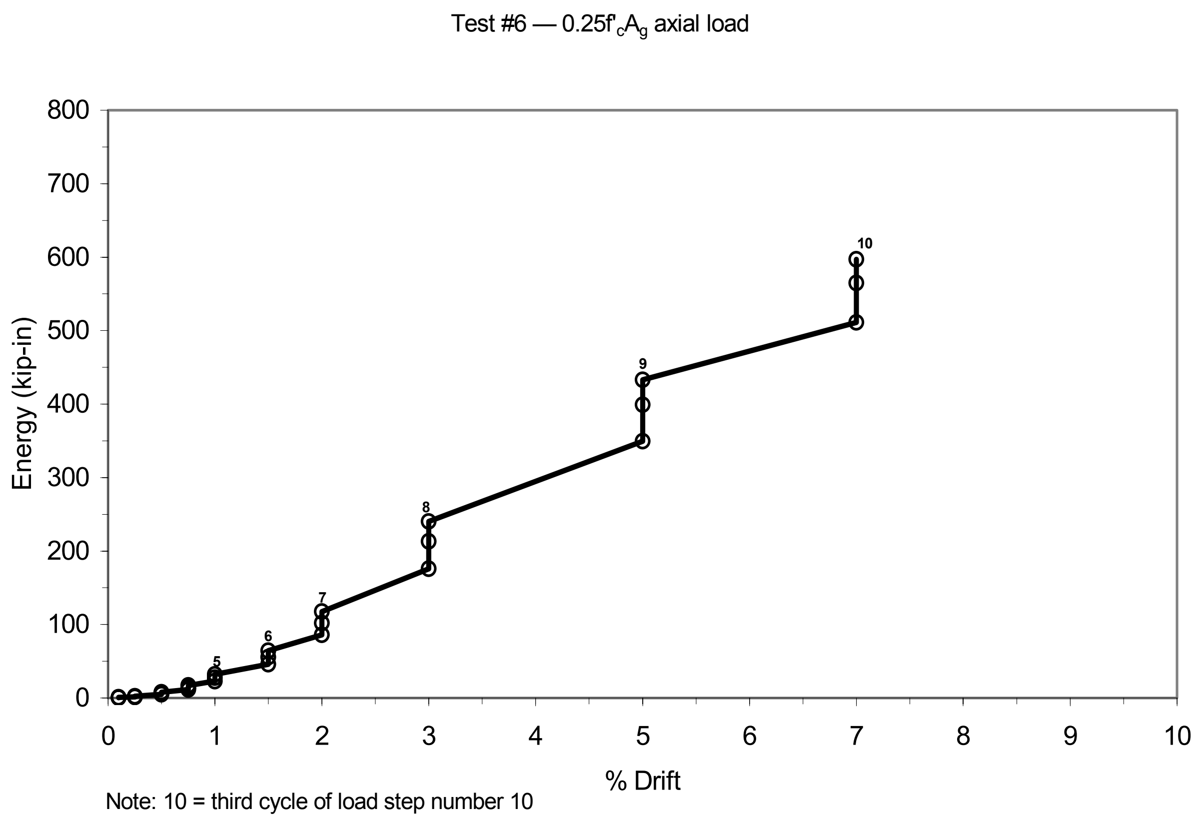


**Fig. 4.28 Unit 6: cumulative energy dissipation**

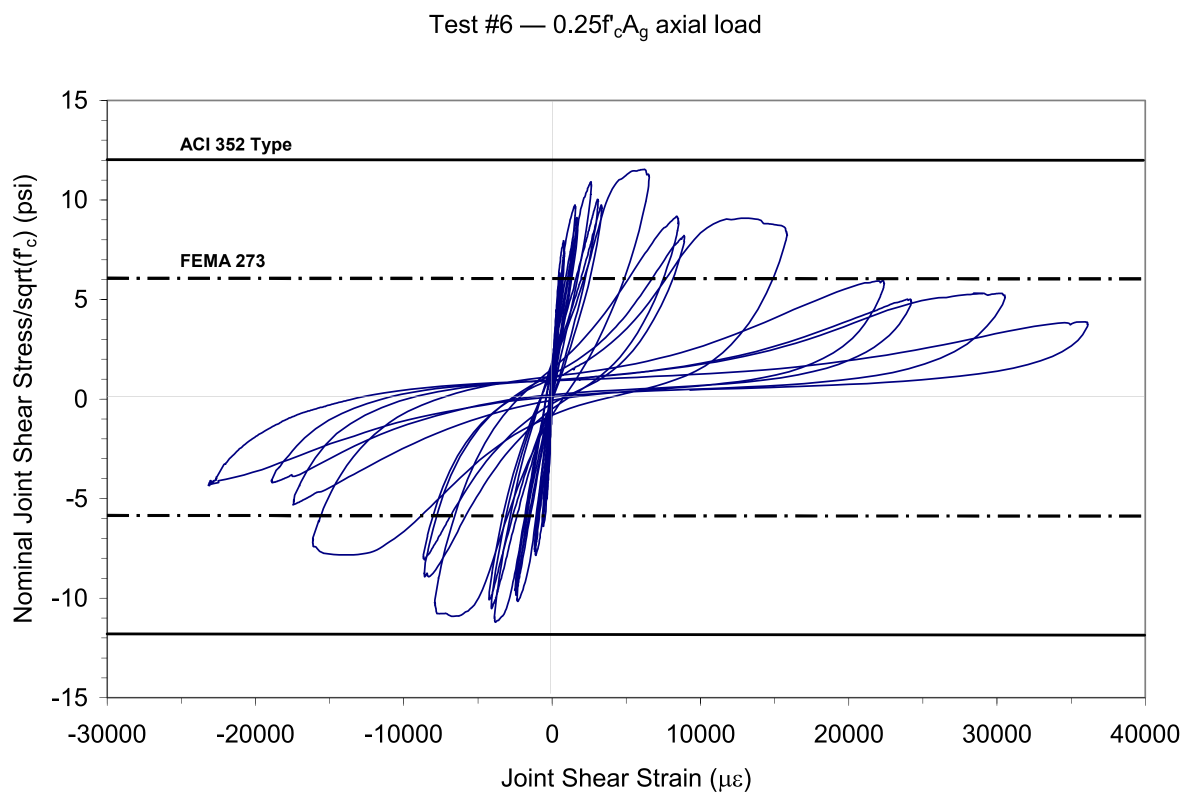


**Fig. 4.29 Unit 6: joint shear stress versus joint shear strain**

**Table 4.2 Theoretical and actual beam moment capacities**

| Test Unit | $\frac{P}{f_c^{'} A_g}$ | Theoretical Beam Moment Capacity (kip-in.) | Actual Moment Capacity —Upward (kip-in.) | Actual Moment Capacity ––Downward (kip-in.) |
|---|---|---|---|---|
| 1 | 0.10 | 3024 | 1229 | 2600 |
| 2 | 0.25 | 3024 | 1686 | 2508 |
| 3 | 0.10 | 3024 | 2508 | 2460 |
| 4 | 0.25 | 3024 | 2682 | 2826 |
| 5 | 0.10 | 3024 | 2622 | 2268 |
| 6 | 0.25 | 3024 | 2640 | 2550 |

# 5 Performance-Based Evaluation

## 5.1 DESCRIPTION OF PARAMETERS

Existing performance-based evaluation methods include the FEMA 273 (BSSC 1997) descriptions for buildings and the performance-based categories developed as part of the Pacific Earthquake Engineering Research Center (PEER). The PEER Bridge Performance Database was used as a guideline in evaluating the performance of the four exterior building joint specimens (Hose et al. 2000). A five-level performance evaluation was performed based on the analysis of a variety of parameters. These performance categories are well-suited for experimental evaluations such as the present study. In addition, for specific subassemblies, the parameters included in the performance categories can be expanded with relevant quantities. The parameters in the PEER database include drift, concrete and steel strains, principal stress states, displacement ductility, plastic rotation, residual deformation index, equivalent viscous damping ratio, and effective stiffness ratio. Explicit procedures on how to calculate these parameters are given by Hose et al. (2000). Several other parameters, in addition to those used for bridges, were evaluated for the six building joint units tested in this investigation. They included joint strength coefficient $\gamma$, cumulative dissipated energy, joint shear strain, lateral load, and crack width. The joint strength coefficient was calculated as follows:

$$\gamma = \frac{\tau_{xy}}{\sqrt{f'_c}} \tag{5.1}$$

where $\tau_{xy}$ = nominal joint shear stress and $f'_c$ = concrete compressive strength. The cumulative dissipated energy was determined as the area under the force-displacement hysteresis curves. The joint shear strain was calculated from experimental LVDT strain data using plane strain transformation. Lateral load was measured during the tests from the load cell attached between the hydraulic cylinder and the beam-loading collar. Crack widths were marked and visually measured during the tests. A peak value for each parameter was calculated or measured for each cycle of each load step with the exception of crack width, which was measured only at the end of each load step. These parameters were prepared for each test with the up and down loading directions considered separately. These results are presented in Tables 5.1 through 5.12. The values of the various parameters were used to delineate the five performance levels.

# Table 5.1 Test #1: Performance parameters ($0.1f'_cA_g$) up direction

| Load Step | Cycle | BEAM Steel Strain | COLN Steel Strain | BEAM Concrete Strain | COLN Concrete Strain | Crack Width in Joint | Lateral Load | Plastic Rotation | Principal Comp. Stress | Principal Tension Stress | Drift Ratio | Disp. Ductility Factor | Residual Deform. Index | Equiv. Visc Viscous Damping Ratio | Eff. Stiffness Ratio | Joint Strength Coeff. | Joint Shear Strain | Cumm. Energy |
|---|---|---|---|---|---|---|---|---|---|---|---|---|---|---|---|---|---|---|
| | | $\varepsilon_s$ | $\varepsilon_s$ | $\varepsilon_c$ | $\varepsilon_c$ | (in) | (kip) | $(\ )_p$ | $p_c$ (psi/f'$_c$) | $p_t$ (psi/√f'$_c$) | $\Delta$ (%) | $\mu_\Delta$ | RDI | $\xi_{eq}$ | $n_k$ | $\gamma$ | | (k-in) |
| | 1 | 4.63E-04 | 1.43E-04 | -2.80E-04 | -1.12E-04 | | 10.13 | 0.0000 | -0.012 | 7.814 | 0.10 | 0.498 | 0.00 | 0.084 | 1.25 | 2.5 | 1.77E-04 | 0.9 |
| 1 | 2 | 3.45E-04 | 8.59E-05 | -1.35E-04 | -1.27E-04 | | 6.07 | 0.0000 | -0.004 | 7.221 | 0.10 | 0.241 | 0.00 | 0.097 | 1.55 | 1.5 | 7.77E-05 | 1.2 |
| | 3 | 5.34E-04 | 8.45E-05 | -1.10E-04 | -1.35E-04 | 0.000 | 5.44 | 0.0000 | -0.003 | 7.048 | 0.10 | 0.223 | 0.00 | 0.108 | 1.50 | 1.4 | 7.65E-05 | 1.5 |
| | 4 | 5.65E-04 | 1.59E-04 | -3.32E-04 | -1.05E-04 | | 12.03 | 0.0000 | -0.016 | 8.131 | 0.25 | 0.564 | 0.00 | 0.048 | 1.31 | 3.0 | 1.84E-04 | 2.2 |
| 2 | 5 | 1.23E-03 | 4.74E-04 | -1.58E-03 | -3.22E-04 | | 17.12 | 0.0000 | -0.013 | 7.857 | 0.25 | 1.075 | 0.05 | 0.071 | 1.02 | 2.8 | 4.65E-04 | 5.0 |
| | 6 | 5.86E-04 | 2.79E-04 | -3.63E-04 | -2.16E-04 | 0.000 | 8.70 | 0.0000 | -0.009 | 7.481 | 0.25 | 0.524 | 0.03 | 0.063 | 1.02 | 2.2 | 1.61E-04 | 5.6 |
| | 7 | 9.74E-04 | 5.17E-04 | -1.22E-03 | -2.89E-04 | | 15.35 | 0.0000 | -0.024 | 8.767 | 0.50 | 1.007 | 0.07 | 0.069 | 0.93 | 3.8 | 3.85E-04 | 7.9 |
| 3 | 8 | 9.99E-04 | 5.50E-04 | -1.17E-03 | -3.01E-04 | | 15.00 | 0.0000 | -0.023 | 8.579 | 0.50 | 0.941 | 0.04 | 0.050 | 1.11 | 3.7 | 3.90E-04 | 9.7 |
| | 9 | 1.02E-03 | 6.14E-04 | -1.16E-03 | -2.95E-04 | Hairline | 15.33 | 0.0000 | -0.023 | 8.666 | 0.50 | 0.999 | 0.06 | 0.054 | 0.94 | 3.8 | 3.99E-04 | 11.5 |
| | 10 | 1.14E-03 | 9.15E-03 | -3.65E-03 | 1.58E-03 | | 18.36 | 0.0016 | -0.031 | 9.590 | 0.75 | 1.452 | 0.23 | 0.085 | 0.79 | 4.6 | 8.24E-04 | 16.3 |
| 4 | 11 | 1.00E-03 | 8.01E-04 | -5.32E-03 | -2.49E-04 | | 17.13 | 0.0023 | -0.028 | 9.330 | 0.75 | 1.471 | 0.19 | 0.062 | 0.73 | 4.3 | 8.25E-04 | 19.6 |
| | 12 | 9.91E-04 | 8.59E-04 | -5.91E-03 | -2.24E-04 | 0.003 | 16.79 | 0.0026 | -0.026 | 9.229 | 0.75 | 1.515 | 0.17 | 0.059 | 0.68 | 4.2 | 8.77E-04 | 22.9 |
| | 13 | 1.15E-03 | 1.43E-02 | -7.68E-03 | 2.69E-03 | | 19.58 | 0.0041 | -0.034 | 9.951 | 1.00 | 1.974 | 0.41 | 0.080 | 0.61 | 4.9 | 1.49E-03 | 29.6 |
| 5 | 14 | 1.10E-03 | 8.27E-03 | -7.02E-03 | -5.12E-04 | | 18.40 | 0.0048 | -0.030 | 9.763 | 1.00 | 2.003 | 0.43 | 0.075 | 0.57 | 4.6 | 1.66E-03 | 35.6 |
| | 15 | 1.08E-03 | 5.11E-03 | -6.54E-03 | -3.52E-04 | 0.008 | 18.08 | 0.0051 | -0.029 | 9.691 | 1.00 | 2.055 | 0.39 | 0.068 | 0.54 | 4.5 | 1.80E-03 | 41.1 |
| | 16 | 1.07E-02 | 1.41E-03 | -4.73E-03 | -3.31E-03 | | 20.74 | 0.0096 | -0.037 | 10.283 | 1.50 | 2.978 | 0.98 | 0.129 | 0.43 | 5.2 | 3.52E-03 | 58.2 |
| 6 | 17 | 1.57E-02 | 2.23E-03 | -2.04E-03 | -2.18E-03 | | 17.88 | 0.0110 | -0.030 | 9.662 | 1.50 | 3.067 | 1.03 | 0.106 | 0.36 | 4.5 | 4.27E-03 | 70.9 |
| | 18 | 1.39E-02 | 2.23E-03 | 1.37E-03 | -1.27E-03 | 0.008 | 16.46 | 0.0116 | -0.026 | 9.330 | 1.50 | 3.075 | 0.92 | 0.102 | 0.33 | 4.1 | 4.65E-03 | 82.1 |
| | 19 | 1.58E-02 | 1.57E-02 | 1.59E-03 | 1.70E-03 | | 18.32 | 0.0162 | -0.031 | 9.691 | 2.00 | 3.900 | 1.61 | 0.159 | 0.28 | 4.6 | 7.25E-03 | 107.4 |
| 7 | 20 | 1.58E-02 | 1.19E-02 | -3.30E-03 | -3.18E-05 | | 15.43 | 0.0173 | -0.024 | 8.940 | 2.00 | -- | 1.31 | 0.141 | 0.24 | 3.8 | 9.52E-03 | 126.2 |
| | 21 | 1.60E-02 | 1.50E-02 | -9.96E-03 | -2.97E-03 | 0.04 | 13.81 | 0.0175 | -0.020 | 8.521 | 2.00 | -- | 1.09 | 0.134 | 0.22 | 3.4 | 1.29E-02 | 142.0 |
| | 22 | 1.48E-02 | 1.54E-02 | -7.94E-04 | -9.31E-03 | | 14.58 | 0.0288 | -0.021 | 9.041 | 3.00 | -- | 3.08 | 0.268 | 0.15 | 3.6 | 2.27E-02 | 191.6 |
| 8 | 23 | 1.45E-02 | 1.24E-02 | -- | -- | | 10.42 | 0.0303 | -0.012 | 8.160 | 3.00 | -- | 1.74 | 0.220 | 0.11 | 2.6 | -- | 221.1 |
| | 24 | 1.59E-02 | 1.59E-02 | -- | -- | 0.08 | 8.83 | 0.0310 | -0.009 | 7.640 | 3.00 | -- | 1.13 | 0.194 | 0.09 | 2.2 | -- | 243.0 |
| | 25 | 1.13E-02 | 1.45E-02 | -- | -- | | 9.37 | 0.0560 | -0.010 | 8.059 | 5.00 | -- | -- | 0.350 | 0.06 | 2.3 | -- | 315.3 |
| 9 | 26 | 1.38E-02 | 1.55E-02 | -- | -- | | 7.12 | 0.0577 | -0.005 | 7.265 | 5.00 | -- | -- | 0.207 | 0.04 | 1.8 | -- | 348.8 |
| | 27 | 1.44E-02 | 9.21E-03 | -- | -- | 0.10 | 5.94 | 0.0549 | -0.004 | 6.831 | 5.00 | -- | -- | 0.181 | 0.04 | 1.5 | -- | 371.9 |
| | 28 | 1.57E-02 | 1.40E-02 | -- | -- | | 6.89 | 0.0778 | -0.006 | 7.554 | 7.00 | -- | -- | 0.247 | 0.03 | 1.7 | -- | 423.1 |
| 10 | 29 | 1.62E-02 | 1.39E-02 | -- | -- | | 5.63 | 0.0785 | -0.004 | 6.976 | 7.00 | -- | -- | 0.163 | 0.03 | 1.4 | -- | 451.1 |
| | 30 | 1.56E-02 | 1.55E-02 | -- | -- | 0.30 | 5.18 | 0.0784 | -0.004 | 6.918 | 7.00 | -- | -- | 0.144 | 0.02 | 1.3 | -- | 473.7 |
| | 31 | 1.52E-02 | 6.48E-03 | -- | -- | | 5.83 | 0.0994 | -0.004 | 7.525 | 8.82 | -- | -- | 0.183 | 0.02 | 1.5 | -- | 514.6 |
| 11 | 32 | 1.63E-02 | 1.24E-02 | -- | -- | | 4.87 | 0.0998 | -0.003 | 7.424 | 8.82 | -- | -- | 0.128 | 0.02 | 1.2 | -- | 538.4 |
| | 33 | 1.14E-02 | 1.21E-02 | -- | -- | 0.80 | 4.34 | 0.0998 | -0.002 | 7.265 | 8.82 | -- | -- | 0.117 | 0.02 | 1.1 | -- | 558.2 |

## Table 5.2 Test #1: Performance parameters ($0.1f'_cA_g$) down direction

| Load Step | Cycle | BEAM Steel Strain | COLN Steel Strain | BEAM Concrete Strain | COLN Concrete Strain | Crack Width in Joint | Lateral Load | Plastic Rotation | Principal Comp. Stress | Principal Tension Stress | Drift Ratio | Disp. Ductility Factor | Residual Deform. Index | Equiv. Visc Viscous Damping Ratio | Eff. Stiffness Ratio | Joint Strength Coeff. | Joint Shear Strain | Cumm. Energy |
|---|---|---|---|---|---|---|---|---|---|---|---|---|---|---|---|---|---|---|
| | | $\varepsilon_s$ | $\varepsilon_s$ | $\varepsilon_c$ | $\varepsilon_c$ | (in) | (kip) | $(\ )_p$ | $p_c$ (psi/f'$_c$) | $p_t$ (psi/$\sqrt{f'_c}$) | $\Delta$ (%) | $\mu_\Delta$ | RDI | $\xi_{eq}$ | $n_k$ | $\gamma$ | | (k-in) |
| 1 | 1 | 3.69E-04 | 9.93E-05 | -7.85E-05 | -1.54E-04 | | 8.61 | 0.0000 | -0.009 | 7.294 | 0.10 | 0.191 | 0.03 | 0.150 | 1.32 | 2.1 | 1.24E-04 | 0.9 |
| | 2 | 5.17E-04 | 9.36E-05 | -1.83E-05 | -1.44E-04 | | 7.37 | 0.0000 | -0.007 | 7.120 | 0.10 | 0.201 | 0.05 | 0.056 | 1.08 | 1.8 | 1.42E-04 | 1.2 |
| | 3 | 5.98E-04 | 1.04E-04 | -7.52E-05 | -1.59E-04 | 0.000 | 8.19 | 0.0000 | -0.008 | 7.221 | 0.10 | 0.217 | 0.07 | 0.043 | 1.11 | 2.0 | 1.21E-04 | 1.5 |
| 2 | 4 | 7.61E-04 | 2.01E-04 | -7.23E-05 | -2.44E-04 | | 13.52 | 0.0000 | -0.021 | 7.958 | 0.25 | 0.343 | 0.04 | 0.041 | 1.16 | 3.4 | 2.22E-04 | 2.2 |
| | 5 | 8.08E-04 | 1.70E-04 | -5.14E-05 | -3.27E-04 | | 13.82 | 0.0000 | -0.018 | 7.698 | 0.25 | 0.316 | 0.05 | 0.168 | 1.28 | 3.1 | 2.43E-04 | 5.0 |
| | 6 | 6.70E-04 | 1.56E-04 | -5.94E-05 | -2.78E-04 | 0.000 | 12.75 | 0.0000 | -0.019 | 7.684 | 0.25 | 0.325 | 0.04 | 0.041 | 1.15 | 3.2 | 2.08E-04 | 5.6 |
| 3 | 7 | 1.35E-03 | 3.72E-04 | -2.43E-04 | -4.90E-04 | | 23.25 | 0.0000 | -0.050 | 9.677 | 0.50 | 0.634 | 0.10 | 0.042 | 1.08 | 5.8 | 4.55E-04 | 7.9 |
| | 8 | 1.32E-03 | 3.63E-04 | -1.89E-04 | -5.26E-04 | | 22.89 | 0.0000 | -0.049 | 9.576 | 0.50 | 0.640 | 0.08 | 0.031 | 1.05 | 5.7 | 4.68E-04 | 9.7 |
| | 9 | 1.28E-03 | 3.79E-04 | -2.20E-04 | -5.41E-04 | Hairline | 22.57 | 0.0001 | -0.047 | 9.503 | 0.50 | 0.634 | 0.06 | 0.033 | 1.04 | 5.6 | 4.69E-04 | 11.5 |
| 4 | 10 | 1.83E-03 | 6.85E-04 | -2.05E-03 | -8.08E-04 | | 30.21 | 0.0006 | -0.072 | 11.338 | 0.75 | 0.897 | 0.05 | 0.048 | 0.99 | 7.5 | 8.20E-04 | 16.3 |
| | 11 | 1.75E-03 | 6.69E-04 | -9.77E-04 | -1.08E-03 | | 28.87 | 0.0007 | -0.067 | 11.107 | 0.75 | 0.880 | 0.07 | 0.035 | 0.97 | 7.2 | 8.00E-04 | 19.6 |
| | 12 | 1.70E-03 | 6.75E-04 | -1.13E-03 | -1.33E-03 | 0.003 | 28.79 | 0.0006 | -0.067 | 11.005 | 0.75 | 0.871 | 0.04 | 0.035 | 0.97 | 7.2 | 8.05E-04 | 22.9 |
| 5 | 13 | 1.24E-02 | 3.87E-03 | 3.63E-04 | -4.49E-03 | | 35.31 | 0.0014 | -0.088 | 12.681 | 1.00 | 1.141 | 0.06 | 0.044 | 0.91 | 8.8 | 1.12E-03 | 29.6 |
| | 14 | 1.15E-02 | 1.04E-02 | -1.06E-04 | -2.58E-03 | | 34.66 | 0.0016 | -0.086 | 12.421 | 1.00 | 1.144 | 0.04 | 0.040 | 0.89 | 8.6 | 1.12E-03 | 35.6 |
| | 15 | 1.04E-02 | 4.34E-03 | -4.84E-04 | -3.20E-03 | 0.008 | 34.04 | 0.0019 | -0.084 | 12.305 | 1.00 | 1.153 | 0.01 | 0.037 | 0.87 | 8.5 | 1.15E-03 | 41.1 |
| 6 | 16 | 1.49E-02 | 1.14E-02 | -2.30E-04 | -2.26E-03 | | 43.79 | 0.0042 | -0.116 | 14.862 | 1.50 | 1.699 | 0.11 | 0.061 | 0.76 | 10.9 | 1.96E-03 | 58.2 |
| | 17 | 1.15E-02 | 3.19E-03 | -9.13E-04 | -1.37E-03 | | 40.62 | 0.0048 | -0.105 | 14.111 | 1.50 | 1.673 | 0.09 | 0.049 | 0.71 | 10.1 | 1.73E-03 | 70.9 |
| | 18 | 1.33E-02 | 3.23E-03 | -1.53E-02 | -8.33E-04 | 0.008 | 38.90 | 0.0051 | -0.099 | 13.692 | 1.50 | 1.661 | 0.09 | 0.046 | 0.69 | 9.7 | 1.16E-03 | 82.1 |
| 7 | 19 | 1.12E-02 | 1.17E-02 | -1.45E-02 | -1.46E-03 | | 43.21 | 0.0090 | -0.113 | 14.717 | 2.00 | 2.220 | 0.29 | 0.071 | 0.58 | 10.7 | -- | 107.4 |
| | 20 | 3.06E-03 | 1.60E-02 | -2.62E-03 | -- | | 38.49 | 0.0100 | -0.097 | 13.547 | 2.00 | 2.200 | 0.33 | 0.059 | 0.51 | 9.6 | -- | 126.2 |
| | 21 | 1.24E-02 | 1.58E-02 | -- | -- | 0.04 | 35.88 | 0.0108 | -0.090 | 12.825 | 2.00 | 2.225 | 0.34 | 0.053 | 0.48 | 8.9 | -- | 142.0 |
| 8 | 22 | 1.52E-02 | 1.46E-02 | -- | -- | | 38.39 | 0.0194 | -0.097 | 13.677 | 3.00 | 2.400 | 1.04 | 0.106 | 0.35 | 9.6 | -- | 191.6 |
| | 23 | 1.45E-02 | 1.42E-02 | -- | -- | | 30.83 | 0.0215 | -0.072 | 11.915 | 3.00 | -- | 1.10 | 0.077 | 0.27 | 7.7 | -- | 221.1 |
| | 24 | 1.36E-02 | 1.55E-02 | -- | -- | 0.08 | 26.53 | 0.0225 | -0.058 | 10.789 | 3.00 | -- | 1.22 | 0.067 | 0.24 | 6.6 | -- | 243.0 |
| 9 | 25 | 1.24E-02 | 1.34E-02 | -- | -- | | 28.91 | 0.0402 | -0.065 | 11.496 | 5.00 | -- | -- | 0.126 | 0.16 | 7.2 | -- | 315.3 |
| | 26 | 1.26E-02 | 9.17E-03 | -- | -- | | 20.28 | 0.0428 | -0.039 | 9.113 | 5.00 | -- | -- | 0.082 | 0.11 | 5.1 | -- | 348.8 |
| | 27 | 1.23E-02 | 4.72E-03 | -- | -- | 0.10 | 16.11 | 0.0430 | -0.028 | 8.059 | 5.00 | -- | -- | 0.072 | 0.09 | 4.0 | -- | 371.9 |
| 10 | 28 | 1.48E-02 | 1.19E-02 | -- | -- | | 19.89 | 0.0609 | -0.040 | 8.868 | 7.00 | -- | -- | 0.092 | 0.08 | 5.0 | -- | 423.1 |
| | 29 | 1.31E-02 | 1.61E-02 | -- | -- | | 13.56 | 0.0623 | -0.022 | 7.424 | 7.00 | -- | -- | 0.074 | 0.05 | 3.4 | -- | 451.1 |
| | 30 | 9.16E-03 | 1.58E-02 | -- | -- | 0.30 | 10.80 | 0.0633 | -0.015 | 7.077 | 7.00 | -- | -- | 0.074 | 0.04 | 2.7 | -- | 473.7 |
| 11 | 31 | 1.21E-02 | 1.39E-02 | -- | -- | | 13.67 | 0.0793 | -0.022 | 7.380 | 8.82 | -- | -- | 0.085 | 0.04 | 3.4 | -- | 514.6 |
| | 32 | 7.49E-03 | 1.44E-02 | -- | -- | | 8.92 | 0.0802 | -0.010 | 6.499 | 8.82 | -- | -- | 0.077 | 0.03 | 2.2 | -- | 538.4 |
| | 33 | 1.56E-02 | 1.34E-02 | -- | -- | 0.80 | 6.63 | 0.0801 | -0.006 | 6.701 | 8.82 | -- | -- | 0.085 | 0.02 | 1.7 | -- | 558.2 |

## Table 5.3 Test #2: Performance parameters ($0.25f'_cA_g$) up direction

| Load Step | Cycle | BEAM Steel Strain | COLN Steel Strain | BEAM Concrete Strain | COLN Concrete Strain | Crack Width in Joint | Lateral Load | Plastic Rotation | Principal Comp. Stress | Principal Tension Stress | Drift Ratio | Disp. Ductility Factor | Residual Deform. Index | Equiv. Visc Viscous Damping Ratio | Eff. Stiffness Ratio | Joint Strength Coeff. | Joint Shear Strain | Cumm. Energy |
|---|---|---|---|---|---|---|---|---|---|---|---|---|---|---|---|---|---|---|
| | | $\varepsilon_s$ | $\varepsilon_s$ | $\varepsilon_c$ | $\varepsilon_c$ | (in) | (kip) | $(\ )_p$ | $p_c$ (psi/f'$_c$) | $p_t$ (psi/√f'$_c$) | Δ (%) | $\mu_\Delta$ | RDI | $\xi_{eq}$ | $n_k$ | $\gamma$ | | (k-in) |
| 1 | 1 | 1.71E-04 | 6.17E-05 | -9.89E-05 | -2.37E-05 | | 4.75 | 0.0000 | -0.001 | 18.803 | 0.10 | 0.190 | 0.00 | 0.0324 | 1.07 | 1.2 | -- | 0.1 |
| | 2 | 1.18E-04 | 5.41E-05 | -4.21E-05 | -9.99E-05 | | 4.14 | 0.0000 | -0.001 | 18.833 | 0.10 | 0.174 | 0.00 | 0.1008 | 0.99 | 1.0 | -- | 0.3 |
| | 3 | 3.16E-04 | 5.98E-05 | -1.56E-04 | -1.57E-04 | 0.000 | 5.20 | 0.0000 | -0.001 | 18.894 | 0.10 | 0.190 | 0.00 | 0.1593 | 1.16 | 1.3 | -- | 0.7 |
| 2 | 4 | 3.95E-04 | 1.86E-04 | -6.18E-04 | -1.45E-04 | | 11.31 | 0.0000 | -0.007 | 19.378 | 0.25 | 0.436 | 0.00 | 0.0586 | 1.09 | 2.8 | -- | 1.4 |
| | 5 | 4.28E-04 | 2.25E-04 | -1.05E-03 | -1.52E-04 | | 13.25 | 0.0000 | -0.009 | 19.619 | 0.25 | 0.523 | 0.00 | 0.0357 | 1.09 | 3.3 | -- | 2.0 |
| | 6 | 4.77E-04 | 2.00E-04 | -9.95E-04 | -1.71E-04 | 0.000 | 11.31 | 0.0000 | -0.007 | 19.483 | 0.25 | 0.445 | 0.00 | 0.0414 | 1.09 | 2.8 | -- | 2.5 |
| 3 | 7 | 5.94E-04 | 3.98E-04 | -6.66E-03 | -1.06E-04 | | 19.20 | 0.0000 | -0.018 | 20.375 | 0.50 | 0.854 | 0.00 | 0.0528 | 0.98 | 4.7 | -- | 4.7 |
| | 8 | 6.55E-03 | 4.06E-04 | -6.46E-03 | -1.18E-04 | | 18.88 | 0.0000 | -0.018 | 20.496 | 0.50 | 0.848 | 0.00 | 0.0407 | 0.96 | 4.7 | -- | 6.3 |
| | 9 | 2.33E-03 | 4.15E-04 | -7.12E-03 | -1.37E-04 | 0.000 | 18.63 | 0.0000 | -0.017 | 20.481 | 0.50 | 0.854 | 0.00 | 0.0323 | 0.94 | 4.6 | -- | 7.6 |
| 4 | 10 | 2.60E-03 | 6.98E-04 | -6.72E-03 | -9.31E-04 | | 24.42 | 0.0006 | -0.029 | 21.358 | 0.75 | 1.277 | 0.07 | 0.0586 | 0.82 | 6.1 | -- | 12.2 |
| | 11 | 2.85E-03 | 5.55E-04 | -1.01E-02 | -1.59E-03 | | 23.50 | 0.0010 | -0.027 | 21.312 | 0.75 | 1.302 | 0.03 | 0.0427 | 0.78 | 5.9 | -- | 15.4 |
| | 12 | 1.15E-02 | 5.40E-04 | -1.54E-02 | -2.08E-03 | 0.000 | 22.89 | 0.0013 | -0.025 | 21.252 | 0.75 | 1.321 | 0.03 | 0.0387 | 0.75 | 5.7 | -- | 18.3 |
| 5 | 13 | 3.69E-03 | 8.62E-04 | -1.01E-02 | -5.94E-03 | | 26.21 | 0.0028 | -0.032 | 21.826 | 1.00 | 1.729 | 0.15 | 0.0622 | 0.66 | 6.5 | -- | 25.3 |
| | 14 | 3.10E-03 | 9.24E-04 | -8.86E-03 | -6.54E-03 | | 24.56 | 0.0033 | -0.029 | 21.675 | 1.00 | 1.752 | 0.11 | 0.0526 | 0.60 | 6.1 | -- | 31.0 |
| | 15 | 3.01E-03 | 8.81E-04 | -8.36E-03 | -6.50E-03 | Hairline | 23.32 | 0.0035 | -0.026 | 21.509 | 1.00 | 1.718 | 0.05 | 0.0483 | 0.59 | 5.8 | -- | 35.8 |
| 6 | 16 | 1.32E-02 | 2.02E-03 | -6.61E-03 | -7.92E-03 | | 28.28 | 0.0069 | -0.037 | 22.416 | 1.50 | 2.538 | 0.48 | 0.1024 | 0.48 | 7.0 | -- | 54.1 |
| | 17 | 4.18E-03 | 1.35E-03 | -5.94E-03 | -7.11E-03 | | 25.37 | 0.0084 | -0.030 | 22.083 | 1.50 | 2.641 | 0.39 | 0.0798 | 0.42 | 6.3 | -- | 67.3 |
| | 18 | 8.48E-03 | 1.51E-03 | -3.85E-03 | -5.15E-03 | 0.01 | 22.69 | 0.0085 | -0.024 | 21.690 | 1.50 | 2.547 | 0.33 | 0.0742 | 0.38 | 5.7 | -- | 78.0 |
| 7 | 19 | 1.35E-02 | 2.42E-03 | -2.52E-03 | -4.30E-03 | | 25.47 | 0.0128 | -0.030 | 21.418 | 2.00 | 2.900 | 0.84 | 0.1366 | 0.32 | 6.3 | -- | 107.6 |
| | 20 | 5.04E-03 | 4.00E-03 | -3.27E-03 | -2.49E-03 | | 20.61 | 0.0143 | -0.020 | 21.463 | 2.00 | -- | 0.69 | 0.1279 | 0.26 | 5.1 | -- | 130.3 |
| | 21 | 5.00E-03 | 1.03E-02 | -2.59E-03 | -1.85E-04 | 0.20 | 18.12 | 0.0153 | -0.016 | 20.995 | 2.00 | -- | 0.56 | 0.1259 | 0.23 | 4.5 | -- | 149.7 |
| 8 | 22 | 1.34E-02 | 1.62E-02 | -6.47E-04 | -1.02E-02 | | 17.91 | 0.0251 | -0.016 | 20.995 | 3.00 | -- | 1.45 | 0.2280 | 0.15 | 4.5 | -- | 202.2 |
| | 23 | 1.01E-02 | 8.04E-03 | -2.66E-04 | -1.20E-02 | | 13.76 | 0.0263 | -0.009 | 20.300 | 3.00 | -- | -- | 0.1697 | 0.12 | 3.4 | -- | 232.1 |
| | 24 | 9.37E-03 | 1.13E-02 | -1.91E-04 | -- | 0.10 | 12.18 | 0.0266 | -0.008 | 20.058 | 3.00 | -- | -- | 0.1405 | 0.10 | 3.0 | -- | 254.0 |
| 9 | 25 | 1.32E-02 | 1.39E-02 | 4.67E-04 | -- | | 13.78 | 0.0463 | -0.009 | 21.539 | 5.00 | -- | -- | 0.2381 | 0.07 | 3.4 | -- | 324.3 |
| | 26 | 9.98E-03 | 8.73E-03 | -1.41E-03 | -- | | 10.74 | 0.0472 | -0.005 | 20.798 | 5.00 | -- | -- | 0.1435 | 0.05 | 2.7 | -- | 357.3 |
| | 27 | 7.53E-03 | 1.14E-02 | -1.04E-03 | -- | > 0.10 | 9.62 | 0.0479 | -0.004 | 20.602 | 5.00 | -- | -- | 0.1205 | 0.05 | 2.4 | -- | 382.3 |
| 10 | 28 | 5.61E-03 | 1.43E-02 | -8.69E-04 | -- | | 10.04 | 0.0682 | -0.005 | 20.677 | 7.00 | -- | -- | 0.1679 | 0.03 | 2.5 | -- | 432.3 |
| | 29 | 4.69E-03 | 1.01E-02 | -7.84E-04 | -- | | 8.30 | 0.0685 | -0.003 | 20.239 | 7.00 | -- | -- | 0.1113 | 0.03 | 2.1 | -- | 460.2 |
| | 30 | 4.51E-03 | 1.49E-02 | -6.23E-04 | -- | > 0.10 | 7.51 | 0.0689 | -0.003 | 20.012 | 7.00 | -- | -- | 0.0986 | 0.03 | 1.9 | -- | 482.3 |
| 11 | 31 | 4.76E-03 | 7.85E-03 | -3.54E-04 | -- | | 7.61 | 0.0864 | -0.003 | 20.043 | 8.82 | -- | -- | 0.1300 | 0.02 | 1.9 | -- | 519.7 |
| | 32 | 4.27E-03 | 8.00E-03 | -4.13E-04 | -- | | 6.11 | 0.0868 | -0.002 | 19.499 | 8.82 | -- | -- | 0.0952 | 0.02 | 1.5 | -- | 541.5 |
| | 33 | 3.90E-03 | 7.93E-03 | -2.53E-04 | -- | > 0.10 | 5.63 | 0.0871 | -0.002 | 19.242 | 8.82 | -- | -- | 0.0988 | 0.02 | 1.4 | -- | 562.5 |

## Table 5.4 Test #2: Performance parameters ($0.25f'_cA_g$) down direction

| Load Step | Cycle | BEAM Steel Strain | COLN Steel Strain | BEAM Concrete Strain | COLN Concrete Strain | Crack Width in Joint | Lateral Load | Plastic Rotation | Principal Comp. Stress | Principal Tension Stress | Drift Ratio | Disp. Ductility Factor | Residual Deform. Index | Equiv. Visc Viscous Damping Ratio | Eff. Stiffness Ratio | Joint Strength Coeff. | Joint Shear Strain | Cumm. Energy |
|---|---|---|---|---|---|---|---|---|---|---|---|---|---|---|---|---|---|---|
| | | $\varepsilon_\sigma$ | $\varepsilon_s$ | $\varepsilon_c$ | $\varepsilon_c$ | (in) | (kip) | $(\ )_p$ | $p_c$ (psi/f'$_c$) | $p_t$ (psi/√f'$_c$) | Δ (%) | $\mu_\Delta$ | RDI | $\xi_{eq}$ | $n_k$ | $\gamma$ | | (k-in) |
| 1 | 1 | 1.39E-04 | 4.51E-05 | -4.83E-05 | -9.39E-05 | | 5.41 | -- | -0.002 | 18.758 | 0.10 | 0.102 | 0.01 | 0.032 | 1.47 | 1.3 | -- | 0.1 |
| | 2 | 3.22E-04 | 4.98E-05 | -1.54E-04 | -1.55E-04 | | 7.36 | -- | -0.003 | 18.954 | 0.10 | 0.132 | 0.01 | 0.046 | 1.54 | 1.8 | -- | 0.3 |
| | 3 | 6.71E-04 | 7.87E-05 | -5.53E-04 | -2.28E-04 | 0.000 | 10.50 | -- | -0.006 | 19.196 | 0.10 | 0.236 | 0.05 | 0.038 | 1.24 | 2.6 | -- | 0.7 |
| 2 | 4 | 8.17E-04 | 9.34E-05 | -8.05E-04 | -2.44E-04 | | 11.85 | -- | -0.008 | 19.302 | 0.25 | 0.263 | 0.04 | 0.057 | 1.24 | 3.0 | -- | 1.4 |
| | 5 | 8.54E-04 | 8.92E-05 | -8.07E-04 | -2.58E-04 | | 11.33 | -- | -0.007 | 19.332 | 0.25 | 0.260 | 0.03 | 0.051 | 1.24 | 2.8 | -- | 2.0 |
| | 6 | 8.81E-04 | 2.18E-04 | -1.14E-03 | -2.27E-04 | 0.000 | 11.04 | -- | -0.006 | 19.302 | 0.25 | 0.256 | 0.01 | 0.045 | 1.22 | 2.7 | -- | 2.5 |
| 3 | 7 | 4.01E-03 | 1.45E-04 | -1.39E-03 | -6.40E-04 | | 20.71 | 0.0002 | -0.021 | 20.496 | 0.50 | 0.523 | 0.06 | 0.047 | 1.09 | 5.1 | -- | 4.7 |
| | 8 | 4.81E-03 | 1.38E-04 | -8.22E-04 | -7.16E-04 | | 21.04 | 0.0002 | -0.022 | 20.602 | 0.50 | 0.531 | 0.06 | 0.023 | 0.72 | 5.2 | -- | 6.3 |
| | 9 | 4.74E-03 | 1.32E-04 | -7.02E-04 | -7.33E-04 | 0.000 | 19.84 | 0.0003 | -0.020 | 20.496 | 0.50 | 0.516 | 0.06 | 0.030 | 1.07 | 4.9 | -- | 7.6 |
| 4 | 10 | 1.28E-02 | 2.97E-04 | -2.56E-03 | -1.28E-03 | | 28.34 | 0.0006 | -0.038 | 21.796 | 0.75 | 0.756 | 0.09 | 0.050 | 1.02 | 7.1 | -- | 12.2 |
| | 11 | 1.43E-02 | 2.97E-04 | -4.21E-03 | -1.32E-03 | | 27.72 | 0.0009 | -0.036 | 21.766 | 0.75 | 0.775 | 0.09 | 0.036 | 1.00 | 6.9 | -- | 15.4 |
| | 12 | 5.39E-03 | 3.11E-04 | -6.43E-03 | -1.35E-03 | 0.000 | 27.30 | 0.0009 | -0.035 | 21.675 | 0.75 | 0.763 | 0.10 | 0.033 | 0.98 | 6.8 | -- | 18.3 |
| 5 | 13 | 6.78E-03 | 4.16E-04 | -5.79E-03 | -3.26E-03 | | 34.19 | 0.0016 | -0.052 | 23.005 | 1.00 | 1.013 | 0.11 | 0.048 | 0.94 | 8.5 | -- | 25.3 |
| | 14 | 7.08E-03 | 5.54E-04 | -5.27E-03 | -3.49E-03 | | 33.70 | 0.0019 | -0.051 | 22.990 | 1.00 | 1.017 | 0.11 | 0.039 | 0.91 | 8.4 | -- | 31.0 |
| | 15 | 7.23E-03 | 6.39E-04 | -2.49E-03 | -3.43E-03 | Hairline | 33.22 | 0.0020 | -0.050 | 22.899 | 1.00 | 1.024 | 0.10 | 0.034 | 0.89 | 8.3 | -- | 35.8 |
| 6 | 16 | 9.87E-03 | 8.31E-04 | -3.30E-03 | -1.03E-02 | | 42.70 | 0.0048 | -0.075 | 25.076 | 1.50 | 1.541 | 0.20 | 0.066 | 0.77 | 10.6 | -- | 54.1 |
| | 17 | 1.14E-02 | 2.88E-03 | -3.17E-03 | -9.93E-03 | | 40.06 | 0.0054 | -0.067 | 24.592 | 1.50 | 1.540 | 0.16 | 0.052 | 0.73 | 10.0 | -- | 67.3 |
| | 18 | 1.47E-02 | 3.00E-03 | -2.11E-03 | -8.77E-03 | 0.01 | 38.82 | 0.0057 | -0.064 | 24.426 | 1.50 | 1.540 | 0.15 | 0.043 | 0.70 | 9.7 | -- | 78.0 |
| 7 | 19 | 1.15E-02 | 5.44E-03 | -1.01E-03 | -4.53E-03 | | 41.19 | 0.0102 | -0.069 | 25.197 | 2.00 | 1.700 | 0.36 | 0.084 | 0.56 | 10.3 | -- | 107.6 |
| | 20 | 1.07E-02 | 5.91E-03 | -9.01E-04 | -2.68E-03 | | 35.14 | 0.0116 | -0.053 | 23.988 | 2.00 | -- | 0.45 | 0.075 | 0.48 | 8.7 | -- | 130.3 |
| | 21 | 1.04E-02 | 9.22E-03 | -1.13E-03 | -1.64E-03 | 0.20 | 32.09 | 0.0124 | -0.045 | 23.428 | 2.00 | -- | 0.48 | 0.070 | 0.43 | 8.0 | -- | 149.7 |
| 8 | 22 | 1.54E-02 | 9.10E-03 | -1.84E-04 | -9.30E-03 | | 32.14 | 0.0223 | -0.045 | 23.534 | 3.00 | -- | 1.35 | 0.130 | 0.30 | 8.0 | -- | 202.2 |
| | 23 | 1.35E-02 | 1.31E-02 | 4.08E-04 | -8.75E-04 | | 24.79 | 0.0242 | -0.028 | 22.174 | 3.00 | -- | -- | 0.094 | 0.22 | 6.1 | -- | 232.1 |
| | 24 | 1.25E-02 | 1.06E-02 | 5.94E-04 | -1.02E-03 | 0.10 | 21.75 | 0.0250 | -0.024 | 20.693 | 3.00 | -- | -- | 0.078 | 0.20 | 5.4 | -- | 254.0 |
| 9 | 25 | 1.33E-02 | 1.58E-02 | -2.95E-03 | -4.92E-04 | | 22.34 | 0.0449 | -0.024 | 20.783 | 5.00 | -- | -- | 0.150 | 0.12 | 5.5 | -- | 324.3 |
| | 26 | 1.08E-02 | 1.50E-02 | -1.16E-03 | -6.73E-03 | | 15.54 | 0.0463 | -0.012 | 20.043 | 5.00 | -- | -- | 0.100 | 0.08 | 3.9 | -- | 357.3 |
| | 27 | 6.85E-03 | 1.13E-02 | -1.16E-03 | -7.51E-04 | > 0.10 | 12.71 | 0.0478 | -0.008 | 19.786 | 5.00 | -- | -- | 0.091 | 0.07 | 3.1 | -- | 382.3 |
| 10 | 28 | 5.13E-03 | 1.22E-02 | -1.48E-03 | -2.84E-04 | | 14.37 | 0.0670 | -0.011 | 19.771 | 7.00 | -- | -- | 0.116 | 0.06 | 3.6 | -- | 432.3 |
| | 29 | 4.59E-03 | 1.12E-02 | -1.14E-03 | -1.03E-03 | | 9.84 | 0.0680 | -0.005 | 19.408 | 7.00 | -- | -- | 0.093 | 0.04 | 2.4 | -- | 460.2 |
| | 30 | 4.31E-03 | 1.07E-02 | -9.77E-04 | -1.48E-03 | > 0.10 | 7.69 | 0.0685 | -0.003 | 19.257 | 7.00 | -- | -- | 0.096 | 0.03 | 1.9 | -- | 482.3 |
| 11 | 31 | 4.22E-03 | 1.32E-02 | -1.36E-03 | -1.43E-02 | | 8.28 | 0.0864 | -0.004 | 18.894 | 8.82 | -- | -- | 0.122 | 0.03 | 2.0 | -- | 519.7 |
| | 32 | 3.66E-03 | 1.24E-02 | -1.11E-03 | -1.04E-02 | | 4.98 | 0.0875 | -0.001 | 18.622 | 8.82 | -- | -- | 0.113 | 0.02 | 1.2 | -- | 541.5 |
| | 33 | 3.28E-03 | 1.23E-02 | -9.35E-04 | -8.25E-03 | > 0.10 | 3.79 | 0.0878 | -0.001 | 18.425 | 8.82 | -- | -- | 0.154 | 0.01 | 0.9 | -- | 562.5 |

## Table 5.5 Test #3: Performance parameters ($0.1f'_cA_g$) up direction

| Load Step | Cycle | BEAM Steel Strain | COLN Steel Strain | BEAM Concrete Strain | COLN Concrete Strain | Crack Width in Joint | Lateral Load | Plastic Rotation | Principal Comp. Stress | Principal Tension Stress | Drift Ratio | Disp. Ductility Factor | Residual Deform. Index | Equiv. Visc Viscous Damping Ratio | Eff. Stiffness Ratio | Joint Strength Coeff. | Joint Shear Strain | Cumm. Energy |
|---|---|---|---|---|---|---|---|---|---|---|---|---|---|---|---|---|---|---|
| | | $\varepsilon_s$ | $\varepsilon_s$ | $\varepsilon_c$ | $\varepsilon_c$ | (in) | (kip) | $(\,)_p$ | $p_c$ (psi/f'$_c$) | $p_t$ (psi/$\sqrt{f'_c}$) | $\Delta$ (%) | $\mu_\Delta$ | RDI | $\xi_{eq}$ | $n_k$ | $\gamma$ | | (k-in) |
| 1 | 1 | 1.99E-04 | 6.36E-05 | -1.27E-04 | -6.11E-05 | | 7.63 | 0.0000 | -0.007 | 7.631 | 0.10 | 0.130 | 0.00 | 0.066 | 1.69 | 1.9 | 6.75E-05 | 0.3 |
| | 2 | 1.93E-04 | 5.78E-05 | -1.14E-04 | -5.95E-05 | | 7.41 | 0.0000 | -0.063 | 7.588 | 0.10 | 0.111 | 0.00 | 0.076 | 1.90 | 1.8 | 4.03E-05 | 0.5 |
| | 3 | 1.85E-04 | 5.31E-05 | -1.15E-04 | -5.82E-05 | 0.000 | 7.06 | 0.0000 | -0.006 | 7.545 | 0.10 | 0.103 | 0.00 | 0.073 | 1.90 | 1.7 | 4.69E-05 | 0.8 |
| 2 | 4 | 6.55E-04 | 1.11E-04 | -1.62E-04 | -1.03E-04 | | 12.99 | 0.0000 | -0.017 | 8.556 | 0.25 | 0.258 | 0.00 | 0.078 | 1.42 | 3.2 | 1.41E-04 | 1.9 |
| | 5 | 7.16E-04 | 1.05E-04 | -1.54E-04 | -1.04E-04 | | 13.09 | 0.0000 | -0.017 | 8.556 | 0.25 | 0.259 | 0.00 | 0.055 | 1.43 | 3.2 | 1.24E-04 | 2.7 |
| | 6 | 7.04E-04 | 9.71E-05 | -1.45E-04 | -1.00E-04 | Hairline | 12.46 | 0.0000 | -0.016 | 8.442 | 0.25 | 0.247 | 0.00 | 0.054 | 1.44 | 3.1 | 1.29E-04 | 3.4 |
| 3 | 7 | 2.87E-03 | 2.54E-04 | 1.06E-04 | -2.85E-04 | | 20.81 | 0.0004 | -0.037 | 10.236 | 0.50 | 0.506 | 0.00 | 0.061 | 1.16 | 5.1 | 2.72E-04 | 6.1 |
| | 8 | 3.41E-03 | 1.69E-04 | 1.99E-04 | -3.14E-04 | | 20.51 | 0.0004 | -0.036 | 10.179 | 0.50 | 0.505 | 0.00 | 0.044 | 1.15 | 5.0 | 2.66E-04 | 8.1 |
| | 9 | 3.78E-03 | 1.70E-04 | 2.72E-04 | -3.76E-04 | Hairline | 20.57 | 0.0005 | -0.036 | 10.208 | 0.50 | 0.512 | 0.00 | 0.042 | 1.13 | 5.0 | 2.55E-04 | 9.9 |
| 4 | 10 | 5.01E-03 | 2.59E-04 | -7.41E-04 | -5.15E-04 | | 27.71 | 0.0013 | -0.056 | 11.902 | 0.75 | 0.753 | 0.00 | 0.052 | 1.04 | 6.8 | 5.27E-04 | 14.6 |
| | 11 | 4.50E-03 | 3.33E-04 | -1.28E-03 | -5.67E-04 | | 27.50 | 0.0015 | -0.055 | 11.859 | 0.75 | 0.766 | 0.00 | 0.042 | 1.01 | 6.7 | 5.22E-04 | 18.4 |
| | 12 | 4.53E-03 | 3.58E-04 | -8.23E-04 | -6.30E-04 | 0.004 | 26.96 | 0.0015 | -0.054 | 11.774 | 0.75 | 0.763 | 0.00 | 0.041 | 1.00 | 6.6 | 4.92E-04 | 21.9 |
| 5 | 13 | 5.00E-03 | 7.60E-04 | -4.39E-03 | -9.06E-04 | | 32.57 | 0.0027 | -0.070 | 13.197 | 1.00 | 1.002 | 0.04 | 0.051 | 0.92 | 8.0 | 8.92E-04 | 29.0 |
| | 14 | 1.04E-02 | 1.35E-03 | -2.47E-03 | -1.28E-03 | | 31.74 | 0.0030 | -0.067 | 13.083 | 1.00 | 1.016 | 0.01 | 0.045 | 0.88 | 7.8 | 9.08E-04 | 35.1 |
| | 15 | 1.47E-02 | 1.86E-03 | -1.78E-03 | -1.38E-03 | 0.006 | 30.94 | 0.0031 | -0.064 | 12.870 | 1.00 | 1.008 | 0.04 | 0.042 | 0.86 | 7.6 | 8.53E-04 | 40.6 |
| 6 | 16 | 4.64E-03 | 2.51E-03 | -8.33E-03 | -2.79E-03 | | 39.29 | 0.0063 | -0.088 | 15.133 | 1.50 | 1.515 | 0.09 | 0.064 | 0.73 | 9.7 | 1.91E-03 | 56.9 |
| | 17 | 4.30E-03 | 3.10E-03 | -9.53E-03 | -4.15E-03 | | 36.33 | 0.0069 | -0.078 | 14.507 | 1.50 | 1.506 | 0.08 | 0.050 | 0.68 | 8.9 | 2.04E-03 | 68.4 |
| | 18 | 3.66E-03 | 7.49E-03 | -1.08E-02 | -2.04E-03 | 0.02 | 35.26 | 0.0073 | -0.075 | 14.279 | 1.50 | 1.520 | 0.09 | 0.047 | 0.65 | 8.7 | 2.18E-03 | 79.1 |
| 7 | 19 | 4.30E-03 | 4.89E-03 | -1.80E-02 | -4.28E-03 | | 42.16 | 0.0107 | -0.094 | 16.158 | 2.00 | 2.030 | 0.20 | 0.070 | 0.59 | 10.4 | 3.28E-03 | 104.5 |
| | 20 | 4.92E-03 | 3.62E-03 | -1.77E-02 | -2.76E-03 | | 37.70 | 0.0117 | -0.081 | 15.133 | 2.00 | 2.018 | 0.24 | 0.061 | 0.53 | 9.3 | 4.17E-03 | 124.2 |
| | 21 | 4.33E-03 | 2.95E-03 | -1.79E-02 | -2.03E-03 | 0.05 | 36.01 | 0.0119 | -0.076 | 14.763 | 2.00 | 2.007 | 0.12 | 0.056 | 0.51 | 8.9 | 4.68E-03 | 141.3 |
| 8 | 22 | 6.65E-03 | 3.09E-03 | -1.68E-02 | -3.73E-04 | | 41.72 | 0.0208 | -0.092 | 16.301 | 3.00 | 2.500 | 0.62 | 0.117 | 0.39 | 10.2 | 7.15E-03 | 203.0 |
| | 23 | 8.63E-03 | 4.09E-03 | -3.77E-03 | -1.41E-03 | | 32.17 | 0.0230 | -0.064 | 13.880 | 3.00 | -- | -- | 0.092 | 0.30 | 7.9 | 1.07E-02 | 241.0 |
| | 24 | 6.97E-03 | 5.53E-03 | -4.59E-03 | -4.80E-04 | 0.10 | 27.87 | 0.0240 | -0.052 | 12.742 | 3.00 | -- | -- | 0.078 | 0.26 | 6.9 | 1.29E-02 | 268.9 |
| 9 | 25 | 1.58E-02 | 6.04E-03 | -3.09E-03 | -4.95E-04 | | 30.01 | 0.0435 | -0.058 | 13.283 | 5.00 | -- | -- | 0.149 | 0.16 | 7.4 | 2.11E-02 | 361.7 |
| | 26 | 1.37E-02 | 4.62E-03 | -1.58E-02 | -3.86E-03 | | 20.07 | 0.0456 | -0.033 | 10.649 | 5.00 | -- | -- | 0.103 | 0.11 | 5.0 | 2.63E-02 | 406.1 |
| | 27 | 1.38E-02 | 4.59E-03 | -1.29E-02 | -3.55E-03 | 0.10 | 17.01 | 0.0473 | -0.026 | 9.809 | 5.00 | -- | -- | 0.085 | 0.09 | 4.2 | 2.88E-02 | 437.5 |
| 10 | 28 | 1.57E-02 | 1.16E-02 | -7.67E-03 | -1.30E-03 | | 17.93 | 0.0662 | -0.028 | 9.880 | 7.00 | -- | -- | 0.118 | 0.07 | 4.4 | 4.37E-02 | 500.2 |
| | 29 | 5.59E-03 | 4.47E-03 | -8.75E-03 | -3.94E-03 | | 13.59 | 0.0671 | -0.019 | 8.684 | 7.00 | -- | -- | 0.101 | 0.05 | 3.4 | 5.00E-02 | 541.4 |
| | 30 | 1.10E-02 | 4.52E-03 | -7.51E-03 | -4.51E-03 | > 0.10 | 11.41 | 0.0678 | -0.014 | 8.072 | 7.00 | -- | -- | 0.095 | 0.05 | 2.8 | 5.48E-02 | 573.9 |
| 11 | 31 | 1.44E-02 | 1.53E-02 | -6.81E-03 | -3.30E-03 | | 10.94 | 0.0860 | -0.014 | 7.745 | 8.82 | -- | -- | 0.122 | 0.03 | 2.7 | -- | 623.9 |
| | 32 | 2.96E-03 | 4.08E-03 | -9.29E-03 | -4.30E-03 | | 7.81 | 0.0866 | -0.075 | 7.033 | 8.82 | -- | -- | 0.136 | 0.02 | 1.9 | -- | 659.5 |
| | 33 | 2.16E-03 | 4.09E-03 | -9.47E-03 | -3.09E-03 | > 0.10 | 5.87 | 0.0869 | -0.004 | 7.517 | 8.82 | -- | -- | 0.109 | 0.02 | 1.4 | -- | 683.2 |

# Table 5.6 Test #3: Performance parameters ($0.1f'_cA_g$) down direction

| Load Step | Cycle | BEAM Steel Strain | COLN Steel Strain | BEAM Concrete Strain | COLN Concrete Strain | Crack Width in Joint | Lateral Load | Plastic Rotation | Principal Comp. Stress | Principal Tension Stress | Drift Ratio | Disp. Ductility Factor | Residual Deform. Index | Equiv. Visc Viscous Damping Ratio | Eff. Stiffness Ratio | Joint Strength Coeff. | Joint Shear Strain | Cumm. Energy |
|---|---|---|---|---|---|---|---|---|---|---|---|---|---|---|---|---|---|---|
| | | $\varepsilon_s$ | $\varepsilon_s$ | $\varepsilon_c$ | $\varepsilon_c$ | (in) | (kip) | $(\,)_p$ | $p_c$ (psi/f'$_c$) | $p_t$ (psi/$\sqrt{f'_c}$) | $\Delta$ (%) | $\mu_\Delta$ | RDI | $\xi_{eq}$ | $n_k$ | $\gamma$ | | (k-in) |
| 1 | 1 | 1.56E-04 | 5.39E-05 | -1.48E-04 | -4.58E-05 | | 5.68 | 0.0000 | -0.004 | 7.147 | 0.10 | 0.098 | 0.03 | 0.107 | 1.68 | 1.4 | 1.23E-04 | 0.3 |
| | 2 | 1.58E-04 | 5.20E-05 | -1.45E-04 | -4.42E-05 | | 5.45 | 0.0000 | -0.004 | 7.132 | 0.10 | 0.098 | 0.03 | 0.107 | 1.60 | 1.3 | 1.27E-04 | 0.5 |
| | 3 | 1.60E-04 | 5.06E-05 | -1.44E-04 | -4.54E-05 | 0.000 | 5.42 | 0.0000 | -0.003 | 7.118 | 0.10 | 0.098 | 0.03 | 0.091 | 1.57 | 1.3 | 1.26E-04 | 0.8 |
| 2 | 4 | 4.42E-04 | 1.08E-04 | -1.92E-04 | -8.58E-05 | | 10.70 | 0.0000 | -0.013 | 7.616 | 0.25 | 0.233 | 0.06 | 0.096 | 1.35 | 2.6 | 2.39E-04 | 1.9 |
| | 5 | 4.93E-04 | 1.05E-04 | -1.81E-04 | -8.71E-05 | | 10.41 | 0.0000 | -0.012 | 7.574 | 0.25 | 0.233 | 0.06 | 0.070 | 1.30 | 2.5 | 2.40E-04 | 2.7 |
| | 6 | 4.70E-04 | 1.05E-04 | -1.89E-04 | -8.43E-05 | Hairline | 10.24 | 0.0000 | -0.012 | 7.560 | 0.25 | 0.234 | 0.05 | 0.063 | 1.26 | 2.5 | 2.41E-04 | 3.4 |
| 3 | 7 | 1.29E-03 | 6.33E-04 | -3.36E-04 | -5.81E-05 | | 19.03 | 0.0002 | -0.035 | 8.940 | 0.50 | 0.464 | 0.08 | 0.067 | 1.18 | 4.6 | 4.86E-04 | 6.1 |
| | 8 | 1.49E-03 | 6.05E-04 | -2.60E-04 | -1.15E-04 | | 18.32 | 0.0002 | -0.033 | 8.812 | 0.50 | 0.462 | 0.09 | 0.049 | 1.14 | 4.5 | 5.09E-04 | 8.1 |
| | 9 | 1.22E-03 | 6.03E-04 | -3.31E-04 | -1.01E-04 | Hairline | 18.12 | 0.0004 | -0.032 | 8.798 | 0.50 | 0.464 | 0.07 | 0.048 | 1.13 | 4.4 | 5.13E-04 | 9.9 |
| 4 | 10 | 3.15E-03 | 2.22E-03 | -6.87E-04 | -2.00E-05 | | 25.59 | 0.0009 | -0.055 | 10.293 | 0.75 | 0.695 | 0.12 | 0.056 | 1.06 | 6.3 | 9.48E-04 | 14.6 |
| | 11 | 3.22E-03 | 2.48E-03 | -8.09E-04 | -8.76E-06 | | 24.68 | 0.0011 | -0.052 | 10.108 | 0.75 | 0.691 | 0.11 | 0.048 | 1.03 | 6.1 | 9.86E-04 | 18.4 |
| | 12 | 2.66E-03 | 2.67E-03 | -7.14E-04 | -1.19E-04 | 0.004 | 24.32 | 0.0011 | -0.051 | 10.079 | 0.75 | 0.691 | 0.11 | 0.045 | 1.02 | 6.0 | 1.03E-03 | 21.9 |
| 5 | 13 | 1.51E-02 | 5.78E-03 | -1.05E-05 | -2.77E-04 | | 30.74 | 0.0020 | -0.071 | 11.517 | 1.00 | 0.917 | 0.16 | 0.054 | 0.96 | 7.6 | 1.62E-03 | 29.0 |
| | 14 | 1.48E-02 | 6.52E-03 | -1.02E-04 | -2.36E-04 | | 30.06 | 0.0023 | -0.068 | 11.403 | 1.00 | 0.925 | 0.16 | 0.048 | 0.93 | 7.4 | 1.74E-03 | 35.1 |
| | 15 | 2.12E-03 | 6.81E-03 | -2.36E-03 | -7.61E-04 | 0.006 | 29.20 | 0.0024 | -0.065 | 11.233 | 1.00 | 0.920 | 0.17 | 0.044 | 0.92 | 7.2 | 1.79E-03 | 40.6 |
| 6 | 16 | 3.43E-03 | 1.56E-02 | -6.43E-03 | -6.82E-04 | | 39.12 | 0.0048 | -0.096 | 13.667 | 1.50 | 1.376 | 0.20 | 0.065 | 0.82 | 9.6 | 3.00E-03 | 56.9 |
| | 17 | 6.67E-03 | 1.60E-02 | -7.61E-03 | -7.97E-05 | | 37.92 | 0.0052 | -0.092 | 13.496 | 1.50 | 1.382 | 0.17 | 0.047 | 0.79 | 9.3 | 3.07E-03 | 68.4 |
| | 18 | 3.15E-03 | 1.40E-02 | -5.50E-03 | -8.55E-04 | 0.02 | 36.42 | 0.0055 | -0.086 | 13.211 | 1.50 | 1.377 | 0.16 | 0.046 | 0.76 | 8.9 | 3.11E-03 | 79.1 |
| 7 | 19 | 3.17E-03 | 1.16E-02 | -1.33E-02 | -3.11E-03 | | 41.40 | 0.0092 | -0.101 | 14.607 | 2.00 | 1.832 | 0.30 | 0.072 | 0.66 | 10.2 | 4.29E-03 | 104.5 |
| | 20 | 3.38E-03 | 5.35E-03 | -1.48E-02 | -2.36E-03 | | 38.33 | 0.0100 | -0.091 | 13.937 | 2.00 | 1.830 | 0.19 | 0.060 | 0.60 | 9.4 | 4.27E-03 | 124.2 |
| | 21 | 3.82E-03 | 4.76E-03 | -1.33E-02 | -1.67E-03 | 0.05 | 36.08 | 0.0106 | -0.084 | 13.468 | 2.00 | 1.832 | 0.34 | 0.055 | 0.57 | 8.8 | 4.26E-03 | 141.3 |
| 8 | 22 | 7.50E-03 | 4.97E-03 | -1.71E-02 | -5.51E-04 | | 36.42 | 0.0207 | -0.086 | 13.695 | 3.00 | 1.900 | 0.92 | 0.136 | 0.37 | 9.1 | 8.08E-03 | 203.0 |
| | 23 | 1.06E-02 | 1.09E-02 | -1.09E-02 | -5.94E-04 | | 28.77 | 0.0228 | -0.060 | 11.774 | 3.00 | -- | -- | 0.104 | 0.30 | 7.1 | 7.77E-03 | 241.0 |
| | 24 | 1.62E-02 | 5.85E-03 | -6.17E-03 | -3.14E-04 | 0.10 | 24.48 | 0.0238 | -0.048 | 10.791 | 3.00 | -- | -- | 0.088 | 0.26 | 6.0 | 7.09E-03 | 268.9 |
| 9 | 25 | 1.56E-02 | 9.72E-03 | -1.54E-02 | -4.75E-04 | | 23.12 | 0.0441 | -0.045 | 10.264 | 5.00 | -- | -- | 0.191 | 0.14 | 5.7 | 1.56E-02 | 361.7 |
| | 26 | 8.99E-03 | 1.27E-02 | -1.67E-02 | -5.84E-04 | | 15.40 | 0.0461 | -0.025 | 8.471 | 5.00 | -- | -- | 0.134 | 0.10 | 3.8 | 1.37E-02 | 406.1 |
| | 27 | 1.24E-02 | 9.00E-03 | -1.17E-02 | -4.02E-04 | 0.10 | 12.42 | 0.0472 | -0.017 | 7.844 | 5.00 | -- | -- | 0.118 | 0.08 | 3.1 | 1.41E-02 | 437.5 |
| 10 | 28 | 7.78E-03 | 6.05E-03 | -9.34E-03 | -1.39E-03 | | 13.05 | 0.0667 | -0.020 | 7.560 | 7.00 | -- | -- | 0.162 | 0.06 | 3.2 | 1.37E-02 | 500.2 |
| | 29 | 7.04E-03 | 5.23E-03 | -8.59E-03 | -1.76E-03 | | 8.79 | 0.0678 | -0.010 | 6.663 | 7.00 | -- | -- | 0.159 | 0.04 | 2.2 | -- | 541.4 |
| | 30 | 9.14E-03 | 7.04E-03 | -7.97E-03 | -9.21E-04 | > 0.10 | 6.49 | 0.0684 | -0.006 | 6.250 | 7.00 | -- | -- | 0.163 | 0.03 | 1.7 | -- | 573.9 |
| 11 | 31 | 1.07E-02 | 1.09E-02 | -7.81E-03 | -3.93E-03 | | 6.59 | 0.0867 | -0.007 | 5.581 | 8.82 | -- | -- | 0.207 | 0.02 | 1.6 | -- | 623.9 |
| | 32 | 1.35E-02 | 8.53E-03 | -6.94E-03 | -4.31E-03 | | 3.62 | 0.0875 | -0.002 | 4.698 | 8.82 | -- | -- | 0.281 | 0.01 | 0.9 | -- | 659.5 |
| | 33 | 7.94E-03 | 5.21E-03 | -8.25E-03 | -7.20E-03 | > 0.10 | 1.25 | 0.0881 | 0.000 | 4.783 | 8.82 | -- | -- | 0.605 | 0.00 | 0.3 | -- | 683.2 |

## Table 5.7 Test #4: Performance parameters ($0.25f'_cA_g$) up direction

| Load Step | Cycle | BEAM Steel Strain | COLN Steel Strain | BEAM Concrete Strain | COLN Concrete Strain | Crack Width in Joint | Lateral Load | Plastic Rotation | Principal Comp. Stress | Principal Tension Stress | Drift Ratio | Disp. Ductility Factor | Residual Deform. Index | Equiv. Visc Viscous Damping Ratio | Eff. Stiffness Ratio | Joint Strength Coeff. | Joint Shear Strain | Cumm. Energy |
|---|---|---|---|---|---|---|---|---|---|---|---|---|---|---|---|---|---|---|
| | | $\varepsilon_s$ | $\varepsilon_s$ | $\varepsilon_c$ | $\varepsilon_c$ | (in) | (kip) | $(\ )_p$ | $p_c$ (psi/f'c) | $p_t$ (psi/√f'c) | Δ (%) | $\mu_\Delta$ | RDI | $\xi_{eq}$ | $n_k$ | $\gamma$ | | (k-in) |
| 1 | 1 | 1.55E-04 | 9.35E-05 | -9.80E-05 | -2.03E-05 | | 4.68 | 0.0000 | -0.001 | 18.419 | 0.10 | 0.093 | 0.02 | 0.064 | 1.30 | 1.2 | 5.57E-05 | 0.1 |
| | 2 | 1.76E-04 | 9.30E-05 | -9.51E-05 | -3.20E-05 | | 4.84 | 0.0000 | -0.001 | 18.419 | 0.10 | 0.091 | 0.02 | 0.053 | 1.35 | 1.2 | 6.46E-05 | 0.3 |
| | 3 | 1.87E-04 | 9.49E-05 | -9.38E-05 | -4.38E-05 | 0.000 | 4.81 | 0.0000 | -0.001 | 18.419 | 0.10 | 0.094 | 0.00 | 0.048 | 1.30 | 1.2 | 6.64E-05 | 0.4 |
| 2 | 4 | 1.08E-03 | 2.06E-04 | -9.29E-05 | -5.88E-05 | | 10.66 | 0.0000 | -0.006 | 18.804 | 0.25 | 0.216 | 0.04 | 0.081 | 1.30 | 2.6 | 1.68E-04 | 1.3 |
| | 5 | 1.27E-03 | 1.95E-04 | -2.79E-05 | -5.97E-05 | | 10.96 | 0.0000 | -0.006 | 18.833 | 0.25 | 0.220 | 0.05 | 0.053 | 1.30 | 2.7 | 1.74E-04 | 1.9 |
| | 6 | 1.34E-03 | 1.93E-04 | -1.36E-05 | -6.51E-05 | 0.000 | 11.00 | 0.0000 | -0.006 | 18.833 | 0.25 | 0.224 | 0.02 | 0.045 | 1.26 | 2.7 | 1.75E-04 | 2.5 |
| 3 | 7 | 4.11E-03 | 3.00E-04 | -3.92E-04 | -1.28E-04 | | 19.26 | 0.0000 | -0.018 | 19.794 | 0.50 | 0.431 | 0.05 | 0.059 | 1.14 | 4.7 | 3.29E-04 | 4.9 |
| | 8 | 4.70E-03 | 2.55E-04 | -5.19E-04 | -2.09E-04 | | 19.31 | 0.0000 | -0.018 | 19.809 | 0.50 | 0.436 | 0.06 | 0.043 | 1.14 | 4.8 | 3.36E-04 | 6.7 |
| | 9 | 4.84E-03 | 2.50E-04 | -7.27E-04 | -2.89E-04 | Hairline | 18.88 | 0.0001 | -0.017 | 19.750 | 0.50 | 0.433 | 0.03 | 0.039 | 1.12 | 4.7 | 3.40E-04 | 8.3 |
| 4 | 10 | 6.64E-03 | 4.13E-04 | -5.47E-04 | -3.31E-04 | | 26.76 | 0.0005 | -0.033 | 21.213 | 0.75 | 0.647 | 0.08 | 0.048 | 1.06 | 6.6 | 5.51E-04 | 12.5 |
| | 11 | 6.76E-03 | 6.22E-04 | -8.28E-04 | -6.67E-04 | | 26.32 | 0.0006 | -0.032 | 21.184 | 0.75 | 0.646 | 0.02 | 0.040 | 1.05 | 6.5 | 5.60E-04 | 15.9 |
| | 12 | 6.80E-03 | 7.08E-04 | -8.39E-04 | -6.89E-04 | Hairline | 26.15 | 0.0006 | -0.031 | 21.169 | 0.75 | 0.644 | 0.04 | 0.036 | 1.04 | 6.5 | 5.57E-04 | 18.9 |
| 5 | 13 | 7.75E-03 | 1.60E-03 | -9.16E-04 | -6.25E-04 | | 23.08 | 0.0012 | -0.047 | 22.455 | 1.00 | 0.852 | 0.08 | 0.046 | 0.99 | 8.1 | 8.16E-04 | 25.4 |
| | 14 | 6.89E-03 | 1.53E-03 | -7.38E-04 | -5.34E-04 | | 32.42 | 0.0014 | -0.045 | 22.352 | 1.00 | 0.857 | 0.02 | 0.039 | 0.96 | 8.0 | 8.65E-04 | 30.8 |
| | 15 | 6.33E-03 | 1.49E-03 | -6.17E-04 | -6.45E-04 | 0.003 | 32.04 | 0.0015 | -0.045 | 22.322 | 1.00 | 0.859 | 0.02 | 0.036 | 0.96 | 7.9 | 9.11E-04 | 35.7 |
| 6 | 16 | 6.43E-03 | 2.21E-03 | -2.51E-05 | -7.04E-04 | | 41.69 | 0.0040 | -0.068 | 24.466 | 1.50 | 1.284 | 0.08 | 0.059 | 0.83 | 10.2 | 1.76E-03 | 51.4 |
| | 17 | 5.60E-03 | 3.39E-03 | -2.40E-04 | -2.39E-03 | | 40.10 | 0.0045 | -0.064 | 24.199 | 1.50 | 1.292 | 0.04 | 0.045 | 0.79 | 9.9 | 2.00E-03 | 63.0 |
| | 18 | 5.05E-03 | 3.47E-03 | -2.83E-04 | -3.09E-03 | 0.008 | 38.82 | 0.0048 | -0.061 | 23.948 | 1.50 | 1.292 | 0.06 | 0.040 | 0.77 | 9.6 | 2.08E-03 | 73.1 |
| 7 | 19 | 5.41E-03 | 5.76E-03 | -3.59E-04 | -3.49E-03 | | 45.14 | 0.0081 | -0.077 | 25.515 | 2.00 | 1.714 | 0.14 | 0.070 | 0.68 | 11.1 | 3.13E-03 | 99.7 |
| | 20 | 4.73E-03 | 6.25E-03 | -1.35E-04 | -4.00E-03 | | 41.81 | 0.0089 | -0.068 | 24.820 | 2.00 | 1.714 | 0.13 | 0.056 | 0.63 | 10.3 | 3.94E-03 | 119.3 |
| | 21 | 4.44E-03 | 5.84E-03 | -1.20E-03 | -3.80E-03 | 0.04 | 39.97 | 0.0095 | -0.063 | 24.406 | 2.00 | 1.712 | 0.09 | 0.052 | 0.60 | 9.8 | 4.25E-03 | 137.0 |
| 8 | 22 | 5.39E-03 | 4.81E-03 | -8.15E-03 | -2.53E-03 | | 44.69 | 0.0161 | -0.075 | 25.678 | 3.00 | 2.000 | 0.41 | 0.130 | 0.48 | 11.0 | 7.08E-03 | 205.7 |
| | 23 | 6.30E-03 | 4.10E-03 | -6.43E-03 | -2.37E-03 | | 33.89 | 0.0210 | -0.048 | 23.076 | 3.00 | -- | 0.29 | 0.097 | 0.34 | 8.4 | 1.06E-02 | 247.8 |
| | 24 | 6.98E-03 | 1.50E-02 | -1.26E-03 | -6.31E-04 | 0.08 | 29.39 | 0.0223 | -0.038 | 21.952 | 3.00 | -- | 0.17 | 0.084 | 0.29 | 7.2 | 1.22E-02 | 279.6 |
| 9 | 25 | 6.58E-03 | 1.09E-02 | -2.46E-03 | -1.39E-02 | | 30.53 | 0.0431 | -0.039 | 22.854 | 5.00 | -- | 1.18 | 0.178 | 0.16 | 7.5 | 2.07E-02 | 385.2 |
| | 26 | 4.04E-03 | 8.12E-03 | -1.19E-02 | -5.34E-03 | | 16.57 | 0.0457 | -0.014 | 19.247 | 5.00 | -- | -- | 0.128 | 0.10 | 4.1 | 1.14E-02 | 430.5 |
| | 27 | 4.02E-03 | 1.07E-02 | -1.22E-02 | -5.64E-03 | > 0.10 | 11.92 | 0.0470 | -0.009 | 15.064 | 5.00 | -- | -- | 0.154 | 0.07 | 3.0 | -- | 470.1 |
| 10 | 28 | -- | -- | -- | -- | | -- | -- | -- | -- | 7.00 | -- | -- | -- | -- | -- | -- | -- |
| | 29 | -- | -- | -- | -- | | -- | -- | -- | -- | 7.00 | -- | -- | -- | -- | -- | -- | -- |
| | 30 | -- | -- | -- | -- | -- | -- | -- | -- | -- | 7.00 | -- | -- | -- | -- | -- | -- | -- |
| 11 | 31 | -- | -- | -- | -- | | -- | -- | -- | -- | 8.82 | -- | -- | -- | -- | -- | -- | -- |
| | 32 | -- | -- | -- | -- | | -- | -- | -- | -- | 8.82 | -- | -- | -- | -- | -- | -- | -- |
| | 33 | -- | -- | -- | -- | -- | -- | -- | -- | -- | 8.82 | -- | -- | -- | -- | -- | -- | -- |

## Table 5.8 Test #4: Performance parameters ($0.25f'_cA_g$) down direction

| Load Step | Cycle | BEAM Steel Strain | COLN Steel Strain | BEAM Concrete Strain | COLN Concrete Strain | Crack Width in Joint | Lateral Load | Plastic Rotation | Principal Comp. Stress | Principal Tension Stress | Drift Ratio | Disp. Ductility Factor | Residual Deform. Index | Equiv. Visc Viscous Damping Ratio | Eff. Stiffness Ratio | Joint Strength Coeff. | Joint Shear Strain | Cumm. Energy |
|---|---|---|---|---|---|---|---|---|---|---|---|---|---|---|---|---|---|---|
| | | $\varepsilon_s$ | $\varepsilon_s$ | $\varepsilon_c$ | $\varepsilon_c$ | (in) | (kip) | $(\ )_p$ | $p_c$ (psi/$f'_c$) | $p_t$ (psi/$\sqrt{f'_c}$) | $\Delta$ (%) | $\mu_\Delta$ | RDI | $\xi_{eq}$ | $n_k$ | $\gamma$ | | (k-in) |
| 1 | 1 | 1.52E-04 | 4.09E-05 | -1.45E-04 | -1.41E-04 | | 5.99 | -- | -0.002 | 18.375 | 0.10 | 0.094 | -- | 0.051 | 1.65 | 1.5 | 7.43E-05 | 0.1 |
| | 2 | 1.52E-04 | 4.00E-05 | -1.42E-04 | -1.36E-04 | | 5.89 | -- | -0.002 | 18.360 | 0.10 | 0.093 | -- | 0.046 | 1.63 | 1.4 | 6.43E-05 | 0.3 |
| | 3 | 1.52E-04 | 3.95E-05 | -1.40E-04 | -1.34E-04 | 0.000 | 5.75 | -- | -0.002 | 18.360 | 0.10 | 0.092 | -- | 0.043 | 1.61 | 1.4 | 6.43E-05 | 0.4 |
| 2 | 4 | 5.44E-04 | 9.92E-05 | -2.25E-04 | -3.49E-04 | | 12.52 | -- | -0.008 | 18.641 | 0.25 | 0.237 | -- | 0.066 | 1.38 | 3.1 | 1.65E-04 | 1.3 |
| | 5 | 5.38E-04 | 9.39E-05 | -2.12E-04 | -3.40E-04 | | 11.75 | -- | -0.007 | 18.597 | 0.25 | 0.229 | -- | 0.049 | 1.33 | 2.9 | 1.46E-04 | 1.9 |
| | 6 | 5.39E-04 | 9.25E-05 | -2.07E-04 | -3.35E-04 | 0.000 | 11.49 | -- | -0.007 | 18.597 | 0.25 | 0.226 | -- | 0.044 | 1.32 | 2.8 | 1.41E-04 | 2.5 |
| 3 | 7 | 1.70E-03 | 1.72E-04 | -2.30E-03 | -7.48E-04 | | 20.83 | 0.0002 | -0.022 | 19.439 | 0.50 | 0.454 | 0.05 | 0.055 | 1.18 | 5.1 | 3.26E-04 | 4.9 |
| | 8 | 1.66E-03 | 1.64E-04 | -2.85E-03 | -7.67E-04 | | 20.41 | 0.0003 | -0.021 | 19.395 | 0.50 | 0.454 | 0.01 | 0.041 | 1.17 | 5.0 | 3.27E-04 | 6.7 |
| | 9 | 1.42E-03 | 1.59E-04 | -3.23E-03 | -7.69E-04 | Hairline | 20.09 | 0.0003 | -0.020 | 19.351 | 0.50 | 0.451 | 0.04 | 0.037 | 1.16 | 4.9 | 3.22E-04 | 8.3 |
| 4 | 10 | 2.28E-03 | 2.19E-04 | -3.26E-03 | -1.32E-03 | | 28.76 | 0.0009 | -0.038 | 20.755 | 0.75 | 0.677 | 0.05 | 0.045 | 1.10 | 7.1 | 5.33E-04 | 12.5 |
| | 11 | 2.75E-03 | 2.06E-04 | -1.78E-05 | -1.38E-03 | | 28.35 | 0.0010 | -0.037 | 20.711 | 0.75 | 0.682 | 0.07 | 0.037 | 1.08 | 7.0 | 5.40E-04 | 15.9 |
| | 12 | 1.77E-03 | 1.99E-04 | -2.22E-04 | -1.41E-03 | Hairline | 27.72 | 0.0010 | -0.036 | 20.652 | 0.75 | 0.677 | 0.05 | 0.034 | 1.06 | 6.8 | 5.24E-04 | 18.9 |
| 5 | 13 | 3.48E-03 | 3.11E-04 | -4.69E-05 | -2.09E-03 | | 34.79 | 0.0019 | -0.054 | 21.819 | 1.00 | 0.904 | 0.11 | 0.043 | 1.00 | 8.6 | 7.65E-04 | 25.4 |
| | 14 | 2.81E-03 | 3.05E-04 | -7.87E-05 | -2.27E-03 | | 33.81 | 0.0021 | -0.051 | 21.672 | 1.00 | 0.899 | 0.04 | 0.037 | 0.97 | 8.3 | 7.54E-04 | 30.8 |
| | 15 | 1.92E-03 | 3.00E-04 | -2.66E-04 | -2.35E-03 | 0.003 | 33.40 | 0.0022 | -0.050 | 21.612 | 1.00 | 0.899 | 0.08 | 0.035 | 0.96 | 8.2 | 7.44E-04 | 35.7 |
| 6 | 16 | 3.04E-03 | 9.56E-04 | -7.69E-04 | -9.99E-03 | | 43.61 | 0.0049 | -0.077 | 23.682 | 1.50 | 1.350 | 0.12 | 0.056 | 0.84 | 10.7 | 1.42E-03 | 51.4 |
| | 17 | 2.93E-03 | 1.30E-03 | -9.21E-04 | -8.93E-03 | | 41.57 | 0.0053 | -0.071 | 23.357 | 1.50 | 1.350 | 0.18 | 0.044 | 0.80 | 10.2 | 1.43E-04 | 63.0 |
| | 18 | 1.47E-02 | 1.50E-03 | -1.50E-03 | -8.31E-03 | 0.008 | 40.77 | 0.0056 | -0.069 | 23.209 | 1.50 | 1.352 | 0.15 | 0.039 | 0.78 | 10.0 | 1.44E-04 | 73.1 |
| 7 | 19 | 4.33E-03 | 4.49E-03 | -5.20E-04 | -1.27E-02 | | 47.53 | 0.0092 | -0.088 | 24.732 | 2.00 | 1.814 | 0.21 | 0.065 | 0.68 | 11.7 | 2.25E-03 | 99.7 |
| | 20 | 4.37E-03 | 4.62E-03 | -5.99E-05 | -1.15E-02 | | 43.45 | 0.0099 | -0.076 | 23.919 | 2.00 | 1.798 | 0.23 | 0.053 | 0.63 | 10.7 | 2.29E-03 | 119.3 |
| | 21 | 4.16E-03 | 1.11E-02 | -2.35E-04 | -9.80E-03 | 0.04 | 41.40 | 0.0104 | -0.070 | 23.505 | 2.00 | 1.800 | 0.24 | 0.050 | 0.60 | 10.2 | 2.31E-03 | 137.0 |
| 8 | 22 | 8.07E-03 | 1.57E-02 | -3.61E-03 | -8.87E-03 | | 41.63 | 0.0206 | -0.071 | 23.534 | 3.00 | -- | 0.77 | 0.145 | 0.45 | 10.2 | 4.73E-03 | 205.7 |
| | 23 | 6.11E-03 | 1.56E-02 | -1.25E-03 | -4.03E-04 | | 32.50 | 0.0225 | -0.047 | 21.539 | 3.00 | -- | 0.84 | 0.102 | 0.31 | 8.0 | 5.23E-03 | 247.8 |
| | 24 | 6.06E-03 | 4.14E-03 | -1.22E-03 | -2.32E-03 | 0.08 | 27.72 | 0.0236 | -0.036 | 20.578 | 3.00 | -- | 0.99 | 0.089 | 0.27 | 6.8 | 5.62E-03 | 279.6 |
| 9 | 25 | 6.19E-03 | 1.09E-02 | -4.88E-03 | -3.57E-03 | | 23.52 | 0.0448 | -0.027 | 20.060 | 5.00 | -- | 2.65 | 0.218 | 0.13 | 5.8 | 1.74E-02 | 385.2 |
| | 26 | 4.03E-03 | 6.93E-03 | -5.64E-03 | -5.81E-03 | | 14.21 | 0.0468 | -0.011 | 17.858 | 5.00 | -- | -- | 0.149 | 0.08 | 3.5 | 3.24E-02 | 430.5 |
| | 27 | 2.68E-03 | 1.13E-02 | -6.26E-03 | -5.59E-03 | > 0.10 | 12.53 | 0.0472 | -0.011 | 13.393 | 5.00 | -- | -- | 0.148 | 0.07 | 3.1 | -- | 470.1 |
| 10 | 28 | -- | -- | -- | -- | | -- | -- | -- | -- | 7.00 | -- | -- | -- | -- | -- | -- | -- |
| | 29 | -- | -- | -- | -- | | -- | -- | -- | -- | 7.00 | -- | -- | -- | -- | -- | -- | -- |
| | 30 | -- | -- | -- | -- | -- | -- | -- | -- | -- | 7.00 | -- | -- | -- | -- | -- | -- | -- |
| 11 | 31 | -- | -- | -- | -- | | -- | -- | -- | -- | 8.82 | -- | -- | -- | -- | -- | -- | -- |
| | 32 | -- | -- | -- | -- | | -- | -- | -- | -- | 8.82 | -- | -- | -- | -- | -- | -- | -- |
| | 33 | -- | -- | -- | -- | -- | -- | -- | -- | -- | 8.82 | -- | -- | -- | -- | -- | -- | -- |

## Table 5.9 Test #5: Performance parameters (0.1f'$_c$A$_g$) up direction

| Load Step | Cycle | BEAM Steel Strain | COLN Steel Strain | BEAM Concrete Strain | COLN Concrete Strain | Crack Width in Joint | Lateral Load | Plastic Rotation | Principal Comp. Stress | Principal Tension Stress | Drift Ratio | Disp. Ductility Factor | Residual Deform. Index | Equiv. Visc Viscous Damping Ratio | Eff. Stiffness Ratio | Joint Strength Coeff. | Joint Shear Strain | Cumm. Energy |
|---|---|---|---|---|---|---|---|---|---|---|---|---|---|---|---|---|---|---|
| | | $\varepsilon_s$ | $\varepsilon_s$ | $\varepsilon_c$ | $\varepsilon_c$ | (in) | (kip) | $(\ )_p$ | $p_c$ (psi/f'$_c$) | $p_t$ (psi/$\sqrt{f'_c}$) | $\Delta$ (%) | $\mu_\Delta$ | RDI | $\xi_{eq}$ | $n_k$ | $\gamma$ | | (k-in) |
| 1 | 1 | 3.19E-04 | 5.53E-04 | -1.64E-04 | -5.74E-05 | | 10.38 | 0.0000 | -0.013 | 8.024 | 0.10 | 0.206 | 0.00 | 0.064 | 1.41 | 2.6 | 1.57E-04 | 0.8 |
| | 2 | 1.74E-04 | 2.81E-04 | -1.93E-03 | -7.95E-05 | | 5.13 | 0.0000 | -0.003 | 7.272 | 0.10 | 0.083 | 0.00 | 0.102 | 1.71 | 1.3 | 7.04E-05 | 1.0 |
| | 3 | 1.63E-04 | 2.58E-04 | -2.01E-03 | -8.01E-05 | 0.000 | 4.65 | 0.0000 | -0.003 | 7.243 | 0.10 | 0.077 | 0.00 | 0.110 | 1.69 | 1.2 | 7.37E-05 | 1.3 |
| 2 | 4 | 3.22E-04 | 5.40E-04 | -2.21E-03 | -4.49E-05 | | 9.86 | 0.0000 | -0.012 | 7.951 | 0.25 | 0.189 | 0.00 | 0.081 | 1.45 | 2.5 | 1.36E-04 | 2.1 |
| | 5 | 3.60E-04 | 5.77E-04 | -2.66E-03 | -3.65E-05 | | 10.13 | 0.0000 | -0.012 | 7.995 | 0.25 | 0.192 | 0.00 | 0.071 | 1.47 | 2.6 | 1.49E-04 | 2.9 |
| | 6 | 3.65E-04 | 5.61E-04 | -2.62E-03 | -3.37E-05 | 0.000 | 9.75 | 0.0000 | -0.012 | 7.921 | 0.25 | 0.187 | 0.00 | 0.070 | 1.45 | 2.5 | 1.29E-04 | 3.6 |
| 3 | 7 | 7.47E-04 | 1.11E-03 | -3.13E-03 | -4.34E-04 | | 17.03 | 0.0001 | -0.030 | 9.352 | 0.50 | 0.377 | 0.00 | 0.072 | 1.27 | 4.4 | 3.02E-04 | 6.3 |
| | 8 | 7.75E-04 | 1.24E-03 | -1.99E-03 | -6.23E-04 | | 16.89 | 0.0001 | -0.029 | 9.308 | 0.50 | 0.377 | 0.00 | 0.054 | 1.24 | 4.3 | 2.99E-04 | 8.3 |
| | 9 | 7.71E-04 | 1.23E-03 | -1.74E-03 | -7.61E-04 | 0.00 | 16.58 | 0.0002 | -0.029 | 9.249 | 0.50 | 0.375 | 0.00 | 0.052 | 1.23 | 4.2 | 3.00E-04 | 10.1 |
| 4 | 10 | 1.10E-03 | 1.96E-03 | -1.59E-03 | -9.06E-04 | | 23.58 | 0.0007 | -0.049 | 10.871 | 0.75 | 0.563 | 0.02 | 0.057 | 1.17 | 6.0 | 5.94E-04 | 14.4 |
| | 11 | 1.12E-03 | 2.12E-03 | -1.19E-03 | -5.95E-04 | | 23.68 | 0.0009 | -0.049 | 10.901 | 0.75 | 0.585 | 0.01 | 0.046 | 1.13 | 6.0 | 6.50E-04 | 18.1 |
| | 12 | 1.08E-03 | 1.92E-03 | -1.14E-03 | -6.57E-04 | 0.004 | 22.46 | 0.0010 | -0.045 | 10.620 | 0.75 | 0.567 | 0.01 | 0.043 | 1.10 | 5.7 | 6.32E-04 | 21.2 |
| 5 | 13 | 1.35E-03 | 2.27E-03 | -1.57E-03 | -1.63E-03 | | 28.21 | 0.0018 | -0.063 | 12.096 | 1.00 | 0.750 | 0.02 | 0.053 | 1.06 | 7.2 | 1.05E-03 | 27.5 |
| | 14 | 1.32E-03 | 1.80E-03 | -1.07E-03 | -1.87E-03 | | 27.40 | 0.0021 | -0.060 | 11.904 | 1.00 | 0.753 | 0.01 | 0.045 | 1.01 | 7.0 | 1.03E-03 | 32.7 |
| | 15 | 1.30E-03 | 6.67E-03 | -1.11E-03 | -1.78E-03 | 0.008 | 26.93 | 0.0022 | -0.059 | 11.815 | 1.00 | 0.749 | 0.02 | 0.040 | 1.00 | 6.8 | 1.15E-03 | 37.4 |
| 6 | 16 | 1.82E-03 | 9.68E-03 | -2.22E-03 | -2.62E-03 | | 36.48 | 0.0045 | -0.088 | 14.515 | 1.50 | 1.130 | 0.06 | 0.059 | 0.90 | 9.3 | 2.25E-03 | 51.3 |
| | 17 | 1.68E-03 | 1.42E-03 | -1.25E-03 | -2.14E-03 | | 32.65 | 0.0055 | -0.075 | 13.585 | 1.50 | 1.125 | 0.05 | 0.044 | 0.81 | 8.3 | 2.26E-03 | 60.5 |
| | 18 | 1.65E-03 | 1.45E-03 | -1.38E-03 | -2.12E-03 | 0.020 | 32.09 | 0.0057 | -0.073 | 13.453 | 1.50 | 1.124 | 0.05 | 0.040 | 0.79 | 8.2 | 2.28E-03 | 68.7 |
| 7 | 19 | 2.11E-03 | 1.99E-03 | -1.41E-03 | -2.49E-03 | | 40.09 | 0.0084 | -0.097 | 15.842 | 2.00 | 1.498 | 0.10 | 0.057 | 0.75 | 10.2 | 3.34E-03 | 88.1 |
| | 20 | 2.36E-03 | 1.73E-03 | -1.01E-03 | -2.25E-03 | | 37.37 | 0.0092 | -0.088 | 15.134 | 2.00 | 1.503 | 0.09 | 0.050 | 0.69 | 9.5 | 3.64E-03 | 104.1 |
| | 21 | 2.41E-03 | 1.91E-03 | -8.94E-04 | -2.04E-03 | 0.025 | 36.05 | 0.0095 | -0.084 | 14.824 | 2.00 | 1.498 | 0.07 | 0.042 | 0.67 | 9.2 | 3.88E-03 | 117.1 |
| 8 | 22 | 2.38E-03 | 2.72E-03 | -1.41E-03 | -1.89E-03 | | 43.61 | 0.0176 | -0.106 | 17.258 | 3.00 | 2.100 | 0.28 | 0.096 | 0.53 | 11.1 | 6.10E-03 | 169.7 |
| | 23 | 2.11E-03 | 3.21E-03 | -2.17E-03 | -1.37E-03 | | 35.65 | 0.0195 | -0.080 | 15.193 | 3.00 | -- | -- | 0.069 | 0.44 | 9.1 | 1.06E-02 | 201.2 |
| | 24 | 2.48E-03 | 2.45E-03 | -8.92E-04 | -1.42E-03 | 0.20 | 32.21 | 0.0207 | -0.070 | 14.264 | 3.00 | -- | -- | 0.058 | 0.40 | 8.2 | 1.25E-02 | 225.2 |
| 9 | 25 | 2.30E-03 | 2.43E-03 | -2.55E-03 | -1.57E-03 | | 35.36 | 0.0401 | -0.078 | 15.237 | 5.00 | -- | -- | 0.140 | 0.25 | 9.0 | 1.96E-02 | 326.2 |
| | 26 | 3.69E-03 | 5.29E-03 | -7.52E-03 | -4.76E-04 | | 23.74 | 0.0431 | -0.045 | 11.933 | 5.00 | -- | -- | 0.095 | 0.18 | 6.1 | 1.96E-02 | 374.6 |
| | 27 | 4.13E-03 | 5.80E-03 | -5.59E-03 | -2.87E-04 | > 0.20 | 20.32 | 0.0442 | -0.037 | 10.901 | 5.00 | -- | -- | 0.081 | 0.15 | 5.1 | 1.66E-02 | 409.9 |
| 10 | 28 | 4.68E-03 | 6.94E-03 | -2.99E-03 | -1.63E-04 | | 21.19 | 0.0641 | -0.039 | 11.063 | 7.00 | -- | -- | 0.123 | 0.11 | 5.4 | 2.16E-02 | 488.0 |
| | 29 | 9.08E-03 | 9.50E-03 | -- | -2.40E-03 | | 15.45 | 0.0656 | -0.025 | 9.308 | 7.00 | -- | -- | 0.100 | 0.08 | 3.9 | -- | 534.2 |
| | 30 | 1.11E-02 | 8.93E-03 | -- | -6.82E-04 | > 0.20 | 13.21 | 0.0662 | -0.020 | 8.629 | 7.00 | -- | -- | 0.092 | 0.07 | 3.4 | -- | 570.6 |
| 11 | 31 | 1.65E-02 | 3.79E-03 | -- | -1.42E-03 | | 13.63 | 0.0844 | -0.020 | 8.688 | 8.82 | -- | -- | 0.115 | 0.06 | 3.5 | -- | 629.7 |
| | 32 | 1.65E-02 | 4.70E-03 | -- | -3.14E-03 | | 10.61 | 0.0853 | -0.016 | 6.962 | 8.82 | -- | -- | 0.103 | 0.04 | 2.7 | -- | 671.2 |
| | 33 | 1.65E-02 | 3.45E-03 | -- | -4.07E-03 | > 0.20 | 9.070 | 0.0862 | -0.012 | 6.446 | 8.82 | -- | -- | 0.106 | 0.04 | 2.3 | -- | 706.9 |

# Table 5.10 Test #5: Performance parameters ($0.1f'_cA_g$) down direction

| Load Step | Cycle | BEAM Steel Strain | COLN Steel Strain | BEAM Concrete Strain | COLN Concrete Strain | Crack Width in Joint | Lateral Load | Plastic Rotation | Principal Comp. Stress | Principal Tension Stress | Drift Ratio | Disp. Ductility Factor | Residual Deform. Index | Equiv. Visc Viscous Damping Ratio | Eff. Stiffness Ratio | Joint Strength Coeff. | Joint Shear Strain | Cumm. Energy |
|---|---|---|---|---|---|---|---|---|---|---|---|---|---|---|---|---|---|---|
| | | $\varepsilon_s$ | $\varepsilon_s$ | $\varepsilon_c$ | $\varepsilon_c$ | (in) | (kip) | $(\ )_p$ | $p_c$ (psi/f'$_c$) | $p_t$ (psi/$\sqrt{f'_c}$) | $\Delta$ (%) | $\mu_\Delta$ | RDI | $\xi_{eq}$ | $n_k$ | $\gamma$ | | (k-in) |
| 1 | 1 | 2.87E-04 | 1.66E-04 | -2.71E-03 | -8.17E-05 | | 6.44 | 0.0000 | -0.006 | 7.184 | 0.10 | 0.135 | 0.05 | 0.175 | 1.57 | 1.6 | 6.60E-05 | 0.8 |
| | 2 | 2.07E-04 | 1.43E-04 | -2.38E-03 | -7.70E-05 | | 3.88 | 0.0000 | -0.002 | 7.021 | 0.10 | 0.090 | 0.04 | 0.140 | 1.44 | 1.0 | 2.66E-05 | 1.0 |
| | 3 | 2.12E-04 | 9.15E-05 | -2.43E-03 | -7.38E-05 | 0.000 | 4.00 | 0.0000 | -0.002 | 7.007 | 0.10 | 0.092 | 0.04 | 0.122 | 1.42 | 1.0 | 5.73E-05 | 1.3 |
| 2 | 4 | 3.13E-04 | 1.88E-04 | -4.14E-03 | -1.11E-04 | | 8.83 | 0.0000 | -0.010 | 7.449 | 0.25 | 0.209 | 0.07 | 0.090 | 1.41 | 2.2 | 1.07E-04 | 2.1 |
| | 5 | 3.27E-04 | 2.53E-04 | -4.27E-03 | -8.36E-05 | | 8.62 | 0.0000 | -0.010 | 7.405 | 0.25 | 0.209 | 0.07 | 0.087 | 1.35 | 2.2 | 1.19E-04 | 2.9 |
| | 6 | 3.45E-04 | 3.06E-04 | -4.27E-03 | -6.82E-05 | 0.000 | 8.67 | 0.0000 | -0.010 | 7.434 | 0.25 | 0.212 | 0.06 | 0.078 | 1.34 | 2.2 | 1.14E-04 | 3.6 |
| 3 | 7 | 6.42E-04 | 3.95E-04 | -5.12E-03 | -4.17E-04 | | 15.64 | 0.0001 | -0.027 | 8.555 | 0.50 | 0.423 | 0.07 | 0.078 | 1.22 | 3.9 | 3.63E-04 | 6.3 |
| | 8 | 6.28E-04 | 4.04E-04 | -3.24E-03 | -4.51E-04 | | 14.96 | 0.0001 | -0.025 | 8.423 | 0.50 | 0.417 | 0.06 | 0.062 | 1.18 | 3.8 | 3.72E-04 | 8.3 |
| | 9 | 6.24E-04 | 4.13E-04 | -2.89E-03 | -4.67E-04 | 0.00 | 14.80 | 0.0002 | -0.025 | 8.393 | 0.50 | 0.417 | 0.09 | 0.058 | 1.16 | 3.7 | 3.60E-04 | 10.1 |
| 4 | 10 | 7.10E-04 | 8.92E-04 | -2.84E-03 | -6.24E-04 | | 20.94 | 0.0007 | -0.044 | 9.662 | 0.75 | 0.627 | 0.12 | 0.064 | 1.10 | 5.3 | 6.16E-04 | 14.4 |
| | 11 | 5.09E-04 | 9.76E-04 | -2.92E-03 | -4.39E-04 | | 20.44 | 0.0008 | -0.042 | 9.544 | 0.75 | 0.627 | 0.10 | 0.056 | 1.07 | 5.2 | 6.07E-04 | 18.1 |
| | 12 | 4.10E-04 | 1.01E-03 | -1.80E-03 | -3.86E-04 | 0.004 | 20.02 | 0.0010 | -0.041 | 9.455 | 0.75 | 0.624 | 0.12 | 0.049 | 1.07 | 5.1 | 6.18E-04 | 21.2 |
| 5 | 13 | 4.18E-04 | 1.36E-03 | -2.17E-03 | -1.17E-03 | | 25.68 | 0.0017 | -0.059 | 10.709 | 1.00 | 0.839 | 0.12 | 0.057 | 1.01 | 6.5 | 9.95E-04 | 27.5 |
| | 14 | 4.42E-04 | 1.43E-03 | -1.39E-03 | -2.43E-03 | | 24.95 | 0.0019 | -0.057 | 10.547 | 1.00 | 0.839 | 0.12 | 0.049 | 0.98 | 6.3 | 1.01E-03 | 32.7 |
| | 15 | 4.32E-04 | 1.46E-03 | -1.24E-03 | -2.63E-03 | 0.008 | 24.39 | 0.0021 | -0.055 | 10.443 | 1.00 | 0.835 | 0.14 | 0.045 | 0.96 | 6.2 | 1.02E-03 | 37.4 |
| 6 | 16 | 8.56E-04 | 2.58E-03 | -1.87E-03 | -5.60E-03 | | 34.50 | 0.0045 | -0.088 | 12.936 | 1.50 | 1.300 | 0.20 | 0.060 | 0.88 | 8.8 | 2.01E-03 | 51.3 |
| | 17 | 7.24E-04 | 1.88E-03 | -1.82E-03 | -4.90E-03 | | 31.78 | 0.0046 | -0.079 | 12.302 | 1.50 | 1.246 | 0.17 | 0.045 | 0.84 | 8.1 | 1.97E-03 | 60.5 |
| | 18 | 8.34E-04 | 1.46E-03 | -1.84E-03 | -4.91E-03 | 0.020 | 31.58 | 0.0048 | -0.078 | 12.243 | 1.50 | 1.255 | 0.19 | 0.040 | 0.83 | 8.0 | 2.02E-03 | 68.7 |
| 7 | 19 | 1.48E-03 | 1.74E-03 | -1.86E-03 | -5.52E-03 | | 38.24 | 0.0076 | -0.100 | 13.939 | 2.00 | 1.663 | 0.27 | 0.060 | 0.76 | 9.7 | 2.89E-03 | 88.1 |
| | 20 | 2.10E-03 | 2.21E-03 | -1.99E-03 | -3.68E-03 | | 36.79 | 0.0086 | -0.095 | 13.600 | 2.00 | 1.704 | 0.32 | 0.050 | 0.71 | 9.4 | 2.96E-03 | 104.1 |
| | 21 | 2.57E-03 | 2.30E-03 | -1.45E-03 | -2.63E-03 | 0.025 | 33.93 | 0.0089 | -0.085 | 12.922 | 2.00 | 1.666 | 0.31 | 0.045 | 0.67 | 8.6 | 2.91E-03 | 117.1 |
| 8 | 22 | 1.66E-03 | 1.65E-02 | -5.53E-03 | -3.33E-03 | | 37.20 | 0.0178 | -0.095 | 13.984 | 3.00 | 1.800 | 0.71 | 0.113 | 0.49 | 9.4 | 4.39E-03 | 169.7 |
| | 23 | 1.49E-03 | 1.65E-02 | -1.93E-03 | -3.47E-03 | | 31.16 | 0.0199 | -0.074 | 12.553 | 3.00 | -- | -- | 0.080 | 0.42 | 7.9 | 3.45E-03 | 201.2 |
| | 24 | 1.55E-03 | 1.65E-02 | -2.15E-03 | -2.61E-03 | 0.20 | 28.21 | 0.0208 | -0.064 | 11.830 | 3.00 | -- | -- | 0.067 | 0.37 | 7.2 | 2.73E-03 | 225.2 |
| 9 | 25 | 6.85E-03 | 1.10E-02 | -5.60E-03 | -- | | 27.15 | 0.0416 | -0.061 | 11.623 | 5.00 | -- | -- | 0.177 | 0.21 | 6.9 | 1.16E-02 | 326.2 |
| | 26 | 1.12E-02 | 1.06E-02 | -4.02E-03 | -- | | 19.08 | 0.0440 | -0.036 | 9.603 | 5.00 | -- | -- | 0.119 | 0.15 | 4.8 | 1.37E-02 | 374.6 |
| | 27 | 1.34E-02 | 8.98E-03 | -1.51E-03 | -- | > 0.20 | 15.78 | 0.0451 | -0.027 | 8.836 | 5.00 | -- | -- | 0.105 | 0.12 | 4.0 | 1.42E-02 | 409.9 |
| 10 | 28 | 1.64E-02 | 1.01E-02 | -- | -- | | 15.74 | 0.0652 | -0.025 | 9.529 | 7.00 | -- | -- | 0.169 | 0.09 | 4.0 | 1.43E-02 | 488.0 |
| | 29 | 1.65E-02 | 8.81E-03 | -- | -- | | 11.12 | 0.0665 | -0.014 | 8.393 | 7.00 | -- | -- | 0.141 | 0.06 | 2.8 | 2.68E-02 | 534.2 |
| | 30 | 1.65E-02 | 6.58E-03 | -- | -- | > 0.20 | 8.84 | 0.0672 | -0.009 | 7.921 | 7.00 | -- | -- | 0.138 | 0.05 | 2.2 | 2.99E-02 | 570.6 |
| 11 | 31 | 1.65E-02 | 6.94E-03 | -- | -- | | 9.45 | 0.0857 | -0.013 | 7.508 | 8.82 | -- | -- | 0.168 | 0.04 | 2.4 | -- | 629.7 |
| | 32 | 1.65E-02 | 4.60E-03 | -- | -- | | 6.37 | 0.0863 | -0.006 | 6.092 | 8.82 | -- | -- | 0.173 | 0.03 | 1.6 | -- | 671.2 |
| | 33 | 1.65E-02 | 5.35E-03 | -- | -- | > 0.20 | 5.40 | 0.0921 | -0.005 | 6.063 | 8.82 | -- | -- | 0.168 | 0.02 | 1.4 | -- | 706.9 |

## Table 5.11 Test #6: Performance parameters ($0.25f'_cA_g$) up direction

| Load Step | Cycle | BEAM Steel Strain | COLN Steel Strain | BEAM Concrete Strain | COLN Concrete Strain | Crack Width in Joint | Lateral Load | Plastic Rotation | Principal Comp. Stress | Principal Tension Stress | Drift Ratio | Disp. Ductility Factor | Residual Deform. Index | Equiv. Visc Viscous Damping Ratio | Eff. Stiffness Ratio | Joint Strength Coeff. | Joint Shear Strain | Cumm. Energy |
|---|---|---|---|---|---|---|---|---|---|---|---|---|---|---|---|---|---|---|
| | | $\varepsilon_s$ | $\varepsilon_s$ | $\varepsilon_c$ | $\varepsilon_c$ | (in) | (kip) | $(\,)_p$ | $p_c$ (psi/$f'_c$) | $p_t$ (psi/$\sqrt{f'_c}$) | $\Delta$ (%) | $\mu_\Delta$ | RDI | $\xi_{eq}$ | $n_k$ | $\gamma$ | | (k-in) |
| | 1 | 4.48E-04 | 9.13E-05 | -2.17E-04 | -7.02E-05 | | 9.76 | 0.0000 | -0.001 | 14.884 | 0.10 | 0.216 | 0.00 | 0.039 | 1.27 | 0.9 | 1.30E-04 | 0.4 |
| 1 | 2 | 1.99E-04 | 1.06E-04 | -1.39E-04 | -4.82E-05 | | 3.71 | 0.0000 | -0.001 | 14.869 | 0.10 | 0.086 | 0.00 | 0.094 | 1.19 | 0.9 | 3.32E-05 | 0.6 |
| | 3 | 2.04E-04 | 1.07E-04 | -1.39E-04 | -5.09E-05 | 0.000 | 3.89 | 0.0000 | -0.001 | 14.839 | 0.10 | 0.090 | 0.00 | 0.084 | 1.20 | 1.0 | 2.92E-05 | 0.7 |
| | 4 | 4.67E-04 | 1.26E-04 | -2.60E-04 | -6.00E-05 | | 9.42 | 0.0000 | -0.006 | 14.914 | 0.25 | 0.208 | 0.00 | 0.065 | 1.26 | 2.4 | 1.18E-04 | 1.4 |
| 2 | 5 | 5.11E-04 | 1.29E-04 | -6.33E-04 | -6.78E-05 | | 9.60 | 0.0000 | -0.006 | 14.914 | 0.25 | 0.208 | 0.00 | 0.054 | 1.28 | 2.5 | 1.29E-04 | 2.0 |
| | 6 | 6.43E-04 | 1.33E-04 | -7.36E-04 | -7.74E-05 | Hairline | 9.48 | 0.0000 | -0.006 | 14.854 | 0.25 | 0.210 | 0.00 | 0.048 | 1.28 | 2.4 | 1.25E-04 | 2.5 |
| | 7 | 1.36E-03 | 2.13E-04 | -3.67E-03 | -2.81E-04 | | 17.21 | 0.0000 | -0.019 | 15.287 | 0.50 | 0.408 | 0.00 | 0.063 | 1.18 | 4.4 | 2.95E-04 | 4.9 |
| 3 | 8 | 3.10E-03 | 2.13E-04 | -3.65E-03 | -5.92E-03 | | 17.17 | 0.0000 | -0.019 | 15.316 | 0.50 | 0.407 | 0.00 | 0.040 | 1.17 | 4.4 | 2.99E-04 | 6.3 |
| | 9 | 1.14E-03 | 1.75E-04 | -4.35E-03 | -5.43E-04 | Hairline | 17.06 | 0.0000 | -0.019 | 15.302 | 0.50 | 0.409 | 0.00 | 0.035 | 1.16 | 4.3 | 3.01E-04 | 7.7 |
| | 10 | 1.94E-03 | 3.05E-04 | -6.66E-03 | -7.91E-04 | | 24.27 | 0.0002 | -0.036 | 16.122 | 0.75 | 0.609 | 0.00 | 0.047 | 1.11 | 6.2 | 5.15E-04 | 11.4 |
| 4 | 11 | 2.85E-03 | 2.37E-04 | -5.66E-03 | -8.92E-04 | | 23.91 | 0.0004 | -0.035 | 16.137 | 0.75 | 0.610 | 0.00 | 0.038 | 1.09 | 6.1 | 5.18E-04 | 14.3 |
| | 12 | 9.99E-03 | 2.86E-04 | -4.03E-03 | -8.94E-04 | 0.003 | 23.36 | 0.0004 | -0.034 | 16.092 | 0.75 | 0.605 | 0.00 | 0.036 | 1.08 | 5.9 | 5.08E-04 | 16.9 |
| | 13 | 5.65E-03 | 4.83E-04 | -6.39E-03 | -8.63E-04 | | 30.60 | 0.0010 | -0.054 | 17.166 | 1.00 | 0.820 | 0.05 | 0.046 | 1.04 | 7.8 | 8.04E-04 | 23.1 |
| 5 | 14 | 5.70E-03 | 4.72E-04 | -5.86E-03 | -9.18E-04 | | 28.57 | 0.0014 | -0.048 | 16.912 | 1.00 | 0.808 | 0.04 | 0.038 | 0.99 | 7.3 | 8.24E-04 | 27.8 |
| | 15 | 5.82E-03 | 4.58E-04 | -5.85E-03 | -9.02E-04 | 0.004 | 28.20 | 0.0015 | -0.047 | 16.867 | 1.00 | 0.811 | 0.04 | 0.036 | 0.97 | 7.2 | 8.33E-04 | 32.1 |
| | 16 | 1.11E-02 | 9.98E-04 | -8.60E-03 | -1.36E-03 | | 37.53 | 0.0036 | -0.075 | 18.583 | 1.50 | 1.202 | 0.11 | 0.057 | 0.87 | 9.6 | 1.59E-03 | 45.8 |
| 6 | 17 | 1.01E-02 | 9.96E-04 | -5.95E-03 | -1.11E-03 | | 35.00 | 0.0044 | -0.067 | 18.269 | 1.50 | 1.211 | 0.08 | 0.043 | 0.80 | 8.9 | 1.68E-03 | 55.5 |
| | 18 | 8.45E-03 | 9.91E-04 | -5.27E-03 | -1.07E-03 | 0.01 | 33.98 | 0.0047 | -0.063 | 18.120 | 1.50 | 1.209 | 0.07 | 0.040 | 0.79 | 8.7 | 1.74E-03 | 64.3 |
| | 19 | 1.38E-02 | 1.39E-03 | -6.21E-03 | -1.55E-03 | | 41.96 | 0.0073 | -0.088 | 19.791 | 2.00 | 1.609 | 0.15 | 0.060 | 0.73 | 10.7 | 2.65E-03 | 85.9 |
| 7 | 20 | 5.97E-03 | 1.96E-03 | -6.88E-03 | -1.65E-03 | | 38.59 | 0.0084 | -0.077 | 19.224 | 2.00 | 1.612 | 0.11 | 0.050 | 0.67 | 9.8 | 3.12E-03 | 102.2 |
| | 21 | 1.02E-02 | 1.90E-03 | -7.58E-03 | -2.00E-03 | 0.02 | 37.54 | 0.0087 | -0.073 | 19.045 | 2.00 | 1.616 | 0.11 | 0.047 | 0.64 | 9.6 | 3.36E-03 | 117.4 |
| | 22 | 8.91E-03 | 7.45E-03 | -1.30E-02 | -1.78E-03 | | 44.39 | 0.0163 | -0.094 | 20.715 | 3.00 | 2.300 | 0.35 | 0.105 | 0.52 | 11.3 | 6.54E-03 | 176.0 |
| 8 | 23 | 7.43E-03 | 8.58E-03 | -1.22E-02 | -1.07E-02 | | 35.33 | 0.0191 | -0.065 | 18.911 | 3.00 | -- | 0.11 | 0.082 | 0.41 | 9.0 | 8.51E-03 | 213.0 |
| | 24 | 3.91E-03 | 1.76E-03 | -1.12E-02 | -1.03E-02 | 0.10 | 31.54 | 0.0205 | -0.054 | 18.180 | 3.00 | -- | 0.04 | 0.067 | 0.36 | 8.0 | 8.93E-03 | 240.4 |
| | 25 | 1.05E-02 | 1.45E-02 | -1.64E-02 | -8.24E-03 | | 34.91 | 0.0398 | -0.064 | 18.955 | 5.00 | -- | 0.64 | 0.154 | 0.23 | 8.9 | 1.59E-02 | 349.4 |
| 9 | 26 | 1.23E-02 | 1.52E-02 | -1.61E-02 | -4.49E-03 | | 22.80 | 0.0431 | -0.032 | 16.450 | 5.00 | -- | -- | 0.101 | 0.16 | 5.8 | 2.24E-02 | 398.9 |
| | 27 | 1.47E-02 | 1.30E-02 | -1.79E-03 | -5.22E-03 | 0.30 | 19.26 | 0.0443 | -0.023 | 15.764 | 5.00 | -- | -- | 0.083 | 0.13 | 4.9 | 2.42E-02 | 433.2 |
| | 28 | 8.13E-03 | 1.59E-02 | -2.41E-03 | -4.22E-03 | | 20.44 | 0.0639 | -0.025 | 16.584 | 7.00 | -- | -- | 0.128 | 0.10 | 5.2 | 3.05E-02 | 510.9 |
| 10 | 29 | 8.32E-03 | 1.40E-02 | -5.75E-03 | -4.41E-03 | | 14.87 | 0.0656 | -0.016 | 13.452 | 7.00 | -- | -- | 0.122 | 0.07 | 3.8 | 3.61E-02 | 565.0 |
| | 30 | 1.49E-02 | 5.62E-03 | -2.82E-03 | -6.55E-03 | > 0.30 | 12.44 | 0.0663 | -0.012 | 12.811 | 7.00 | -- | -- | 0.086 | 0.06 | 3.1 | 6.35E-02 | 597.0 |
| | 31 | -- | -- | -- | -- | | -- | -- | -- | -- | 8.82 | -- | -- | -- | -- | -- | -- | -- |
| 11 | 32 | -- | -- | -- | -- | | -- | -- | -- | -- | 8.82 | -- | -- | -- | -- | -- | -- | -- |
| | 33 | -- | -- | -- | -- | -- | -- | -- | -- | -- | 8.82 | -- | -- | -- | -- | -- | -- | -- |

## Table 5.12 Test #6: Performance parameters ($0.25f'_cA_g$) down direction

| Load Step | Cycle | BEAM Steel Strain | COLN Steel Strain | BEAM Concrete Strain | COLN Concrete Strain | Crack Width in Joint | Lateral Load | Plastic Rotation | Principal Comp. Stress | Principal Tension Stress | Drift Ratio | Disp. Ductility Factor | Residual Deform. Index | Equiv. Visc Viscous Damping Ratio | Eff. Stiffness Ratio | Joint Strength Coeff. | Joint Shear Strain | Cumm. Energy |
|---|---|---|---|---|---|---|---|---|---|---|---|---|---|---|---|---|---|---|
| | | $\varepsilon_s$ | $\varepsilon_s$ | $\varepsilon_c$ | $\varepsilon_c$ | (in) | (kip) | $(\ )_p$ | $p_c$ (psi/f'$_c$) | $p_t$ (psi/√f'$_c$) | Δ (%) | $\mu_\Delta$ | RDI | $\xi_{eq}$ | $n_k$ | $\gamma$ | | (k-in) |
| 1 | 1 | 1.72E-04 | 1.00E-04 | -1.69E-04 | -5.63E-05 | | 4.75 | 0.0000 | -0.002 | 15.242 | 0.10 | 0.090 | 0.02 | 0.200 | 1.48 | 1.2 | 6.55E-05 | 0.4 |
| | 2 | 1.77E-04 | 1.01E-04 | -1.59E-04 | -5.67E-05 | | 4.40 | 0.0000 | -0.001 | 15.212 | 0.10 | 0.086 | 0.03 | 0.082 | 1.41 | 1.1 | 6.99E-05 | 0.6 |
| | 3 | 1.98E-04 | 1.05E-04 | -1.46E-04 | -5.69E-05 | 0.000 | 4.50 | 0.0000 | -0.001 | 15.212 | 0.10 | 0.088 | 0.02 | 0.078 | 1.42 | 1.1 | 6.70E-05 | 0.7 |
| 2 | 4 | 7.60E-04 | 8.76E-05 | -8.63E-04 | -1.06E-04 | | 9.59 | 0.0000 | -0.006 | 15.719 | 0.25 | 0.213 | 0.06 | 0.065 | 1.24 | 2.4 | 1.49E-04 | 1.4 |
| | 5 | 7.55E-04 | 1.01E-04 | -1.01E-03 | -1.15E-04 | | 9.23 | 0.0000 | -0.005 | 15.615 | 0.25 | 0.210 | 0.05 | 0.058 | 1.23 | 2.3 | 1.44E-04 | 2.0 |
| | 6 | 7.59E-04 | 9.95E-05 | -1.06E-03 | -1.20E-04 | Hairline | 9.14 | 0.0000 | -0.005 | 15.555 | 0.25 | 0.215 | 0.05 | 0.051 | 1.19 | 2.3 | 1.39E-04 | 2.5 |
| 3 | 7 | 3.10E-03 | 1.73E-04 | -8.25E-04 | -4.01E-04 | | 19.35 | 0.0000 | -0.022 | 17.121 | 0.50 | 0.458 | 0.09 | 0.052 | 1.17 | 4.9 | 3.74E-04 | 4.9 |
| | 8 | 4.79E-03 | 1.43E-04 | -9.03E-04 | -5.64E-04 | | 17.37 | 0.0002 | -0.018 | 16.808 | 0.50 | 0.425 | 0.06 | 0.040 | 1.13 | 4.4 | 3.41E-04 | 6.3 |
| | 9 | 3.11E-03 | 1.58E-04 | -9.50E-04 | -6.27E-04 | Hairline | 17.01 | 0.0002 | -0.017 | 16.763 | 0.50 | 0.422 | 0.06 | 0.036 | 1.12 | 4.3 | 3.42E-04 | 7.7 |
| 4 | 10 | 1.37E-02 | 2.75E-04 | -7.64E-04 | -9.70E-04 | | 24.57 | 0.0006 | -0.033 | 18.210 | 0.75 | 0.632 | 0.10 | 0.047 | 1.07 | 6.3 | 6.17E-04 | 11.4 |
| | 11 | 3.77E-03 | 2.71E-04 | -1.68E-03 | -9.44E-04 | | 24.23 | 0.0007 | -0.032 | 18.180 | 0.75 | 0.632 | 0.06 | 0.037 | 1.06 | 6.1 | 6.40E-04 | 14.3 |
| | 12 | 1.53E-02 | 2.69E-04 | -1.59E-03 | -9.38E-04 | 0.003 | 23.76 | 0.0007 | -0.031 | 18.120 | 0.75 | 0.629 | 0.09 | 0.035 | 1.05 | 6.0 | 6.38E-04 | 16.9 |
| 5 | 13 | 3.37E-03 | 4.71E-04 | -1.49E-03 | -1.06E-03 | | 30.21 | 0.0015 | -0.046 | 19.597 | 1.00 | 0.840 | 0.10 | 0.048 | 0.99 | 7.7 | 1.13E-03 | 23.1 |
| | 14 | 1.89E-03 | 4.74E-04 | -2.88E-03 | -1.11E-03 | | 29.41 | 0.0016 | -0.044 | 19.492 | 1.00 | 0.840 | 0.09 | 0.037 | 0.97 | 7.5 | 1.18E-03 | 27.8 |
| | 15 | 2.75E-03 | 4.74E-04 | -1.26E-03 | -1.09E-03 | 0.004 | 29.10 | 0.0017 | -0.043 | 19.433 | 1.00 | 0.839 | 0.11 | 0.035 | 0.96 | 7.4 | 1.19E-03 | 32.1 |
| 6 | 16 | 8.95E-03 | 9.34E-04 | -1.60E-03 | -1.30E-03 | | 39.12 | 0.0039 | -0.069 | 22.087 | 1.50 | 1.257 | 0.16 | 0.055 | 0.87 | 10.0 | 2.38E-03 | 45.8 |
| | 17 | 7.91E-03 | 8.79E-04 | -1.79E-03 | -1.29E-03 | | 37.89 | 0.0043 | -0.065 | 21.908 | 1.50 | 1.261 | 0.11 | 0.040 | 0.83 | 9.6 | 2.46E-03 | 55.5 |
| | 18 | 7.43E-03 | 8.43E-04 | -1.81E-03 | -1.29E-03 | 0.01 | 36.87 | 0.0045 | -0.062 | 21.744 | 1.50 | 1.259 | 0.14 | 0.037 | 0.81 | 9.4 | 2.51E-03 | 64.3 |
| 7 | 19 | 1.41E-02 | 1.34E-03 | -1.28E-02 | -2.56E-03 | | 43.12 | 0.0078 | -0.078 | 23.608 | 2.00 | 1.674 | 0.15 | 0.059 | 0.71 | 11.0 | 3.89E-03 | 85.9 |
| | 20 | 1.41E-02 | 1.70E-03 | -8.93E-03 | -2.97E-03 | | 40.53 | 0.0085 | -0.071 | 23.027 | 2.00 | 1.678 | 0.22 | 0.047 | 0.67 | 10.3 | 4.11E-03 | 102.2 |
| | 21 | 1.60E-02 | 2.19E-03 | -4.98E-03 | -3.28E-03 | 0.02 | 38.64 | 0.0090 | -0.066 | 22.624 | 2.00 | 1.679 | 0.24 | 0.046 | 0.64 | 9.8 | 4.26E-03 | 117.4 |
| 8 | 22 | 3.28E-03 | 5.30E-03 | -4.75E-03 | -6.97E-03 | | 42.02 | 0.0183 | -0.074 | 23.579 | 3.00 | 1.700 | 0.68 | 0.110 | 0.46 | 10.7 | 7.91E-03 | 176.0 |
| | 23 | 3.51E-03 | 2.92E-03 | -4.70E-03 | -1.09E-02 | | 34.37 | 0.0204 | -0.054 | 21.565 | 3.00 | -- | 0.77 | 0.084 | 0.38 | 8.7 | 8.64E-03 | 213.0 |
| | 24 | 3.45E-03 | 2.54E-03 | -4.52E-03 | -9.46E-03 | 0.10 | 31.03 | 0.0213 | -0.046 | 20.715 | 3.00 | -- | 0.84 | 0.069 | 0.34 | 7.9 | 8.68E-03 | 240.4 |
| 9 | 25 | 5.86E-03 | 1.52E-02 | -1.60E-02 | -7.27E-03 | | 30.11 | 0.0420 | -0.045 | 20.148 | 5.00 | -- | 2.34 | 0.178 | 0.20 | 7.7 | 1.61E-02 | 349.4 |
| | 26 | 1.35E-02 | 1.47E-02 | -1.30E-02 | -1.17E-02 | | 20.42 | 0.0445 | -0.024 | 17.285 | 5.00 | -- | -- | 0.113 | 0.13 | 5.2 | 1.74E-02 | 398.9 |
| | 27 | 6.05E-03 | 1.59E-02 | -3.13E-03 | -1.21E-02 | 0.30 | 16.14 | 0.0456 | -0.016 | 16.181 | 5.00 | -- | -- | 0.101 | 0.11 | 4.1 | 1.89E-02 | 433.2 |
| 10 | 28 | 1.54E-02 | 1.59E-02 | -8.32E-03 | -1.03E-02 | | 16.69 | 0.0654 | -0.017 | 16.301 | 7.00 | -- | -- | 0.156 | 0.08 | 4.2 | 2.32E-02 | 510.9 |
| | 29 | 1.47E-02 | 1.45E-02 | -1.26E-02 | -7.00E-03 | | 12.77 | 0.0755 | -0.012 | 13.064 | 7.00 | -- | -- | 0.126 | 0.05 | 3.3 | 2.08E-02 | 565.0 |
| | 30 | 1.57E-02 | 8.84E-03 | -3.55E-03 | -7.53E-03 | > 0.30 | 6.50 | 0.0683 | -0.003 | 11.752 | 7.00 | -- | -- | 0.16646494 | 0.03 | 1.6 | -- | 597.0 |
| 11 | 31 | -- | -- | -- | -- | | -- | -- | -- | -- | 8.82 | -- | -- | -- | -- | -- | -- | -- |
| | 32 | -- | -- | -- | -- | | -- | -- | -- | -- | 8.82 | -- | -- | -- | -- | -- | -- | -- |
| | 33 | -- | -- | -- | -- | -- | -- | -- | -- | -- | 8.82 | -- | -- | -- | -- | -- | -- | -- |

## 5.2 PERFORMANCE LEVELS

Five levels of performance were used to characterize the exterior joints. These levels were determined based on the evaluation and comparison of the previously tabulated parameters. After analysis of the six joint test units, the governing parameters for delineating between performance levels were found to be drift, plastic rotation, joint crack width, and the joint strength coefficient $\gamma$. The type and extent of damage in the joint associated with each step was also used as a parameter for determining the performance levels. The difference in axial compression load caused slight differences but did not affect the order or description of the performance levels. The most significant factor was the difference in the detailing of test units 1 and 2 versus 3, 4, 5, and 6, which caused different modes of failure. Owing to the different modes of failure, two sets of performance levels were developed.

For test units 1 and 2, Level I is the first yielding of longitudinal reinforcement, which was characterized by barely visible, initial cracking in the joint or no cracking at all. Level II represents the full development of the bond-slip mechanism of the bottom beam bars in the joint. This level occurred at the peak lateral load and was characterized by cracking in the joint less than 0.01 in. wide. Level III represents significant diagonal cracking in the joint ( > 0.02 in. wide) and the extension of these cracks into the column. Level IV was characterized by the spalling of concrete at the corner of the joint where the bottom beam bars were slipping. Level V is total loss of lateral-load-carrying capacity.

For test units 3, 4, 5, and 6, Level I is also the first yielding of longitudinal reinforcement and was characterized by barely visible, initial cracking in the joint or no cracking at all. Level II represents significant diagonal cracking in the joint ( > 0.02 in. wide) and the extension of these cracks into the column. Level III represents the full development of the joint shear mechanism. This level occurred at the peak lateral load and was characterized by extensive cracking in the joint and the extension of diagonal joint cracks into the column. Level IV was characterized by the spalling of concrete in the core of the joint. Level V is total loss of gravity-load-carrying capacity.

The performance levels with detailed descriptions are shown for each beam-column joint test unit in Tables 5.13 through 5.18. Accompanying these tables are Figures 5.1 through 5.12, which include performance levels marked on each joint's respective hysteretic-envelope curve and photographic documentation of each joint at all five performance levels.

It should be noted that these performance levels are based on only six joint tests. The parameters are average values. Further studies are needed to generalize the findings of this investigation and to determine the performance levels for higher axial load levels.

## Table 5.13 Test #1 performance levels ($0.1f'_cA_g$)

| Level | Performance Description | Cycle | Drift % | Lateral Load kip (kN) | Plastic Rotation radians | $\gamma$ psi (Mpa) | Crack Width in (mm) |
|---|---|---|---|---|---|---|---|
| I | First yield in longitudinal reinforcement (column) | 10 | .75 | 18.4 (82) | 0.002 | 4.6 (0.38) | Hairline |
| II | Formation of bond slip mechanism | 16 | 1.5 | 20.7 (92) | 0.016 | 5.2 (0.43) | 0.008 (0.2) |
| III | Significant cracking in joint, w > 0.02 in (0.5mm) | 19 | 2.0 | 18.3 (81) | 0.010 | 4.6 (0.38) | 0.04 (1.0) |
| IV | Significant spalling of concrete at corner | 22 | 3.0 | 14.6 (65) | 0.029 | 3.6 (0.30) | 0.08 (2.0) |
| V | Loss of lateral load | 28 | 7.0 | 5.6 (25) | 0.078 | 1.7 (0.14) | 0.30 (8.0) |

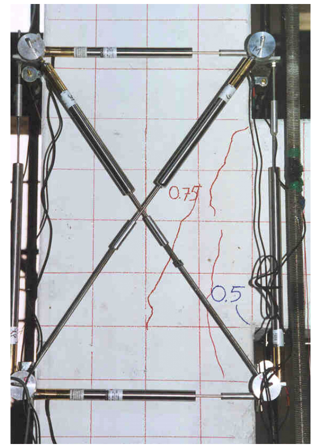

Level I

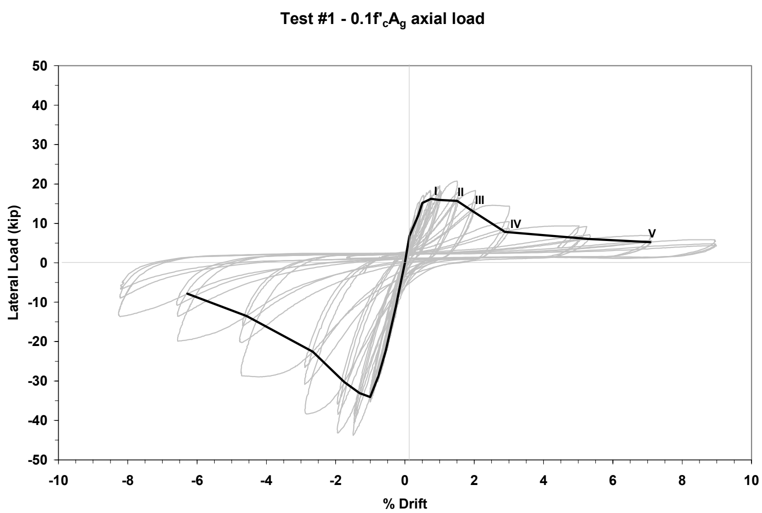


**Fig. 5.1 Test #1 performance level identification curve**

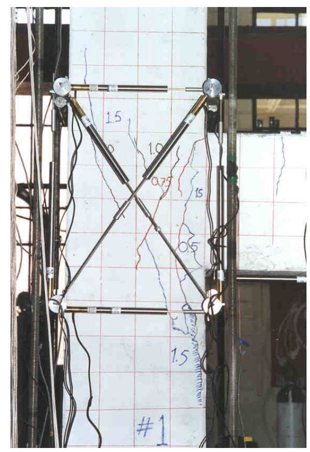

Level II

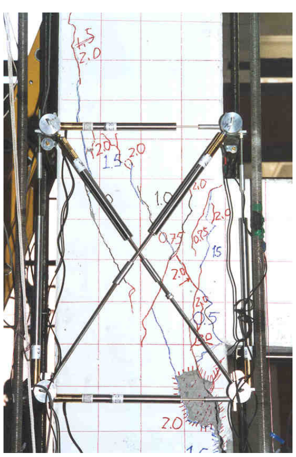

Level III

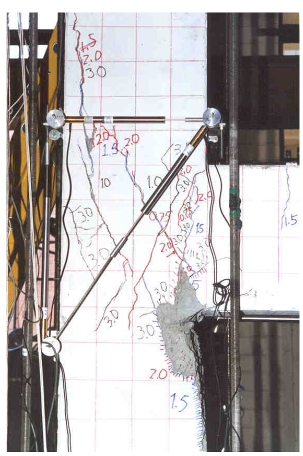

Level IV

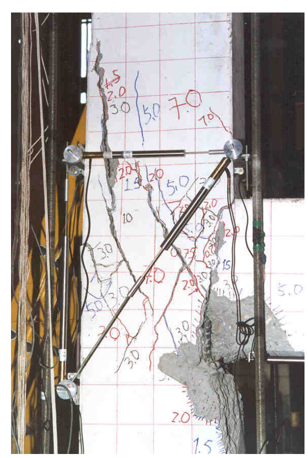

Level V

**Fig. 5.2 Test #1 photo documentation of performance levels**

**Table 5.14 Test #2 performance levels ($0.25f'_cA_g$)**

| Level | Performance Description | Cycle | Drift % | Lateral Load kip (kN) | Plastic Rotation radians | $\gamma$ psi (Mpa) | Crack Width in (mm) |
|---|---|---|---|---|---|---|---|
| I | First yield in longitudinal reinforcement (beam) | 8 | .50 | 18.9 (84) | 0.000 | 4.7 (0.39) | None |
| II | Formation of bond slip mechanism | 16 | 1.5 | 28.3 (126) | 0.007 | 7.0 (0.58) | 0.01 (0.3) |
| III | Significant cracking in joint, w > 0.02 in (0.5mm) | 19 | 2.0 | 25.5 (113) | 0.013 | 6.3 (0.53) | 0.02 (0.5) |
| IV | Significant spalling of concrete at corner | 22 | 3.0 | 17.9 (80) | 0.025 | 4.5 (0.38) | 0.10 (3.0) |
| V | Loss of lateral load | 28 | 7.0 | 8.3 (37) | 0.068 | 2.1 (0.18) | > 0.10 (3.0) |

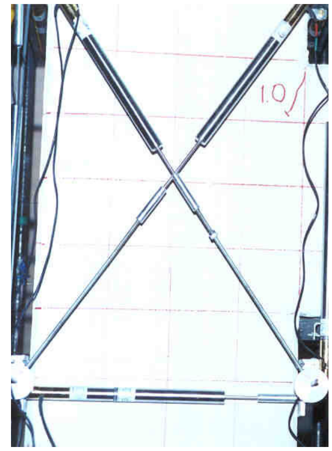


Level I

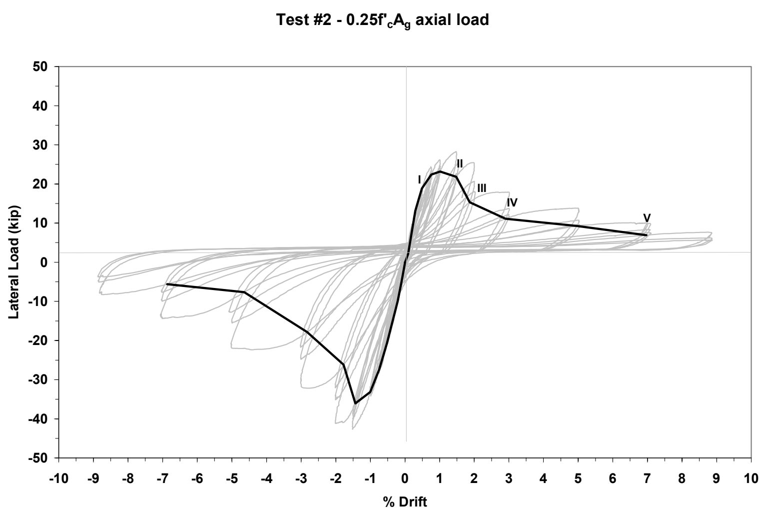


**Fig. 5.3 Test #2 performance level identification curve**

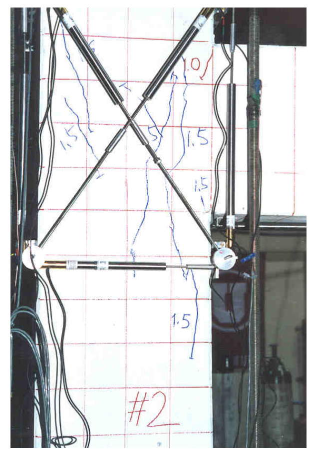


Level II

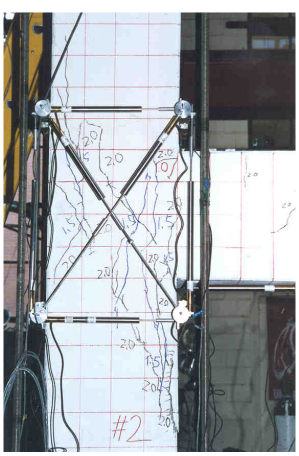


Level III

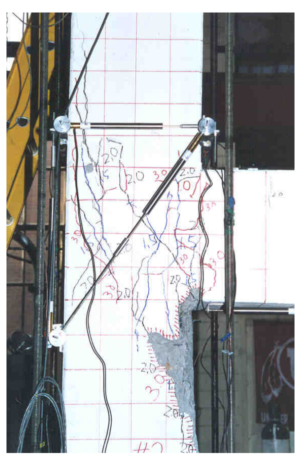

Level IV

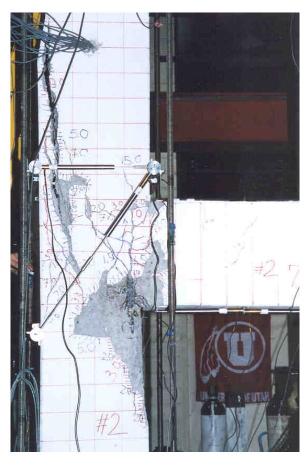


Level V

**Fig. 5.4 Test #2 photo documentation of performance levels**

**Table 5.15 Test #3 performance levels ($0.1f'_cA_g$)**

| Level | Performance Description | Cycle | Drift % | Lateral Load kip (kN) | Plastic Rotation radians | $\gamma$ psi (Mpa) | Crack Width in (mm) |
|---|---|---|---|---|---|---|---|
| I | First yield in longitudinal reinforcement (beam) | 7 | .50 | 20.8 (93) | 0.0004 | 5.1 (0.43) | Hairline |
| II | Significant cracking in joint, w > 0.02 in (0.5mm) | 16 | 1.5 | 39.3 (175) | 0.006 | 9.7 (0.81) | 0.02 (0.4) |
| III | Formation of joint shear mechanism | 19 | 2.0 | 42.2 (188) | 0.011 | 10.4 (0.87) | 0.05 (1.3) |
| IV | Significant spalling of concrete in core | 25 | 5.0 | 30.0 (133) | 0.044 | 7.4 (0.62) | 0.1 (3.0) |
| V | Loss of gravity load | 31 | 9.0 | 10.9 (48) | 0.086 | 2.7 (0.23) | >0.1 (3.0) |

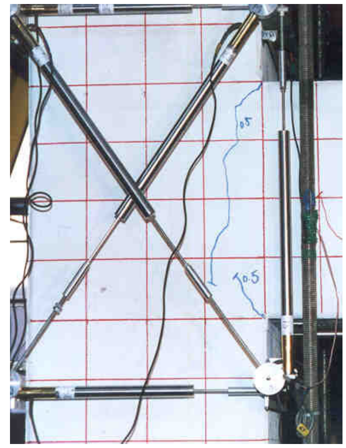

Level I

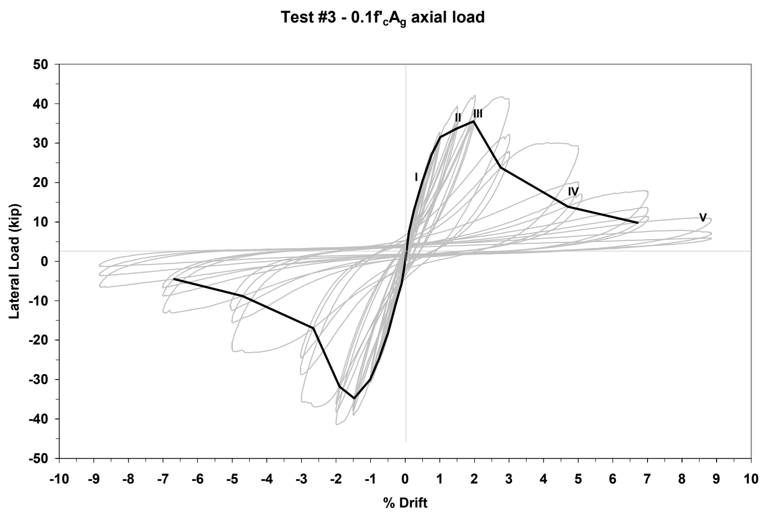


**Fig. 5.5 Test #3 performance level identification curve**

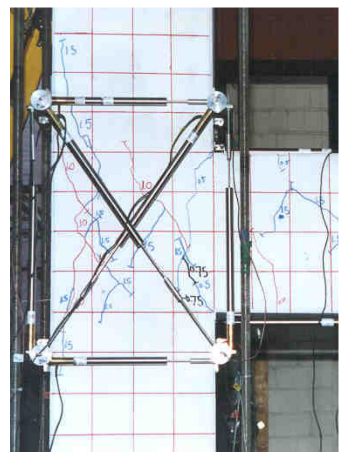

Level II

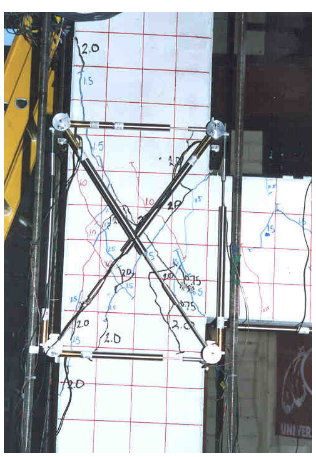

Level III

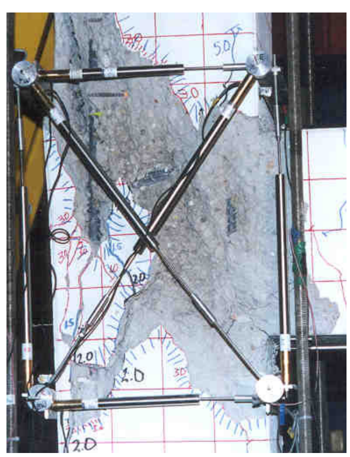

Level IV

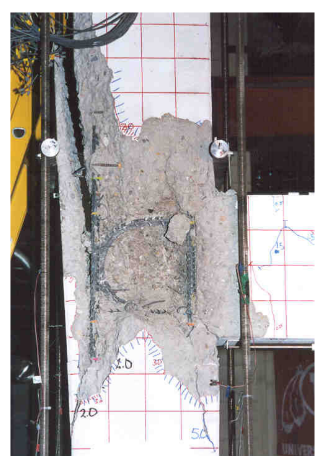

Level V

**Fig. 5.6 Test #3 photo documentation of performance levels**

**Table 5.16 Test #4 performance levels (0.25f′$_c$A$_g$)**

| Level | Performance Description | Cycle | Drift % | Lateral Load Kip (kN) | Plastic Rotation radians | $\gamma$ psi (Mpa) | Crack Width in (mm) |
|---|---|---|---|---|---|---|---|
| I | First yield in longitudinal reinforcement (beam) | 7 | .50 | 19.3 (86) | 0.000 | 4.7 (0.39) | Hairline |
| II | Significant cracking in joint, w > 0.02 in (0.5mm) | 16 | 1.5 | 41.7 (185) | 0.004 | 10.2 (0.85) | 0.008 (0.2) |
| III | Formation of joint shear mechanism | 19 | 2.0 | 45.1 (201) | 0.008 | 11.1 (0.93) | 0.04 (1.0) |
| IV | Significant spalling of concrete in core | 25 | 5.0 | 30.5 (136) | 0.043 | 7.5 (0.63) | >0.1 (3.0) |
| V | Loss of gravity load | 25 | 5.0 | 30.5 (136) | 0.043 | 7.5 (0.63) | >0.1 (3.0) |


Level I

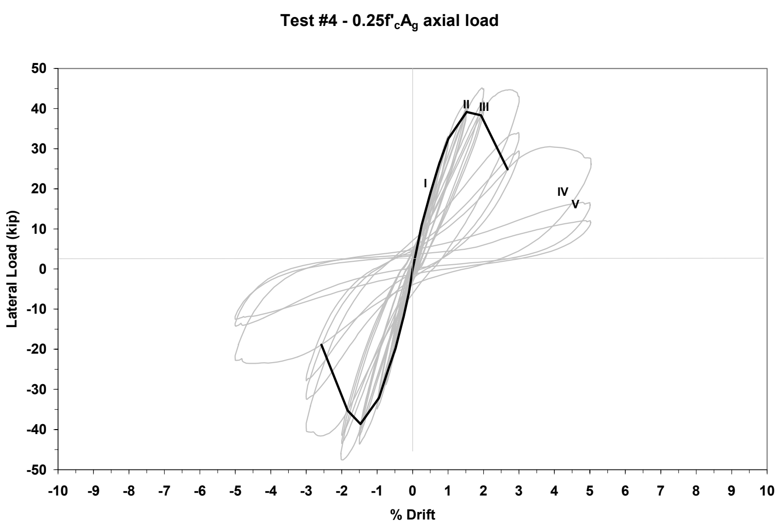


**Fig. 5.7 Test #4 performance level identification curve**

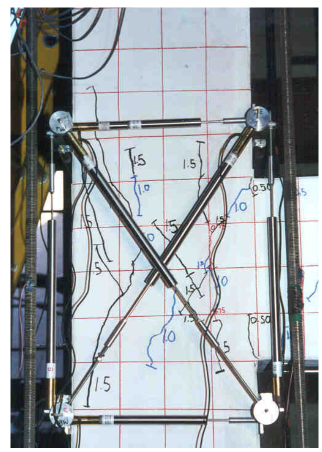

Level II

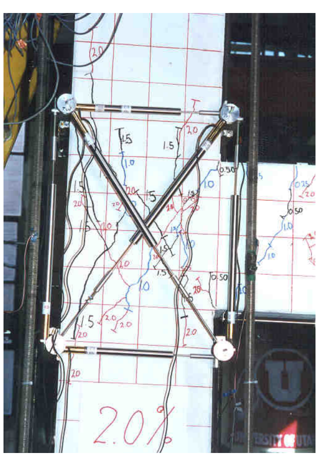


Level III

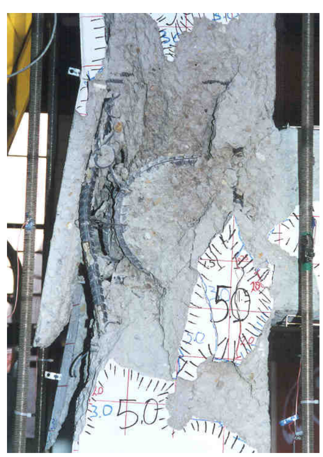

Level IV

Level V

**Fig. 5.8 Test #4 photo documentation of performance levels**

**Table 5.17 Test #5 performance levels ($0.1f'_cA_g$)**

| Level | Performance Description | Cycle | Drift % | Lateral Load Kip (kN) | Plastic Rotation radians | $\gamma$ psi (Mpa) | Crack Width in (mm) |
|---|---|---|---|---|---|---|---|
| I | First yield in longitudinal reinforcement (column) | 16 | 1.5 | 34.5 (153) | 0.004 | 8.8 (0.73) | 0.02 (0.4) |
| II | Significant cracking in joint, w > 0.02 in (0.5mm) | 19 | 2.0 | 38.2 (171) | 0.008 | 9.7 (0.81) | 0.025 (0.6) |
| III | Formation of joint shear mechanism | 19 | 2.0 | 38.2 (171) | 0.008 | 9.7 (0.81) | 0.025 (0.6) |
| IV | Significant spalling of concrete in core | 25 | 5.0 | 27.2 (121) | 0.042 | 6.9 (0.58) | >0.2 (5.0) |
| V | Loss of gravity load | 31 | 9.0 | 9.5 (42) | 0.086 | 2.4 (0.20) | >0.2 (5.0) |

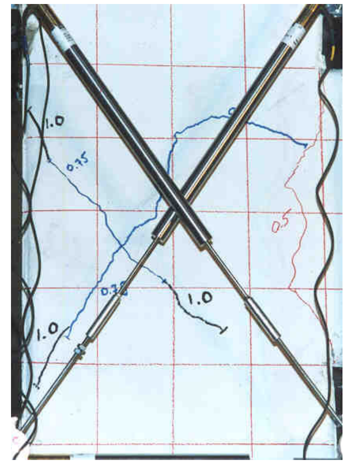

Level I

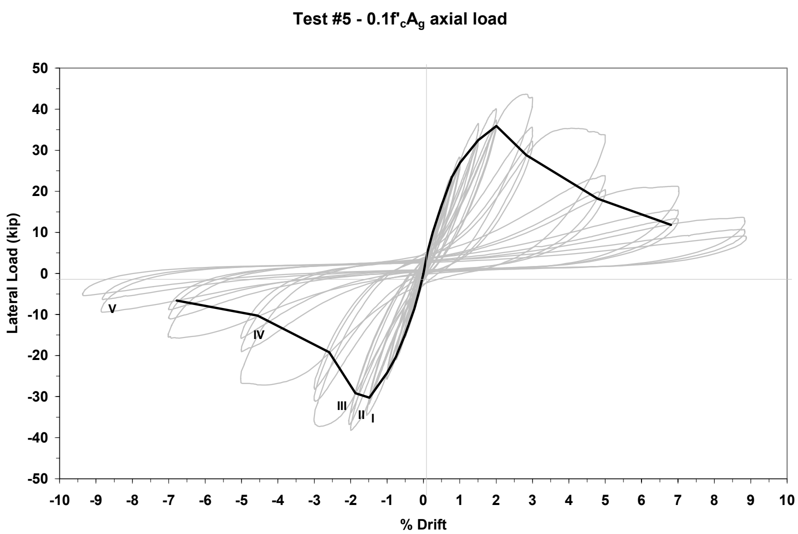


**Fig. 5.9 Test #5 performance level identification curve**

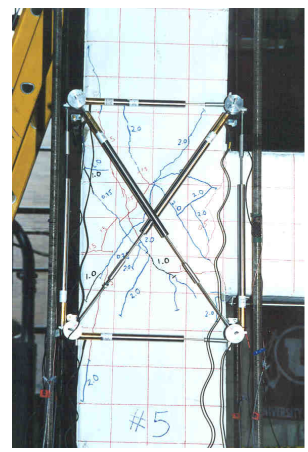

Level II

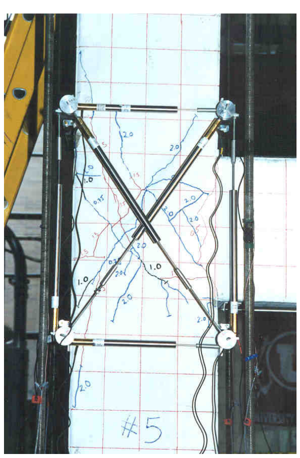

Level III

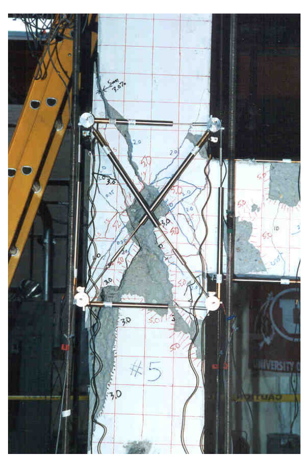

Level IV

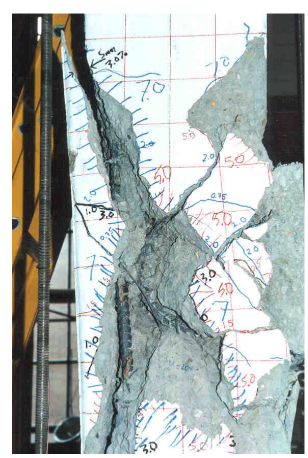

Level V

**Fig. 5.10 Test #5 photo documentation of performance levels**

## Table 5.18  Test #6 performance levels ($0.25f'_cA_g$)

| Level | Performance Description | Cycle | Drift % | Lateral Load Kip (kN) | Plastic Rotation radians | $\gamma$ psi (Mpa) | Crack Width in (mm) |
|---|---|---|---|---|---|---|---|
| I | First yield in longitudinal reinforcement (beam) | 7 | 0.5 | 19.4 (86) | 0.000 | 4.9 (0.41) | Hairline |
| II | Significant cracking in joint, w > 0.02 in (0.5mm) | 16 | 1.5 | 39.1 (174) | 0.004 | 10.0 (0.83) | 0.01 (0.3) |
| III | Formation of joint shear mechanism | 19 | 2.0 | 43.1 (192) | 0.008 | 11.0 (0.92) | 0.02 (0.5) |
| IV | Significant spalling of concrete in core | 25 | 5.0 | 30.1 (134) | 0.042 | 7.7 (0.64) | 0.3 (8.0) |
| V | Loss of gravity load | 28 | 7.0 | 16.7 (74) | 0.065 | 4.2 (0.35) | >0.3 (8.0) |

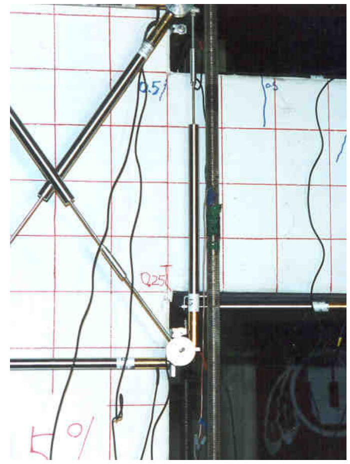

Level I

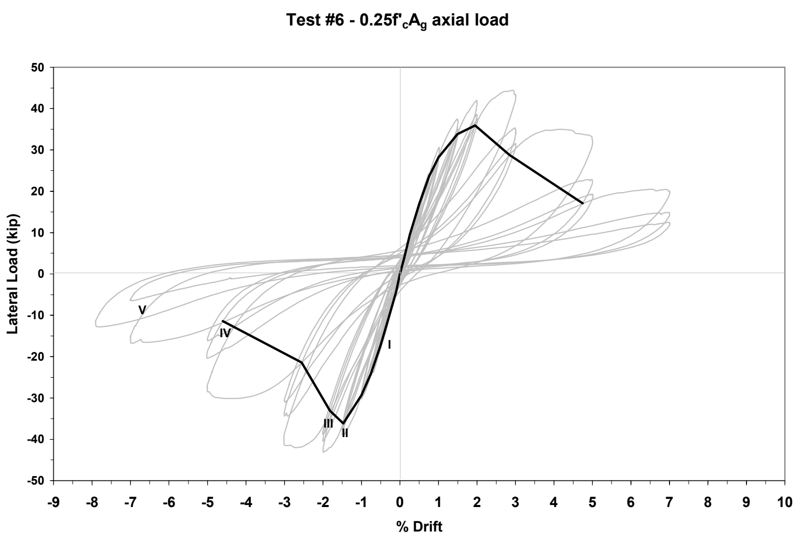


**Fig. 5.11  Test #6 performance level identification curve**

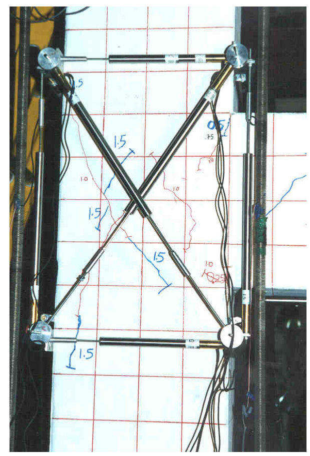

Level II

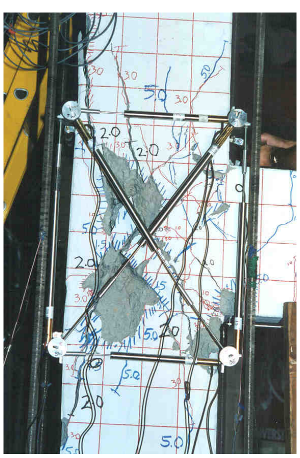

Level III

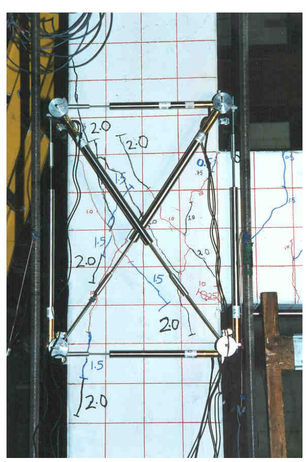

Level IV


Level V

**Fig. 5.12  Test #6 photo documentation of performance levels**

## 5.3 BOND SLIP

Bond slip of the bottom beam bars was measured during tests 1, 2, 3, and 4. Owing to a malfunction in the instrumentation, no data were obtained from test 1. The results from test 2 are shown in Figure 5.13 plotted against plastic rotation. Positive bar pullout is in the direction toward the beam, while negative is toward the back face of the column. A maximum bottom beam bar pullout of 0.67 in. was measured in the upward direction at the end of load step number 9 at a plastic shear angle of 0.054 radian (5.0% drift). Data were unable to be measured beyond step 9 since the back face of the column had spalled off due to the $0.25f'_cA_g$ axial compression load, and the instrument was in danger of being damaged. This was also the case for test 4.

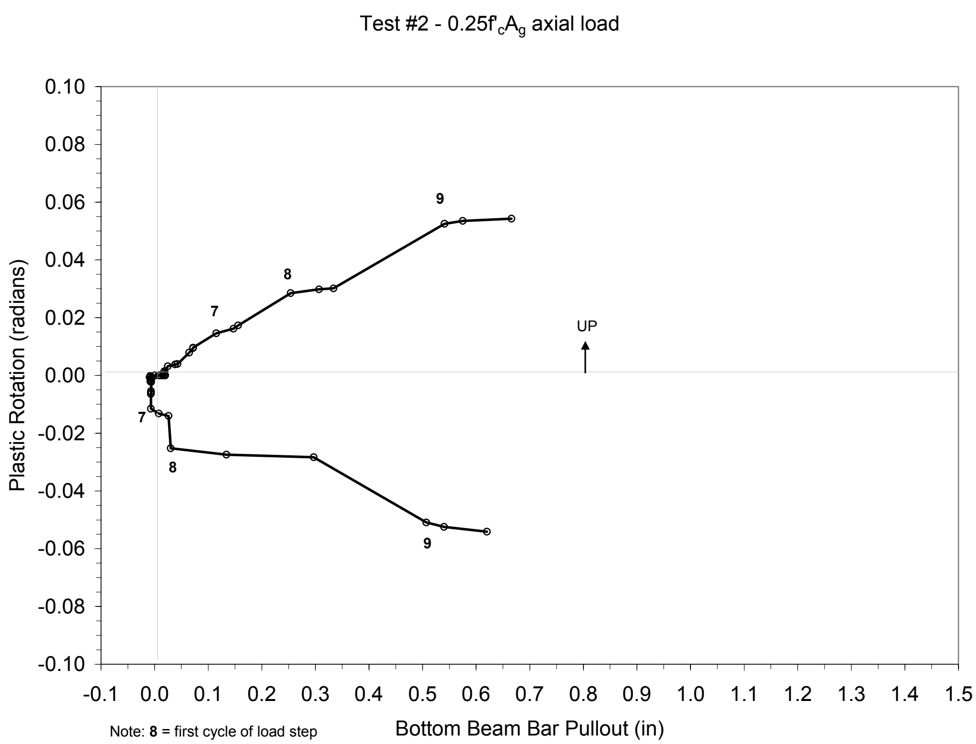


**Fig. 5.13 Unit 2: plastic rotation versus bottom beam bar pullout**

Since test 3 had $0.1f'_cA_g$ axial compression load, and instruments were not in danger of damage from spalling, bar pullout was measured to load step number 10. Corresponding to this step at a shear angle of 0.077 (7.0% drift) is 1.44 in. of bottom beam bar pullout in the upward direction as seen in Figure 5.14.

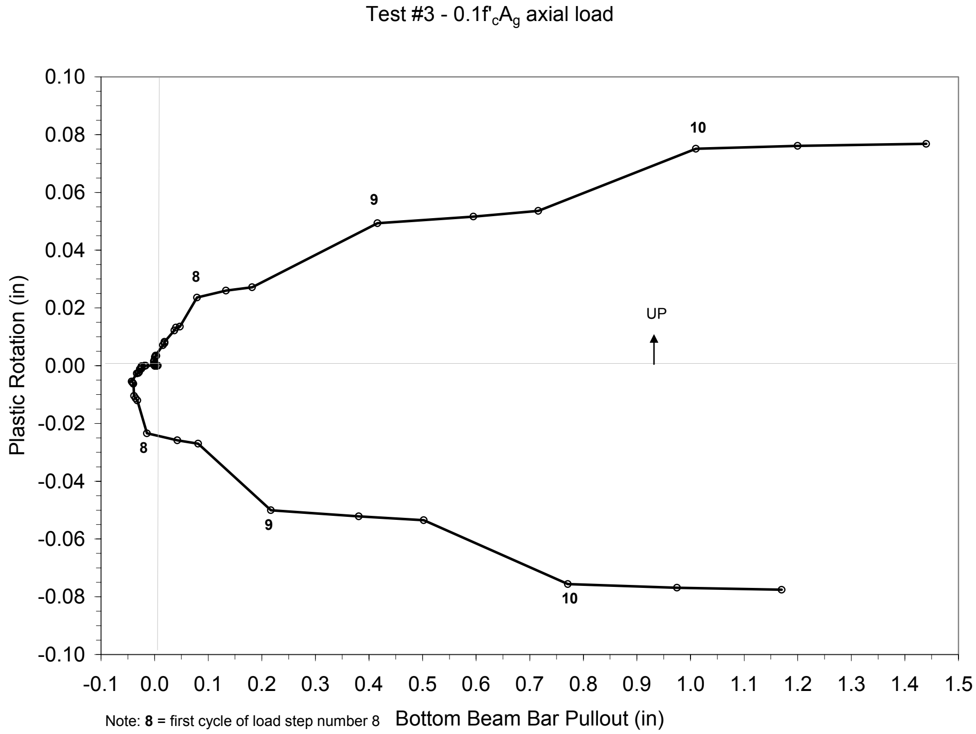


**Fig. 5.14 Unit 3: plastic rotation versus bottom beam bar pullout**

Bottom beam bar pullout in test 4 was measured until the second cycle of load step 9. At a plastic rotation of 0.052 (5.0% drift) the bar slipped 0.363 in. in the upward direction. This is shown in Figure 5.15.

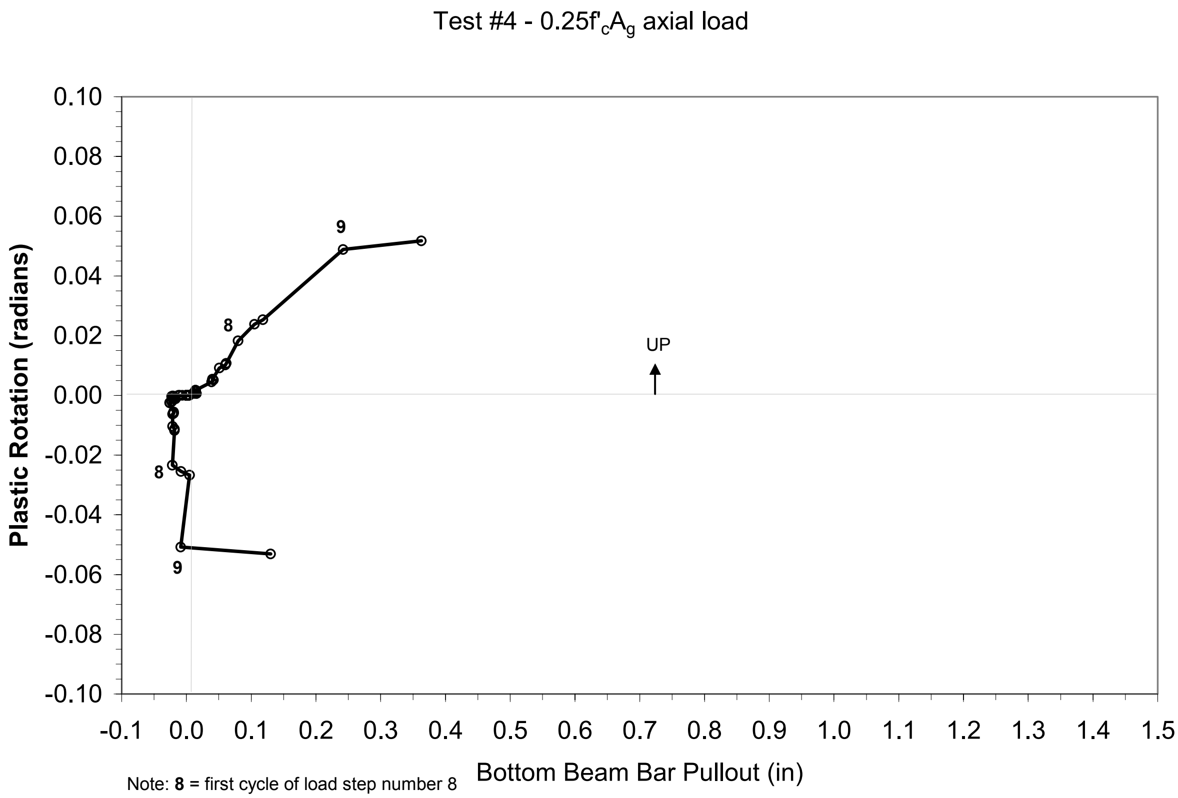


**Fig. 5.15 Unit 4: plastic rotation versus bottom beam bar pullout**

Comparison between the three tests can be made by examining the bottom beam bar pullout for each test at the second cycle of load step number 9. For test 2 at this cycle in the upward direction, the bond slip was 0.575 in. The bond slip for test 3 at this cycle was 0.595 in. and for test 4 it was 0.363 in. The values for tests 2 and 3 are very close. It appears that loading an exterior joint to $0.25f'_cA_g$ that has 6 in. of bottom beam bar embedment has the same effect on bar pullout as that of an exterior joint with only $0.1f'_cA_g$ and 14 in. of bottom beam bar embedment. Also noteworthy is the difference that axial load makes on two joints with identical details. Owing to the increased axial compression load, the bottom beam bar pullout of test 4 at cycle 2 of step 9 was only 0.363 in.; a decrease of 39% compared to test 3.

## 5.4 COMPARISON WITH FEMA 273 AND ACI 352

The test results were compared with the FEMA 273 (BSSC 1997) modeling parameters for RC beam-column joints. Specifically, the shear deformation angle parameters at the end of the peak strength, *d*, and at the collapse level, *e*, and the residual strength ratio, *c,* as defined in Figure 5.16, were compared to Table 6-8 of FEMA 273. FEMA 273 parameters do not exist for an axial load ratio of 0.25 $f'_c A_g$; however, Table 5.19 shows that for an axial load ratio of $0.1f'_c A_g$, the FEMA Guidelines are conservative.

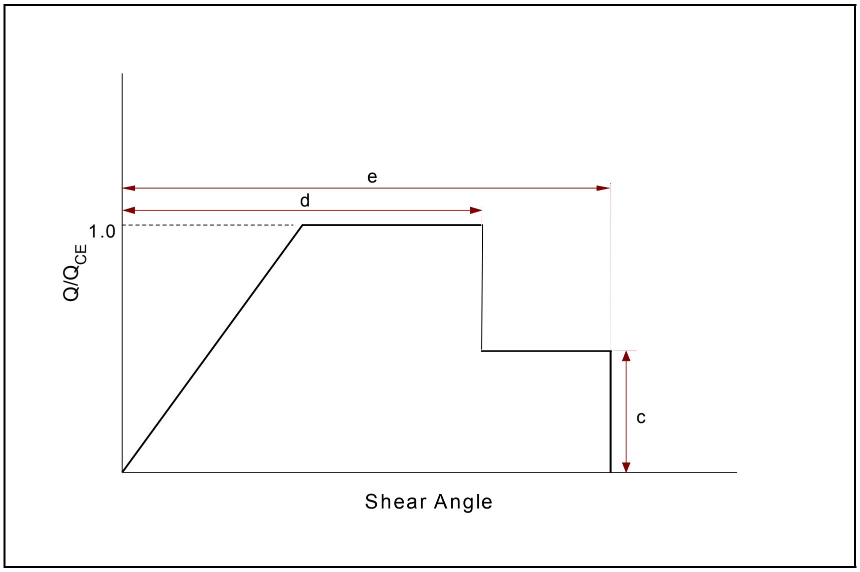


**Fig. 5.16 FEMA modeling parameters**

**Table 5.19 Modeling parameters for specimens in comparison with FEMA 273**

| Test # | $P/f'_c A_g$ [1] | Transverse Reinforcement | $V/V_n$ [2] | d | e | c [5] |
|---|---|---|---|---|---|---|
| 1 | 0.10 | NC [3] | 0.88 | 0.010 | 0.030 | 0.488 |
| 2 | 0.25 | NC [3] | 1.20 | 0.010 | 0.030 | 0.514 |
| FEMA 273 | ≤ 0.1 | NC [4] | ≤ 1.2 | 0.005 | 0.010 | 0.200 |
| 3 | 0.10 | NC | 1.73 | 0.015 | 0.050 | 0.341 |
| 4 | 0.25 | NC | 1.89 | 0.020 | 0.050 | 0.300 |
| 5 | 0.10 | NC | 1.65 | 0.020 | 0.084 | 0.200 |
| 6 | 0.25 | NC | 1.87 | 0.020 | 0.067 | 0.200 |
| FEMA 273 | ≤ 0.1 | NC [4] | ≥ 1.5 | 0.005 | 0.010 | 0.200 |

[1] ratio of the axial column load to the cross-sectional area of the joint and concrete compressive strength
[2] ratio of the design shear force to the shear strength for the joint: $V_n$ is calculated using Equation 6-4 in FEMA 273 Section 5.5.2.3
[3] nonconforming details; no hoops within the joint
[4] nonconforming details; see Table 6-8 footnote 1 of FEMA 273

In terms of the shear strength coefficient, $\gamma$, the FEMA 273 guidelines suggest a value of $\gamma = 6$ (psi) for corner joints (exterior joints without transverse beams). This is comparable to the joints with 6″ bottom bar embedment but conservative for the rest of the test units. For test unit 1 ($0.10f'_cA_g$) with $\gamma = 5.2$ (psi) the FEMA guidelines are slightly unconservative. When axial load is increased to $0.25f'_cA_g$, as in test unit 2, $\gamma = 7.0$ (psi), and the FEMA guidelines become slightly conservative. The test units with 14 in. of bottom bar embedment and those that hooked performed very similarly. Test units 3 and 5, both with $0.1f'_cA_g$, had an average maximum coefficient $\gamma = 10.0$ (psi), while tests #5 and #6 ($0.25f'_cA_g$) had a $\gamma = 11.0$ (psi) nearly twice that given by FEMA.

The exterior joints tested for this research do not qualify as either Type 1 or Type 2 joints per ACI 352 (ACI 1991), since the reinforcement is similar to Type 1 but the loading is of Type 2. When comparing the results for the shear strength coefficient obtained in this research to the coefficient suggested by ACI 352 for new corner joints, which is $\gamma = 12$ (psi), it can be observed that nonductile joints without hoop steel in the joint do not meet the Type 2 joint design value. This is true for the exterior joints tested here with the reinforcement details described, regardless of the axial column load level.

## 5.5 LIMIT STATES MODEL

The five performance levels developed in Figures 5.17 through 5.20 are best suited for an evaluation of experimental results. However, for the construction of a limit states model for design, it can be seen that only three parameters are sufficient to describe the behavior of RC exterior joints: plastic rotation, joint shear strength coefficient, and crack width. The results obtained for the two test units with 6″ bottom beam bar embedment are shown in Figure 5.17 for the joint strength coefficient, $\gamma$, and in Figure 5.18 for the crack width. Figure 5.17 indicates that a sequence of steel yielding followed by the formation of a bond-slip mechanism, joint cracking, spalling concrete, and loss of lateral load is representative of these two tests. Figure 5.18, which has a logarithmic vertical axis, indicates that the crack width is an exponential function of the drift.

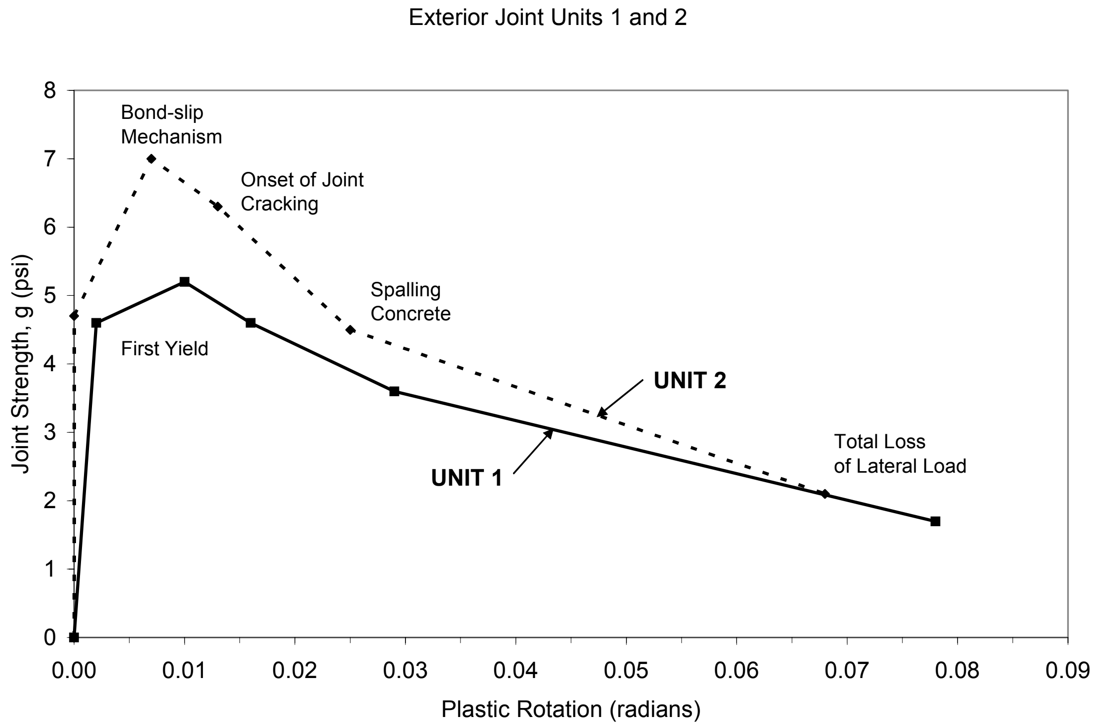


**Fig. 5.17 Limit states model for exterior joint units 1 and 2**

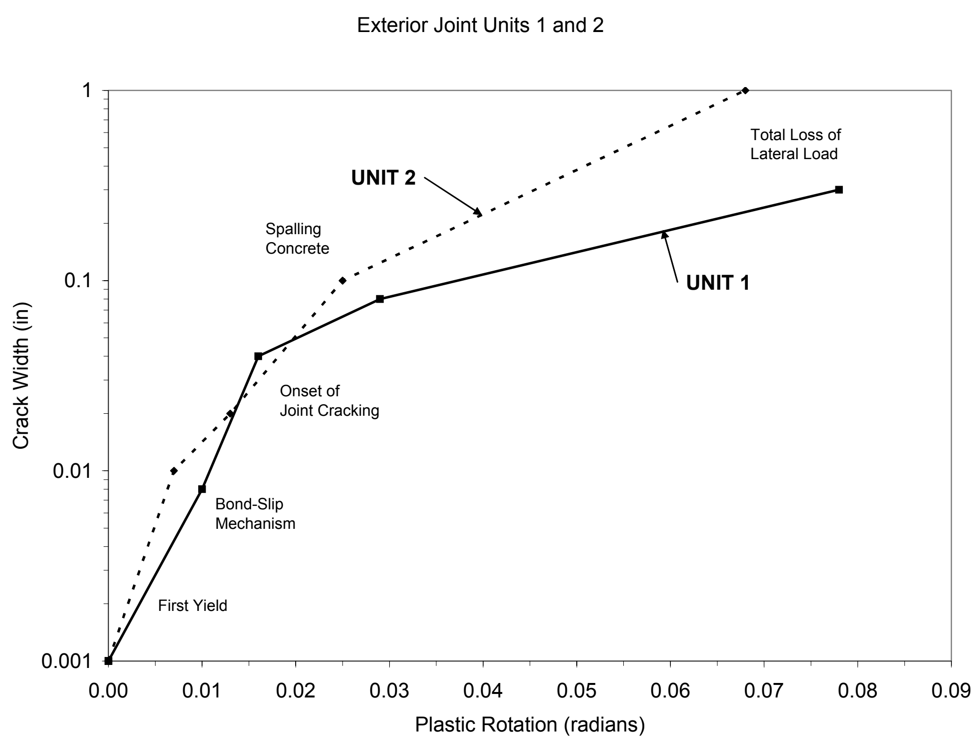


**Fig. 5.18 Crack width model for exterior joint units 1 and 2**

The limit states are different for the other exterior joint units 3, 4, 5, and 6. The sequence for these units is steel yielding, followed by joint cracking, the formation of a joint shear mechanism, spalling of concrete, and loss of gravity load. The behavior of these four tests is shown in Figure 5.19. The crack width relationship with drift is exponential, as shown in Figure 5.20.

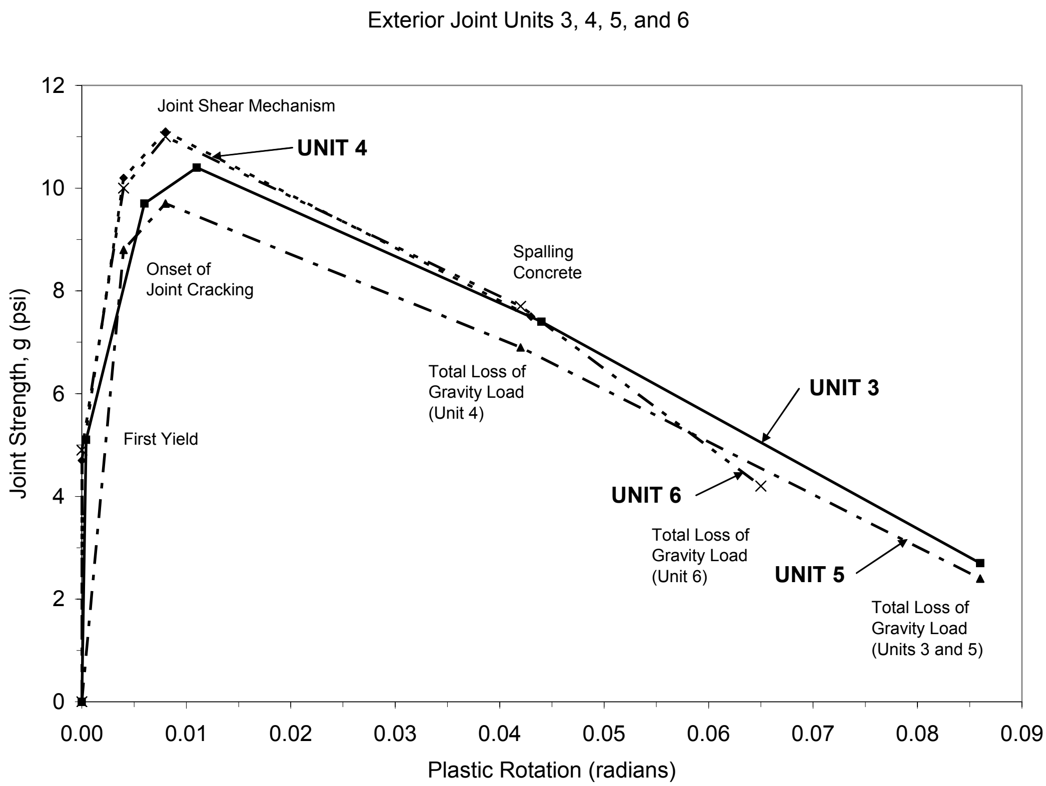


**Fig. 5.19 Limit states model for exterior joint units 3, 4, 5, and 6**

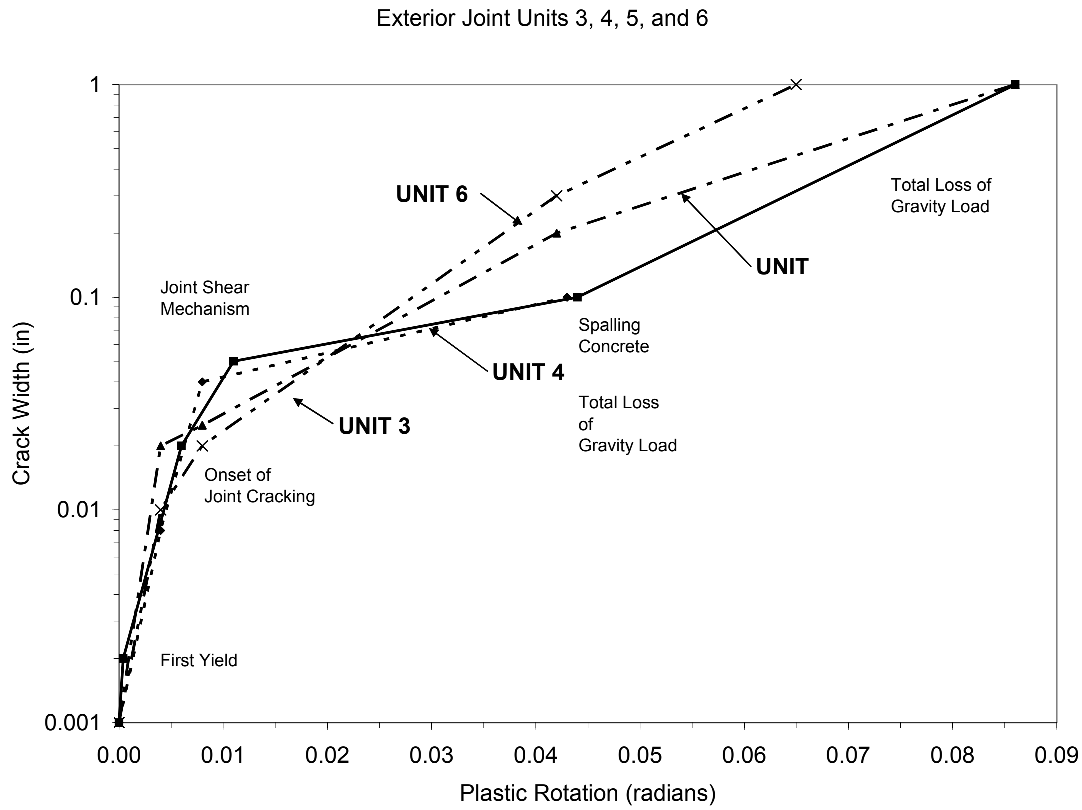


**Fig. 5.20 Crack width model for exterior joint units 3, 4, 5, and 6**

The limit states model could be used for performance evaluation of RC joints after an earthquake. From knowledge of the joint detailing, the axial load, and measurement of the crack width, Figure 5.18 or 5.20 could be used to estimate the corresponding plastic rotation; then by using Figure 5.17 or 5.19, the joint shear strength coefficient could be obtained which corresponds to the remaining shear capacity of the joint.

## 5.6 PROPOSED NEW MODELING CRITERIA FOR EXTERIOR JOINTS WITH SUBSTANDARD DETAILS

The FEMA 273 (1997) document contains modeling parameters for RC concrete beam-column joints (Table 6-8). These criteria are evaluated based on the shear angle and a residual strength ratio. The shear angle is given in terms of quantities *d* and *e*, as shown in Figure 5.21, which also shows the residual strength ratio, *c*. It should be noted that the FEMA 356 (2000) document has a table similar to the one in FEMA 273; however, the quantities *d* and *e* are specified as plastic shear angles (Table 6-9).

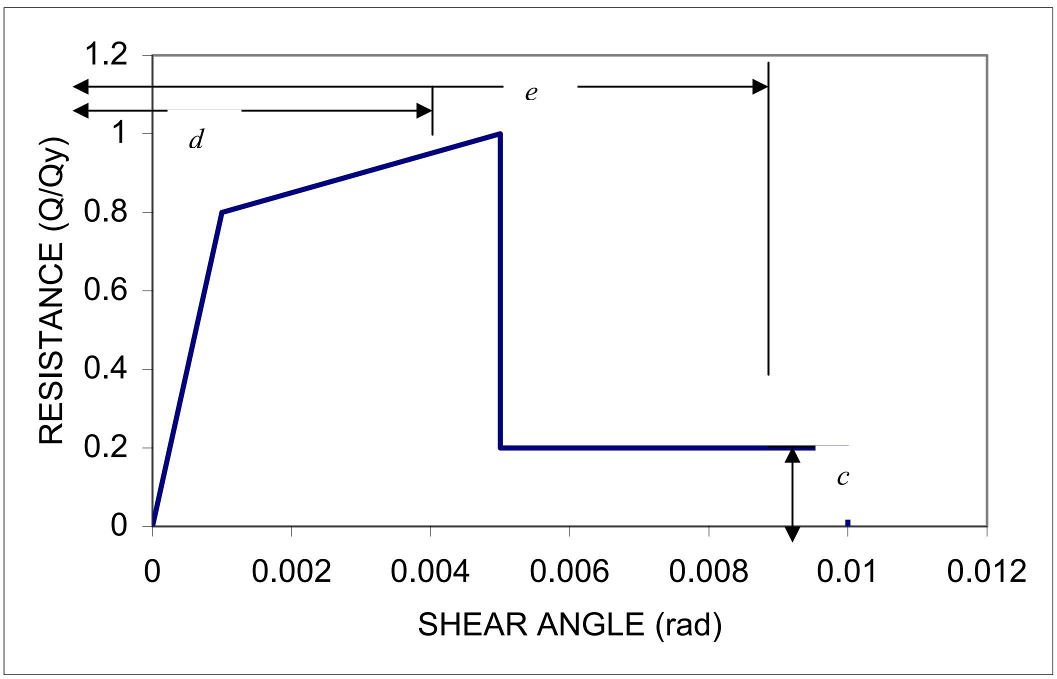


**Fig. 5.21 FEMA 273 generalized deformation relation**

The data from the six units tested in the present research study do not support the information conveyed by Figure 5.21. Instead, depending on the failure mode of the joints, i.e., bond slip or shear failure, the generalized deformation relation varies as shown in Figure 5.22. In addition, the expression of the modeling parameters in terms of *d*, *e,* and *c* does not seem to satisfy the generalized deformation relations obtained in this study. Four parameters are used to establish the new modeling criteria: P1, P2, P3, and P4, which are defined as follows:

P1 = Lateral Load Resistance value at yield
P2 = Peak value of Lateral Load Resistance
P3 = Sudden Reduction in Lateral Load Resistance
P4 = Residual Strength Ratio

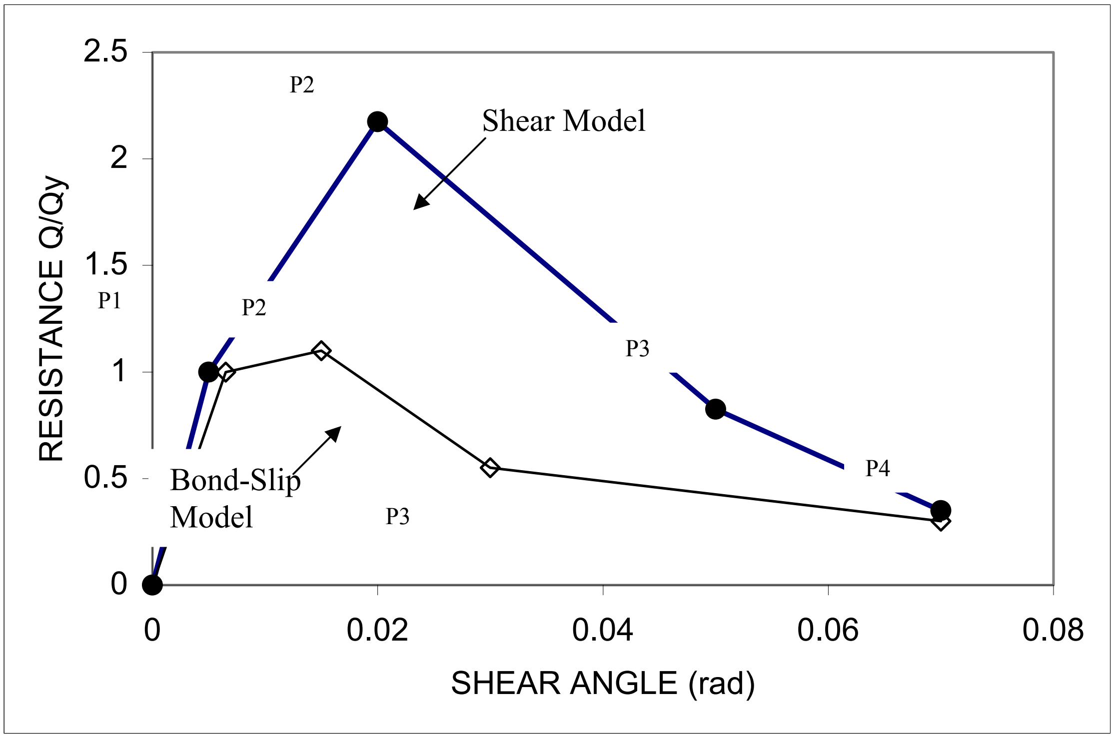


**Fig. 5.22 Proposed generalized deformation relations for exterior beam-column joints**

Adopting the definitions shown in Figure 5.22, the following data are obtained from the test units as shown in Figure 5.23 for the bond-slip failure mode (units 1 and 2), and Figure 5.24 for the shear failure mode (units 3, 4, 5, and 6). The data are also shown in tabular form in Table 5.20. Note that in addition to the shear angle, the plastic shear angle (plastic rotation) is also provided in Table 5.20. Finally, from the six units tested in this research an alternate table is proposed for modeling parameters similar to Table 6-8 of FEMA 273; this is provided in Table 5.21, which should be used in conjunction with Figure 5.20.

**Table 5.20 Modeling parameters for exterior beam-column joints with nonconforming details**

| | **MODELING PARAMETERS** | | | | | | | | | | | |
|---|---|---|---|---|---|---|---|---|---|---|---|---|
| | BOND MODEL | | | | | | | | | | | |
| | P1 | | | P2 | | | P3 | | | P4 | | |
| TEST UNIT (Axial Load) | Resistance Q/Qy | Shear Angle (rad) | Plastic Shear Angle (rad) | Resistance Q/Qy | Shear Angle (rad) | Plastic Shear Angle (rad) | Resistance Q/Qy | Shear Angle (rad) | Plastic Shear Angle (rad) | Resistance Q/Qy | Shear Angle (rad) | Plastic Shear Angle (rad) |
| 1 ($0.10f'_cA_g$) | 1.0 | 0.005 | 0.000 | 1.1 | 0.015 | 0.010 | 0.6 | 0.030 | 0.029 | 0.3 | 0.070 | 0.070 |
| 2 ($0.25f'_cA_g$) | 1.0 | 0.008 | 0.000 | 1.0 | 0.015 | 0.007 | 0.5 | 0.030 | 0.025 | 0.3 | 0.070 | 0.068 |
| | SHEAR MODEL | | | | | | | | | | | |
| | P1 | | | P2 | | | P3 | | | P4 | | |
| TEST UNIT | Resistance Q/Qy | Shear Angle (rad) | Plastic Shear Angle (rad) | Resistance Q/Qy | Shear Angle (rad) | Plastic Shear Angle (rad) | Resistance Q/Qy | Shear Angle (rad) | Plastic Shear Angle (rad) | Resistance Q/Qy | Shear Angle (rad) | Plastic Shear Angle (rad) |
| 3 ($0.10f'_cA_g$) | 1.0 | 0.005 | 0.000 | 2.0 | 0.020 | 0.009 | 0.7 | 0.050 | 0.044 | 0.4 | 0.070 | 0.068 |
| 4 ($0.25f'_cA_g$) | 1.0 | 0.005 | 0.000 | 2.1 | 0.020 | 0.009 | 0.6 | 0.050 | 0.045 | - | - | - |
| 5 ($0.10f'_cA_g$) | 1.0 | 0.005 | 0.000 | 2.3 | 0.020 | 0.008 | 1.1 | 0.050 | 0.042 | 0.6 | 0.070 | 0.065 |
| 6 ($0.25f'_cA_g$) | 1.0 | 0.005 | 0.000 | 2.3 | 0.020 | 0.008 | 0.9 | 0.050 | 0.042 | 0.4 | 0.070 | 0.065 |

**Table 5.21 Proposed modeling parameters for exterior beam-column joints with nonconforming[†] details**

| | EXTERIOR JOINT MODELING PARAMETERS FOR JOINTS WITH NONCONFORMING DETAILS | | | | | | | | | | | |
|---|---|---|---|---|---|---|---|---|---|---|---|---|
| | BOND MODEL | | | | | | | | | | | |
| | P1 | | | P2 | | | P3 | | | P4 | | |
| Axial Load | Resistance Q/Qy | Shear Angle (rad) | Plastic Shear Angle (rad) | Resistance Q/Qy | Shear Angle (rad) | Plastic Shear Angle (rad) | Resistance Q/Qy | Shear Angle (rad) | Plastic Shear Angle (rad) | Resistance Q/Qy | Shear Angle (rad) | Plastic Shear Angle (rad) |
| $0.10f'_cA_g$ | 1.0 | 0.005 | 0.000 | 1.1 | 0.015 | 0.010 | 0.6 | 0.030 | 0.029 | 0.3 | 0.070 | 0.070 |
| $0.25f'_cA_g$ | 1.0 | 0.008 | 0.000 | 1.0 | 0.015 | 0.007 | 0.5 | 0.030 | 0.025 | 0.3 | 0.070 | 0.068 |
| | SHEAR MODEL | | | | | | | | | | | |
| | P1 | | | P2 | | | P3 | | | P4 | | |
| | Resistance Q/Qy | Shear Angle (rad) | Plastic Shear Angle (rad) | Resistance Q/Qy | Shear Angle (rad) | Plastic Shear Angle (rad) | Resistance Q/Qy | Shear Angle (rad) | Plastic Shear Angle (rad) | Resistance Q/Qy | Shear Angle (rad) | Plastic Shear Angle (rad) |
| $0.10f'_cA_g$ | 1.0 | 0.005 | 0.000 | 2.1 | 0.020 | 0.009 | 0.9 | 0.050 | 0.043 | 0.5 | 0.070 | 0.067 |
| $0.25f'_cA_g$ | 1.0 | 0.005 | 0.000 | 2.2 | 0.020 | 0.009 | 0.6 | 0.050 | 0.044 | 0.2 | 0.040 | 0.032 |

[†]Nonconforming according to FEMA 273

# 6 Strut-and-Tie-Model

Over the past few decades the design of concrete structures has changed dramatically. Improvements to codes were implemented for the design of concrete structures based on extensive testing, including the effects of seismic loading. The design of concrete structures in the 1960s did not consider these effects in the details that are currently required by codes. One big difference in the 1960s' design is the absence of steel hoops in the beam-column connections. Several types of buildings were built with no steel hoops through the joint in this era, and with various vertical and horizontal reinforcement details through the joint. It is now important to re-evaluate these buildings to determine their adequacy in a seismic event.

The design of RC joints is very difficult to model using traditional stress-strain relationships, or even using finite element analysis techniques. However, strut-and-tie models, a relatively new design method, may provide a much more accurate model of the joint. Recently, several strut-and-tie models have been developed for various types of beam-column concrete joints (Ali and White 2001, Lowes and Moehle 1999, Hwang and Lee 1999). These models have been developed for joints designed to meet current codes, which consider the benefit of steel hoops in the joint; thus they are not suitable for the evaluation of existing joints with substandard reinforcement details. In these cases, there is a need for a somewhat different strut-and-tie model to be developed. The strut-and-tie model developed here is verified by the experimental results obtained in the present study.

## 6.1 OBJECTIVE

The purpose of this chapter is to develop a strut-and-tie model for one of the beam-column joints tested in the present research. Six beam-column joints with three different reinforcement details based on 1960's construction were tested. Each of the three different joint types was tested at levels of 10% and 25% of the axial load capacity of the column section. A strut-and-tie model was developed for test unit 6, with the reinforcement detail shown in Figure 6.1, at 25% axial load.

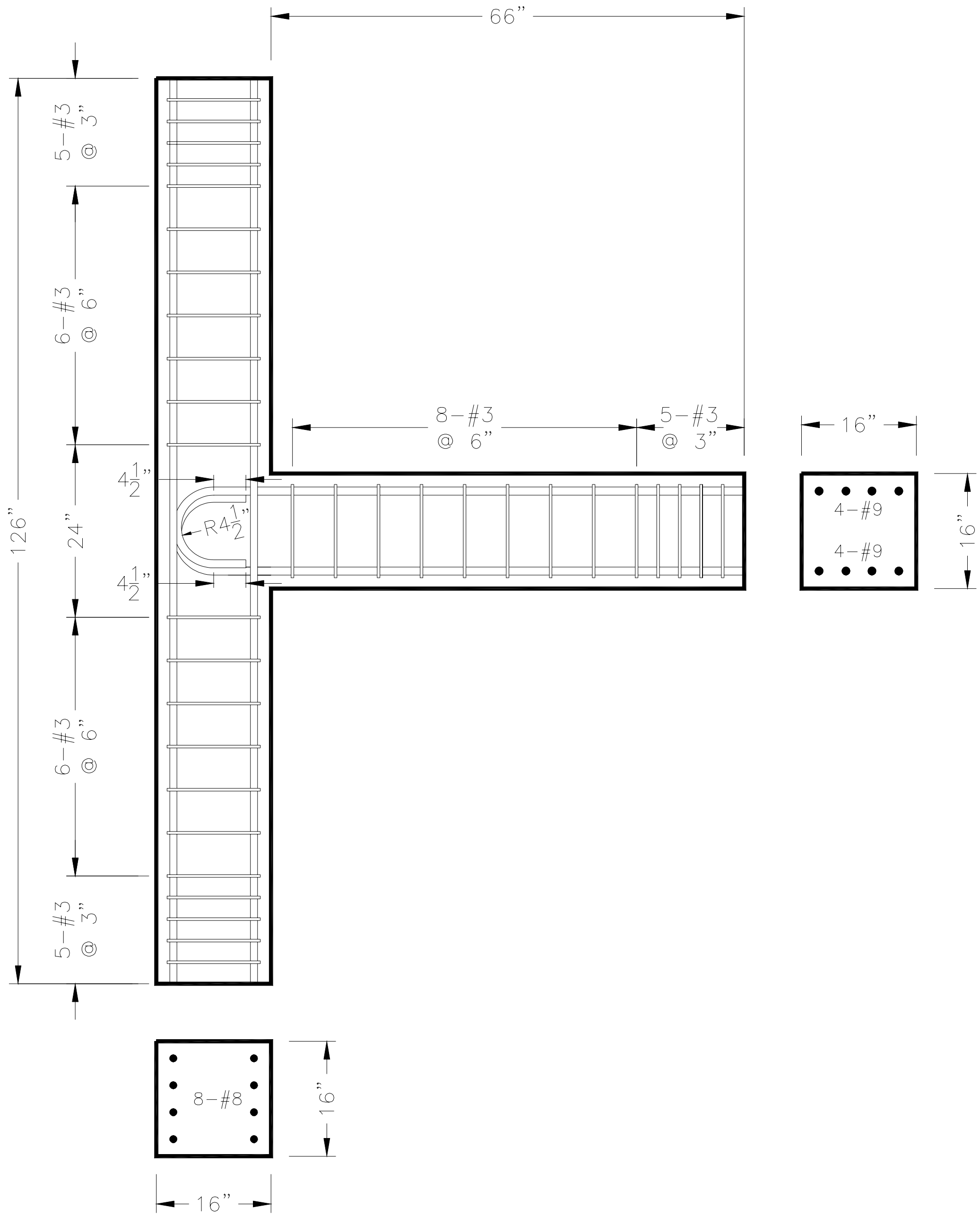


**Fig. 6.1 Joint detail for test unit 6**

## 6.2 TEST UNIT

The joint shown in Figure 6.1 has reinforcement details meeting the requirements of the 1963 ACI Code. This detail represents a very good design for that time due to the large hooks that connect the beam to the column. This detail was used to develop the strut-and-tie model discussed in this Chapter. The concrete compressive strength used in the analysis was $f'_c = 4{,}496$ psi, obtained from tests of three cylinders just prior to testing the joint. The yield stress of the various sizes of steel bars was also obtained from tests and is shown in Table 2.2.

The column was subjected to a static axial load of A = 280 kips, and the beam was cycled up and down in a quasi-static cyclic fashion until failure occurred. The maximum load carried by the joint during the experiment was P = 42 kips. The location of axial load, A, and lateral load, P, is shown in Figure 6.2, which also shows the test setup. The strut-and-tie model developed was based on the upward stroke. The results for the downward stroke are the same due to the symmetry of the joint.

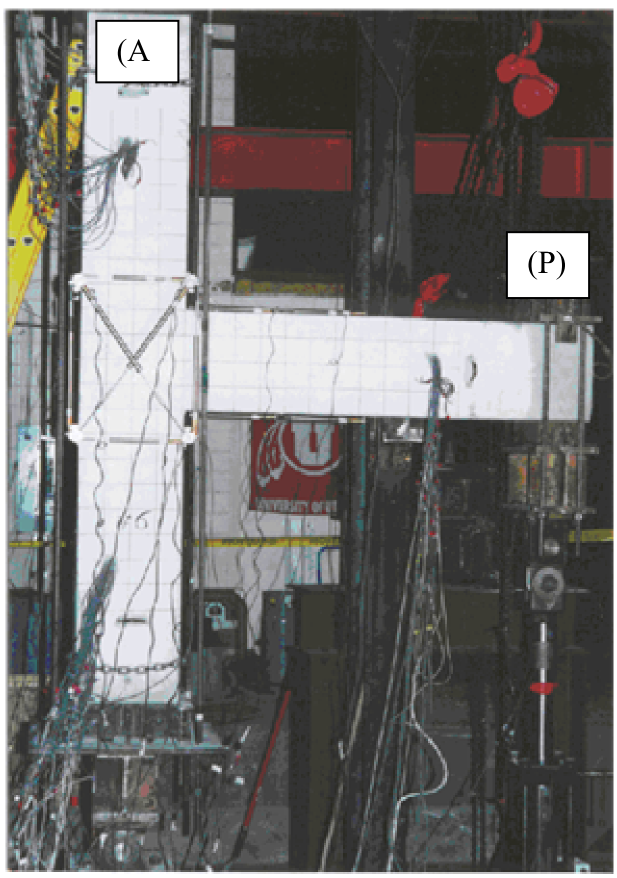


**Fig. 6.2 Test setup**

## 6.3 MODEL DEVELOPMENT

The first step in developing the strut-and-tie model was to determine and isolate the discontinuity, or "D-region," as shown in Figure 6.3. The D-region is considered to be the section where a discontinuity exists due to a change in geometry or where severe loading exists. It is bound by the column hoop steel immediately above and below the joint core and the four faces of the column.

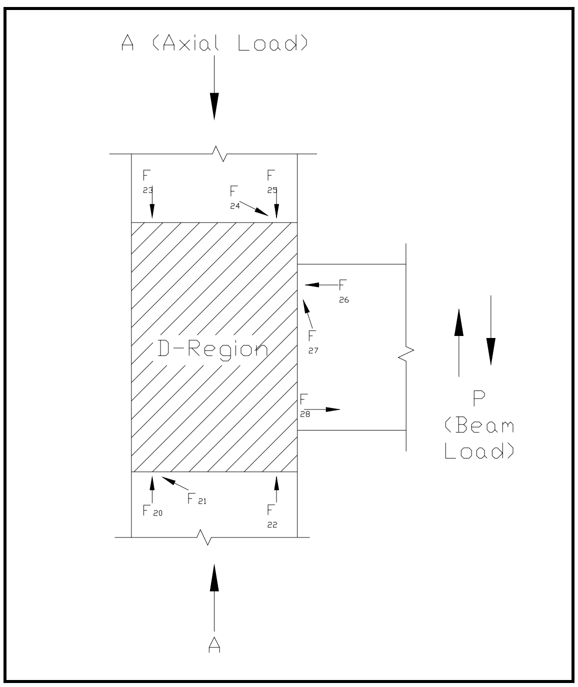


**Fig. 6.3 Discontinuity region**

The second step was to determine the forces acting on the boundary of the D-region. This was a very important step in the development process. In order to determine how the axial load (A) and beam lateral load (P) might be acting on the surface of the D-region, a strut-and-tie model was developed first for the entire specimen excluding the D-region, as shown in Figure

6.4. This model was simple to develop due to the continuity of stresses outside the D-region. It also gave a good idea of how the loads (A) and (P) were acting on the D-region, as shown in Figure 6.3. Once the boundary conditions were defined, that is the forces acting on the boundary of the D-Region in terms of (A) and (P), the truss for the strut-and-tie model of the joint could be drawn.

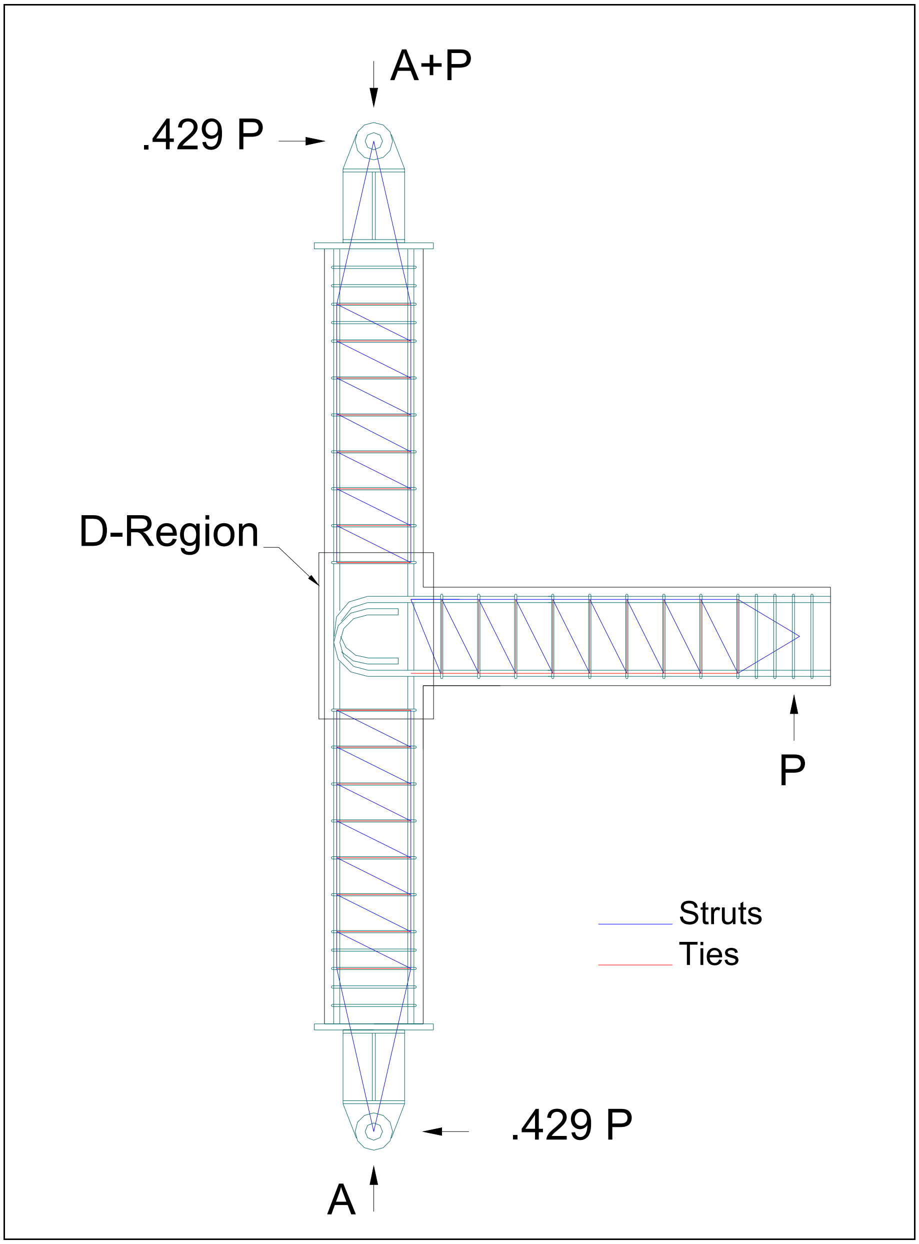


**Fig. 6.4 Truss model**

The truss for the strut-and-tie model of the joint was difficult to construct, mostly due to the lack of stirrups in the joint. Several different strut-and tie truss models were attempted until an optimal model was developed. The strut-and-tie truss that was developed is different from other trusses used in a joint of this type of geometry in several ways. One difference is that the truss extends outside of the joint to the nearest steel tie, which is 4″ outside the joint. Another difference is the use of three major diagonal struts (compression members) through the joint. These struts were developed to model the confining effect of the large steel hooks located within the joint.

The final strut-and-tie model developed is shown in Figure 6.5. The solid lines represent tension ties, whereas the dotted lines represent compression struts. The angles of struts 10, 11, and 12 from the horizontal are 59.7˚, 41.7˚, and 30.3˚, respectively.

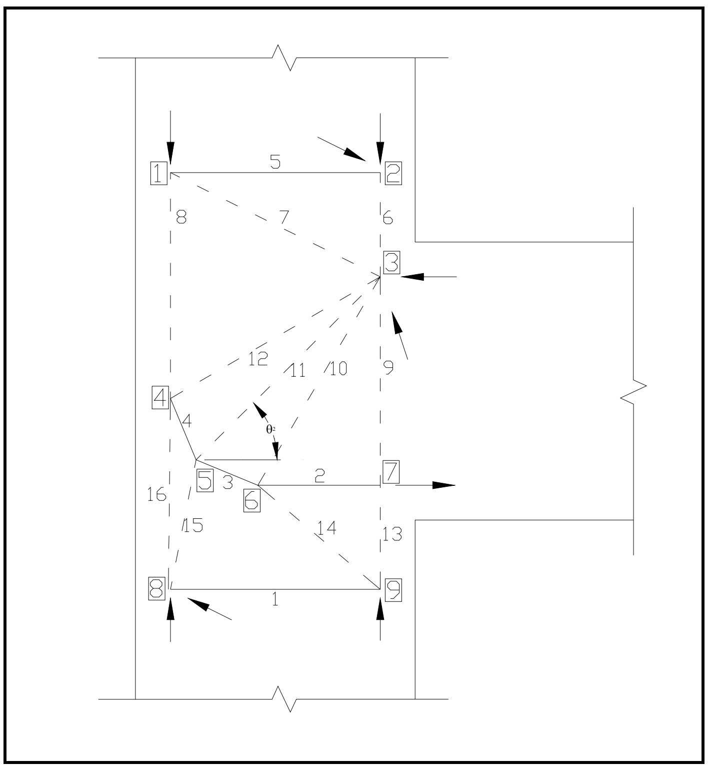


**Fig. 6.5 Member and joint numbers of strut-and-tie model**

It was important to develop a model that captured the failure mechanism observed in the actual test unit. A comparison of the strut-and-tie model of Figure 6.5, with both the up and down loading superimposed, and the actual joint from the test was made before major spalling of the concrete had occurred. As Figure 6.6 shows, the cracking through the joint is similar to the orientation of the struts in the strut-and-tie model, and it extends outside the joint to the nearest steel tie. This was the first evidence that the strut-and-tie model developed would provide a good representation of the performance obtained from test unit 6.

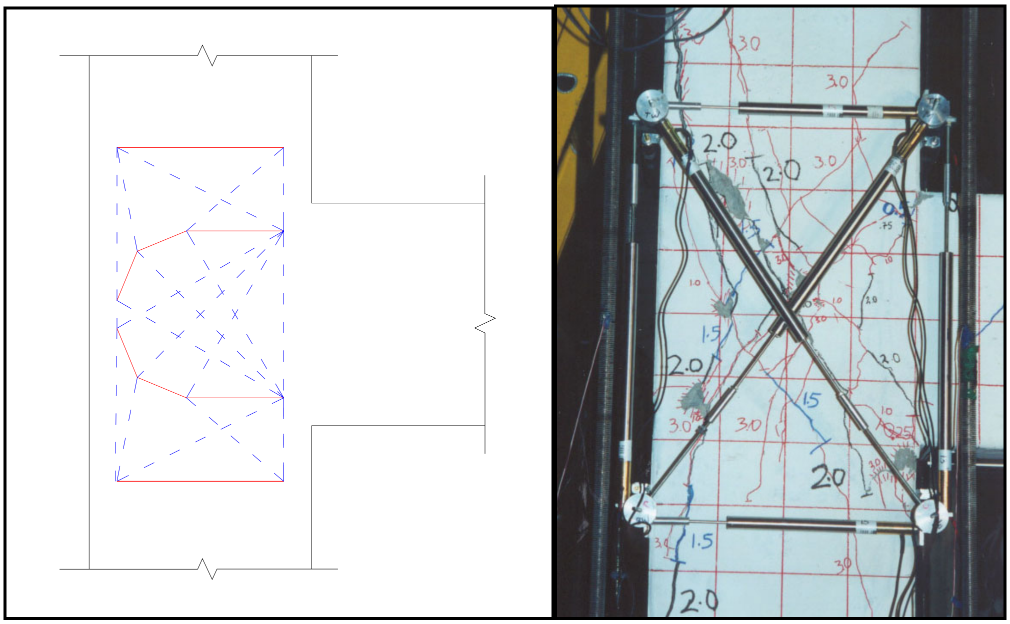


**Figure 6.6. Comparison of truss model to actual joint cracks**

With the strut-and-tie truss model developed, the strut and tie forces could now be calculated. It was assumed that on the upstroke at the ultimate beam lateral load (P), member #1 yields (member #5 on the down stroke); test results confirm this assumption. This led to a statically determinate truss that was solved in terms of the axial load (A) and the beam lateral load (P). Table 6.1 lists the member forces in symbolic form and based on the 280 kips axial load and 42 kips beam lateral load. The table also lists the compression strut widths and the effective compressive strength of the concrete ($f_{ce}$).

**Table 6.1 Member forces and strut widths based on ultimate lateral beam load**

| Member | Symbolic Member Force | $f_{ce}$ (psi) | Force (kips)† | Strut Width (in.) † |
|---|---|---|---|---|
| 1 | $F_1^*$ | -- | +27.2 | -- |
| 2 | 5.256P | -- | +220.8 | -- |
| 3 | $4.543P - 1.297F_1$ | -- | +155.42 | -- |
| 4 | $7.316P - 7.564F_1$ | -- | +100.93 | -- |
| 5 | 0.429P | -- | +18.0 | -- |
| 6 | 0.5A + 2.943P | 3520 | -263.6 | 3.39 |
| 7 | 0.480P | 2290 | -20.2 | 0.55 |
| 8 | 0.5A – 2.158P | 2290 | -49.4 | 0.877 |
| 9 | $0.5A - 2.443P - 0.857F_1$ | 3520 | -14.02 | 0.220 |
| 10 | $2.481P + 0.284F_1$ | 2290 | -112.0 | 3.07 |
| 11 | $1.670P + 3.033F_1$ | 2290 | -152.88 | 4.33 |
| 12 | $2.697P - 2.788F_1$ | 2290 | -37.22 | 0.87 |
| 13 | $0.5A - 2.443P - 0.857F_1$ | 3520 | -14.02 | 0.22 |
| 14 | $1.317F_1$ | 2290 | -35.93 | 1.05 |
| 15 | $8.634F_1 - 3.707P$ | 2290 | -79.84 | 2.62 |
| 16 | $0.5A + 6.125P - 8.576F_1$ | 2290 | -163.30 | 1.33 |

$^*F_1 = A_s f_y$
P = Lateral Beam Load (assumed as 42 kips)
A = Axial Load (Assumed as 280 kips)
† Based on P = 42 kips and A = 280 kips
+ = tension tie
- = compression strut

### 6.4 EVALUATION OF TRUSS

The first members analyzed were the ties, or the tension members. Failure of the ties would indicate a more ductile behavior of the joint, which is the most desirable failure mode. The force required to yield each of the ties was determined using the simple relationship: $F = f_y A_s$, thus ignoring any strain hardening effects. These forces are listed in Table 6.1. Only one of the ties in this model reached the yield stress; therefore the ties were not the primary cause of failure. The only exception is member number 1, in the up stroke, which was assumed to yield; this was confirmed from the test of unit 6.

The other failure modes examined were crushing of the struts, i.e., the concrete compression members, and crushing of the nodes. The first step in determining the capacity of the struts is to determine the effective compressive strength of the struts. The allowable stress was determined using the method outlined by MacGregor (1997). In this method, which is very similar to the method outlined in the ACI code (Concrete International 2001), the effective compressive strength of the concrete ($f_{ce}$) is determined using the following:

$$f_{ce} = \nu_1 \nu_2 f_c^{'} \tag{6.1}$$

$$\nu_2 = 0.55 + \frac{15}{\sqrt{f_c^{'}}} \tag{6.2}$$

where $f'_c$ is in psi units. The value of $\nu_1$ varies, depending on the type of strut or node being examined. For uncracked uniaxially stressed struts $\nu_1 = 1.0$. For struts cracked longitudinally due to bottle-shaped stress fields without transverse reinforcement $\nu_1 = 0.65$. Only strut members 6, 9, and 13 (see Fig. 6.5 for locations of members) were modeled as uncracked uniaxially stressed struts. These members are located at the interface between the column and the beam, which confines the struts and reduces the development of bottle-shaped stress fields. Strut members 7, 8, 10, 11, 12, 14, 15, and 16 were modeled as struts cracked longitudinally due to bottle-shaped stress fields. This is a conservative approach, especially for members 10, 11, and 12 because the hooks in the joint help to confine these members in the transverse direction. However, the hooks do not constrain these struts in the plane perpendicular to the hooks. The test of unit 6 showed that there was a large amount of concrete spalling in this plane.

For the node calculations, $\nu_1 = 1.0$ for nodes with only compression struts (node 3 in Fig. 6.5), 0.85 for nodes with two or more struts and one tie (nodes 1, 2, 4, 8, and 9 in Fig. 6.5), and 0.75 for nodes with two or more ties (nodes 5, 6, and 7 in Fig. 6.5). Based on these values for $\nu_1$ and the value of $\nu_2$ from equation (6.2), the effective compressive strength, ($f_{ce}$), of each node and compression strut was calculated, as shown in Table 6.1.

Once the strut widths have been calculated, a detailed drawing of the model can be drawn to determine the size of the nodes, and also areas of the joint where the struts fail due to overlapping. As can be seen in Figure 6.7, compression struts 10, 11, and 12 overlap each other when drawn to scale. The same overlapping can be seen between compression struts 15 and 16. In these overlapping areas we know the effective concrete strength is exceeded and the concrete will crush.

It can also be seen in Figure 6.7 that node 3 has the most critical loading on the diagonal face, where the three diagonal compression struts (10, 11, and 12) come together. In order to determine the stress on this node, the forces from compression struts 10 and 12 were resolved into components parallel and perpendicular to strut 11. The forces acting on the diagonal face of joint 3 were then calculated as the sum of the forces of the three diagonal members acting in the direction of strut 11. The net force acting on the diagonal face of node 3 was determined to be 296 kips, which results in a stress of 4490 psi. The effective compression strength of this node is 3522 psi, based on equations (6.1) and (6.2), which clearly indicates that the node fails by crushing of the concrete.

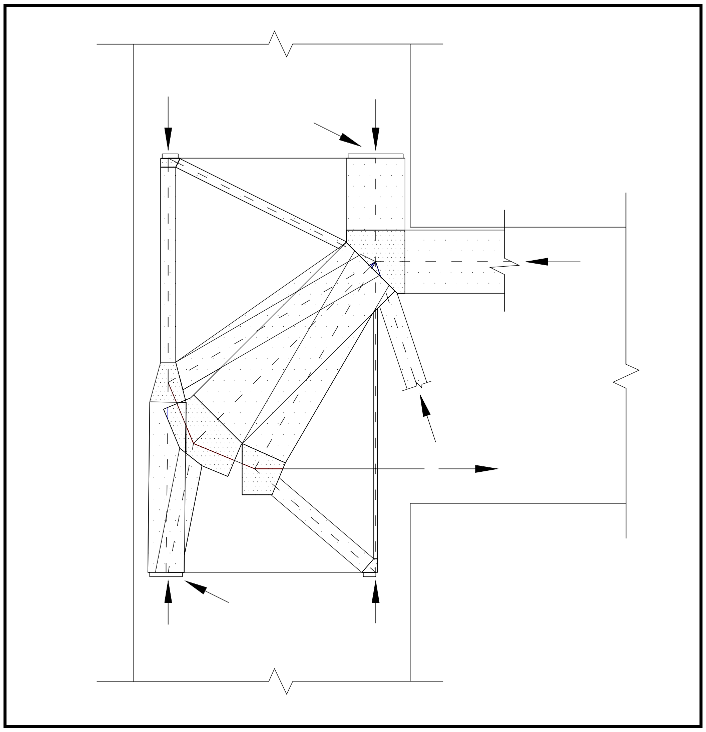

**Fig. 6.7 Strut-and-tie model failure mode showing strut widths**

Based on the initial analysis outlined in this paper the critical areas are nodes 3, 4, 5, and 6, and struts 10, 11, 12, 15, and 16. By using the experimental lateral load of 42 kips, it can be observed from Figure 6.7 that struts 10, 11, and 12 overlap and that nodes 4, 5, and 6 also overlap. It is therefore likely that crushing of the struts within the hooks caused failure.

The strut-and-tie model shown in Figure 6.7 is a good representation of the joint and simulates the results for test unit 6 in a satisfactory manner. The failure zones shown in Figure 6.7 correlate well with the failure zones of the actual joint. It was also observed that massive spalling of the concrete occurred within the hooks, and as much as 3 in. of concrete fell from the joint within the area of the hooks on each side of the beam.

# 7 Conclusions

The present investigation is concerned with the assessment of RC building exterior joints with substandard details. The six test units were full-scale models of typical exterior beam-column joints in RC buildings built in the United States and other countries prior to 1970. The joint details were substandard compared to current seismic codes in the following areas: (a) there was no transverse reinforcement in the joints, (b) the beam depth to column bar ratio was less than the recommended value, (c) the development length for the bottom beam bars was less than the required length for four of the test units, and (d) column bars were present only on two faces of the joint and were not distributed around the joint perimeter. However, all units satisfied the requirement for column to beam flexural ratio, and the top beam reinforcement into the joint satisfied bar anchorage requirements.

The research has shown that there are primarily two failure modes related to joints with the substandard details described above: (a) a bond-slip failure mode, and (b) a joint shear failure mode. Two of the units tested (units 1 and 2) exhibited a bond slip failure mode and the remaining four units (units 3 to 6) exhibited a joint shear failure mode.

One of the findings of this study is that the joint strength coefficient, $\gamma$, changes with the variation of the column compressive axial load. For unit 1 with a bond-slip failure mode and an axial column load of $0.1f'_cA_g$,the value of $\gamma$ was 5.2 (psi); for unit 2 with an axial column load of $0.25f'_cA_g$,the value of $\gamma$ was 7.0 (psi), an increase of 35 percent. For units 3 and 5 with a joint shear failure mode and an axial column load of $0.1f'_cA_g$, the value of $\gamma$ was 10.2 (psi) and 9.7 (psi) respectively; for units 4 and 6 with an axial column load of $0.25f'_cA_g$,the value of $\gamma$ was 11.7 (psi), and 11.0 (psi), respectively; this is an increase of 15 percent for the units with the higher axial column load. The FEMA 273 (BSSC 1997) joint shear strength coefficient is given as $\gamma$ = 6 (psi) for existing exterior joints without transverse beams, which is seen to be very conservative except for unit 1 with the lower column axial load and the bond-slip failure mode.

The ACI 352 (1991) joint shear strength coefficient for new Type II exterior joints is given as $\gamma$ = 12 (psi), which was not reached by any of the units tested in this research regardless of the level of column axial load.

The average value of the joint shear strain for units 1 and 2, exhibiting the bond-slip failure mode, at the peak lateral load was 0.0035; the maximum measured joint shear strain was 0.0227. The average value of the joint shear strain for units 3-6, exhibiting the joint shear failure mode, at the peak lateral load was 0.0033; the maximum measured joint shear strain was 0.0242.

The principal tensile stress in the joint for unit 1 with a bond-slip failure mode and axial column load of $0.1f'_cA_g$ was $10.3\sqrt{f'_c}$ (psi); for unit 2 with an axial column load of $0.25f'_cA_g$ the principal tensile stress was $22.4\sqrt{f'_c}$ (psi), an increase of 117 percent. For units 3 and 5 with a joint shear failure mode and an axial column load of $0.1f'_cA_g$,the average value of the principal tensile stress was $14.3\sqrt{f'_c}$ (psi); for units 4 and 6 with an axial column load of $0.25f'_cA_g$,the average value of the principal tensile stress was $24.2\sqrt{f'_c}$ (psi); this is an increase of 69 percent for the units with the higher axial column load.

The plastic shear angle at peak lateral load for the joint for all units tested was 0.01 (rad); for unit 1 with a bond-slip failure mode and axial column load of $0.1f'_cA_g$, the plastic shear angle after sudden reduction of the lateral load was 0.03 (rad); for unit 2 with an axial column load of $0.25f'_cA_g$ the corresponding plastic shear angle was 0.02 (rad). For units 3 to 6 with a joint shear failure mode, regardless of the level of the axial column load, the average value of the plastic shear angle after sudden reduction of the lateral load was 0.04 (rad).

The displacement ductility ratios of unit 1 ($0.1f'_cA_g$) and unit 2 ($0.25f'_cA_g$) with the bond-lip failure mode were 3.9 and 2.9, respectively; for units 3 and 5 with the joint shear failure mode and axial column load of $0.1f'_cA_g$, the displacement ductility ratio was 1.9, and for units 4 and 6 with axial column load of $0.25f'_cA_g$, the displacement ductility ratio was 1.8. In addition, units 3 to 6 with the joint shear failure mode had a cumulative displacement ductility of 31% to 39% smaller than units 1 and 2 with the bond-slip failure mode.

The units with $0.10f'_cA_g$ column axial load that failed by joint shear had a 24% higher hysteretic energy dissipation compared to unit 1 that failed by a bond-slip mechanism. The units with $0.25f'_cA_g$ column axial load that failed by joint shear had the same hysteretic energy dissipation compared to unit 2 that failed by a bond-slip mechanism.

For each of the two failure modes of bond slip and joint shear five performance levels were identified. For units 1 and 2 with the bond-slip failure mode the following performance levels were identified: (I) first yield of the reinforcement, (II) formation of the bond-slip mechanism, (III) cracking in the joint, (IV) spalling of concrete at the corner of the joint where bond slip occurs, and (V) loss of lateral load capacity. For units 3 to 6 with the joint shear failure mode the following performance levels were identified: (I) first yield of the reinforcement, (II) cracking in the joint, (III) formation of the joint shear mechanism, (IV) spalling of concrete at the joint core, and (V) loss of gravity load capacity. The above performance levels were used to identify corresponding limit states, which were delineated in terms of joint strength coefficient versus plastic rotation and crack width versus plastic rotation for both the bond-slip failure mode and the joint shear failure mode.

It can be observed that the presence of the higher axial load was beneficial in terms of the joint strength coefficient and principal tensile stress, but was detrimental for displacement ductility and energy dissipation. The four units (units 3 to 6) with the joint shear failure mode failed at the end of the test due to loss of the column axial compression load capacity. The remaining two units (units 1 and 2) with the bond-slip failure mode failed at the end of the test due to the loss of lateral load capacity. The units that had a bond-slip failure mode had a lower joint strength coefficient, ultimate plastic shear angle, principal tensile stress, and energy dissipation than the units with the joint shear failure mode.

A strut-and-tie model was developed for units 5 and 6 of the experimental program. The analytical model is unique in that it incorporates bent bars in the beam-column joint. The tensile tie elements that were used to represent the bent bars in the beam-column joint were idealized by linear chord segments. Correlation with experimental values of the lateral load and column compression axial load was excellent.

This research has resulted in a recommendation for new modeling criteria for exterior concrete joints with substandard details based on either a bond-slip failure model or a joint shear failure model. In the opinion of the authors, the proposed modeling criteria for exterior joints that are prone to either bond-slip or shear failure modes capture the characteristics of the units tested in this research in a more satisfactory manner than do the current FEMA 273 (1997) modeling criteria.

# REFERENCES


ACI Standard 318-63. 1963. *Building code requirements for reinforced concrete (ACI 318-63).* American Concrete Institute, Detroit, MI.

ACI Committee 352. 1991. *Recommendations for design of beam-column joints in monolithic reinforced concrete structures (ACI 352R-91).* American Concrete Institute, Farmington Hills, MI.

ACI Committee 318. 1999. *Building code requirements for structural concrete (ACI 318-99) and commentary (ACI 318R-99).* American Concrete Institute, Farmington Hills, MI.

Ali, M.A., and White, R.N. 2001. *Automatic Generation of Truss Model for Optimal Design of Reinforced Concrete Structures, ACI Structural Journal,*98(4), 431-442.

American Society of Civil Engineers. 2000. FEMA 356: *Prestandard and Commentary for the Seismic Rehabilitation of Buildings*. Federal Emergency Management Agency, Washington, DC.

Beres, A., White, A.N., and Gergely, P. 1992. *Seismic behavior of RC frame structures with nonductile details: Part I-Summary of experimental findings of full scale beam-column joint tests,* Report NCEER-92-0024, NCEER, SUNY Buffalo, NY.

Building Seismic Safety Council. 1997. FEMA 273: *NEHRP Guidelines for the Seismic Rehabilitation of Buildings*. Federal Emergency Management Agency, Washington, DC.

Concrete International. 2001. *Chapter 22, ACI 318 Code Building code requirements for structural concrete (ACI 318-99) and commentary (ACI 318R-99).* American Concrete Institute, Farmington Hills, MI, 125-132.

Clyde, C., Pantelides, C.P., and Reaveley, L.D. 2000. *Performance-based evaluation of exterior reinforced concrete building joints for seismic excitation*. Pacific Earthquake Engineering Research Center, PEER Report 2000/05, University of California, Berkeley, CA.

Durrani, A.J., and Zerbe, H.E.. 1987. *Seismic resistance of R/C exterior connections with floor slab*. Journal of Structural Engineering, 113 (8), 1850-64.

Earthquake Engineering Research Institute. 1999a. EERI Special Earthquake Report – September 1999. The Tehuacan, Mexico, Earthquake of June 15, 1999. http://www.eeri.org/earthquakes/earthquakes.html

Earthquake Engineering Research Institute. 1999b. EERI Special Earthquake Report – November 1999. The Athens, Greece Earthquake of September 7, 1999.
http://www.eeri.org/earthquakes/earthquakes.html

Earthquake Engineering Research Institute. 1999b. EERI Special Earthquake Report – December 1999. The Chi-Chi, Taiwan Earthquake of September 21, 1999.
http://www.eeri.org/earthquakes/earthquakes.html

Ehsani, M.R., and Wight, J.K. 1985. *Exterior reinforced concrete beam-to-column connections subjected to earthquake-type loading*. ACI Journal, 82(4), 492-499.

Hakuto, S., Park, R., and Tanaka, H. 2000. *Seismic load tests on interior and exterior beam-column joints with substandard reinforcing details.* ACI Journal, 97(1), 11-25.

Hose, Y.D., Eberhard, M., and Seible, F. 1999. *Performance Library of Concrete Bridge Components, Sub-assemblages and Systems under simulated Seismic Loads*. SSRP 99/08 Structural Systems Research Program, UCSD, San Diego, CA.

Hwang, S-J., and Lee, H-J. 1999. *Analytical Model for Predicting Shear Strengths of Exterior Reinforced Concrete Beam-Column Joints for Seismic Resistance. ACI Structural Journal,* 96(5), 846-857.

Kaku, T., and Asakusa, H. 1991. *Bond and anchorage of bars in reinforced concrete beam-column joints.* ACI SP-123, Design of Beam-Column Joints for Seismic Resistance, J.O. Jirsa, ed., American Concrete Institute, Detroit, MI., 401-423.

Kurose, Y. 1987. *Recent studies on reinforced concrete beam column joints in Japan*. PMFSEL Report No. 87-8 Department of Civil Engineering, University of Texas at Austin, Austin, TX.

Lowes, L.N., and Moehle, J.P. 1999. *Evaluation and Retrofit of Beam-Column T-Joints in Older Reinforced Concrete Bridge Structures*. *ACI Structural Journal,* 96(4), 519-532.

MacGregor, J.G. 1997 *Reinforced Concrete - Mechanics and Design,* Third Edition, Prentice Hall, Inc., Upper Saddle River, NJ.

Megget, L.M. 1974. *Cyclic behaviour of exterior reinforced concrete beam-column joints*. Bulletin of the New Zealand National Society for Earthquake Engineering, 7(1).

Meinheit, D.F. and Jirsa, J.O., The shear strength of reinforced concrete beam-column joints, CESRL Report No. 77-1, University of Texas, Austin, TX, Jan. 1977.

Moehle, J.P. and Mahin, S.A. 1991. Observations on the behavior of reinforced concrete buildings during earthquakes. *Earthquake-Resistant Concrete Structures Inelastic Response and Design SP-127*, American Concrete Institute, ed. S.K. Ghosh, Detroit.

Pantazapoulou, S.J., and J.F. Bonacci. 1992. Consideration of questions about beam-column joints. ACI Structural Journal, 89 (1), 27-36.

Pantazapoulou, S.J., and J.F. Bonacci. 1994. *On earthquake-resistant reinforced concrete frame connections*. Canadian Journal of Civil Engineering, 21, 307-28.

Park, R.; et al. 1995. The Hyogo-ken Nanbu earthquake (the great Hanshin earthquake) of 17 January 1995: report of the NZNSEE Reconnaissance Team, Bulletin of the New Zealand National Society for Earthquake Engineering, 28, 1, Mar. 1995, pg. 1-98.

Park, R. (1997). *A static force-based procedure for the seismic assessment of existing reinforced concrete moment resisting frames*. Bulletin of the New Zealand National Society for Earthquake Engineering, 30(3), 213-26.

Paulay, T., and Scarpas, A. 1981. *The behaviour of exterior beam-column joints*. Bulletin of the New Zealand National Society for Earthquake Engineering, 14(3), 131-44.

Priestley, M.J.N., Seible, F., and Calvi, G.M. 1996. *Seismic Design and Retrofit of Bridges*. John Wiley & sons, Inc., New York, NY.

Sezen, H., Elwood, K.J., Whittaker, A.S., Mosalam, K. M., Wallace, J.W., and Stanton, J.F. 2000. Structural engineering reconnaissance of the August 17, 1999 earthquake: Kocaeli (Izmit), Turkey, PEER-2000/09, Berkeley: Pacific Earthquake Engineering Research Center, University of California, Dec.

Tsonos, A.G., Tegos, I.A., and Penelis, G.G. 1995. Influence of Axial Force Variations on the Seismic Behavior of Exterior Beam-Column Joints. European Earthquake Engineering, 3, 51-63.

Uang, C-M., Elgamal, A., Li, W-S., and Chou, C-C. 1999. Ji-Ji Taiwan Earthquake of September 21, 1999: A Brief Reconnaissance Report, Department of Structural Engineering, University of California, San Diego, http://www.structures.ucsd.edu/Taiwaneq

Uzumeri, S. M. 1977. *Strength and Ductility of Cast-In-Place Beam-Column Joints*. ACI Publication SP 53-12: Reinforced Concrete Structures in Seismic Zones, 293-350.

# PEER REPORTS

PEER reports are available from the National Information Service for Earthquake Engineering (NISEE). To order PEER reports, please contact the Pacific Earthquake Engineering Research Center, 1301 South 46th Street, Richmond, California 94804-4698. Tel.: (510) 231-9468; Fax: (510) 231-9461.

**PEER 2002/18** *Assessment of Reinforced Concrete Building Exterior Joints with Substandard Details.* Chris P. Pantelides, Jon Hansen, Justin Nadauld, and Lawrence D. Reaveley. May 2002.

**PEER 2002/17** *Structural Characterization and Seismic Response Analysis of a Highway Overcrossing Equipped with Elastomeric Bearings and Fluid Dampers: A Case Study.* Nicos Makris and Jian Zhang. November 2002.

**PEER 2002/16** *Estimation of Uncertainty in Geotechnical Properties for Performance-Based Earthquake Engineering.* Allen L. Jones, Steven L. Kramer, and Pedro Arduino. December 2002.

**PEER 2002/15** *Seismic Behavior of Bridge Columns Subjected to Various Loading Patterns.* Asadollah Esmaeily-Gh. and Yan Xiao. December 2002.

**PEER 2002/14** *Inelastic Seismic Response of Extended Pile Shaft Supported Bridge Structures.* T.C. Hutchinson, R.W. Boulanger, Y.H. Chai, and I.M. Idriss. December 2002.

**PEER 2002/13** *Probabilistic Models and Fragility Estimates for Bridge Components and Systems.* Paolo Gardoni, Armen Der Kiureghian, and Khalid M. Mosalam. June 2002.

**PEER 2002/12** *Effects of Fault Dip and Slip Rake on Near-Source Ground Motions: Why Chi-Chi Was a Relatively Mild M7.6 Earthquake.* Brad T. Aagaard, John F. Hall, and Thomas H. Heaton. December 2002.

**PEER 2002/11** *Analytical and Experimental Study of Fiber-Reinforced Strip Isolators*. James M. Kelly and Shakhzod M. Takhirov. September 2002.

**PEER 2002/10** *Centrifuge Modeling of Settlement and Lateral Spreading with Comparisons to Numerical Analyses***.** Sivapalan Gajan and Bruce L. Kutter. January 2003.

**PEER 2002/09** *Documentation and Analysis of Field Case Histories of Seismic Compression during the 1994 Northridge, California, Earthquake.* Jonathan P. Stewart, Patrick M. Smith, Daniel H. Whang, and Jonathan D. Bray. October 2002.

**PEER 2002/08** *Component Testing, Stability Analysis and Characterization of Buckling-Restrained Unbonded Braces™.* Cameron Black, Nicos Makris, and Ian Aiken. September 2002.

**PEER 2002/07** *Seismic Performance of Pile-Wharf Connections.* Charles W. Roeder, Robert Graff, Jennifer Soderstrom, and Jun Han Yoo. December 2001.

**PEER 2002/06** *The Use of Benefit-Cost Analysis for Evaluation of Performance-Based Earthquake Engineering Decisions*. Richard O. Zerbe and Anthony Falit-Baiamonte. September 2001.

PEER 2002/05 *Guidelines, Specifications, and Seismic Performance Characterization of Nonstructural Building Components and Equipment*. André Filiatrault, Constantin Christopoulos, and Christopher Stearns. September 2001.

PEER 2002/03 *Investigation of Sensitivity of Building Loss Estimates to Major Uncertain Variables for the Van Nuys Testbed.* Keith A. Porter, James L. Beck, and Rustem V. Shaikhutdinov. August 2002.

PEER 2002/02 *The Third U.S.-Japan Workshop on Performance-Based Earthquake Engineering Methodology for Reinforced Concrete Building Structures*. July 2002.

PEER 2002/01 *Nonstructural Loss Estimation: The UC Berkeley Case Study. Mary C. Comerio and John C. Stallmeyer.* December 2001.

PEER 2001/16 *Statistics of SDF-System Estimate of Roof Displacement for Pushover Analysis of Buildings.* Anil K. Chopra, Rakesh K. Goel, and Chatpan Chintanapakdee. December 2001.

PEER 2001/15 *Damage to Bridges during the 2001 Nisqually Earthquake.* R. Tyler Ranf, Marc O. Eberhard, and Michael P. Berry. November 2001.

PEER 2001/14 *Rocking Response of Equipment Anchored to a Base Foundation.* Nicos Makris and Cameron J. Black. September 2001.

PEER 2001/13 *Modeling Soil Liquefaction Hazards for Performance-Based Earthquake Engineering.* Steven L. Kramer and Ahmed-W. Elgamal. February 2001.

PEER 2001/12 *Development of Geotechnical Capabilities in OpenSees.* Boris Jeremic. September 2001.

PEER 2001/11 *Analytical and Experimental Study of Fiber-Reinforced Elastomeric Isolators*. James M. Kelly and Shakhzod M. Takhirov. September 2001.

PEER 2001/10 *Amplification Factors for Spectral Acceleration in Active Regions.* Jonathan P. Stewart, Andrew H. Liu, Yoojoong Choi, and Mehmet B. Baturay. December 2001.

PEER 2001/09 *Ground Motion Evaluation Procedures for Performance-Based Design.* Jonathan P. Stewart, Shyh-Jeng Chiou, Jonathan D. Bray, Robert W. Graves, Paul G. Somerville, and Norman A. Abrahamson. September 2001.

PEER 2001/08 *Experimental and Computational Evaluation of Reinforced Concrete Bridge Beam-Column Connections for Seismic Performance*. Clay J. Naito, Jack P. Moehle, and Khalid M. Mosalam. November 2001.

PEER 2001/07 *The Rocking Spectrum and the Shortcomings of Design Guidelines.* Nicos Makris and Dimitrios Konstantinidis. August 2001.

PEER 2001/06 *Development of an Electrical Substation Equipment Performance Database for Evaluation of Equipment Fragilities*. Thalia Agnanos. April 1999.

PEER 2001/05 *Stiffness Analysis of Fiber-Reinforced Elastomeric Isolators.* Hsiang-Chuan Tsai and James M. Kelly. May 2001.

PEER 2001/04 *Organizational and Societal Considerations for Performance-Based Earthquake Engineering.* Peter J. May. April 2001.

**PEER 2001/03** *A Modal Pushover Analysis Procedure to Estimate Seismic Demands for Buildings: Theory and Preliminary Evaluation.* Anil K. Chopra and Rakesh K. Goel. January 2001.

**PEER 2001/02** *Seismic Response Analysis of Highway Overcrossings Including Soil-Structure Interaction.* Jian Zhang and Nicos Makris. March 2001.

**PEER 2001/01** *Experimental Study of Large Seismic Steel Beam-to-Column Connections.* Egor P. Popov and Shakhzod M. Takhirov. November 2000.

**PEER 2000/10** *The Second U.S.-Japan Workshop on Performance-Based Earthquake Engineering Methodology for Reinforced Concrete Building Structures.* March 2000.

**PEER 2000/09** *Structural Engineering Reconnaissance of the August 17, 1999 Earthquake: Kocaeli (Izmit), Turkey.* Halil Sezen, Kenneth J. Elwood, Andrew S. Whittaker, Khalid Mosalam, John J. Wallace, and John F. Stanton. December 2000.

**PEER 2000/08** *Behavior of Reinforced Concrete Bridge Columns Having Varying Aspect Ratios and Varying Lengths of Confinement.* Anthony J. Calderone, Dawn E. Lehman, and Jack P. Moehle. January 2001.

**PEER 2000/07** *Cover-Plate and Flange-Plate Reinforced Steel Moment-Resisting Connections.* Taejin Kim, Andrew S. Whittaker, Amir S. Gilani, Vitelmo V. Bertero, and Shakhzod M. Takhirov. September 2000.

**PEER 2000/06** *Seismic Evaluation and Analysis of 230-kV Disconnect Switches.* Amir S. J. Gilani, Andrew S. Whittaker, Gregory L. Fenves, Chun-Hao Chen, Henry Ho, and Eric Fujisaki. July 2000.

**PEER 2000/05** *Performance-Based Evaluation of Exterior Reinforced Concrete Building Joints for Seismic Excitation.* Chandra Clyde, Chris P. Pantelides, and Lawrence D. Reaveley. July 2000.

**PEER 2000/04** *An Evaluation of Seismic Energy Demand: An Attenuation Approach.* Chung-Che Chou and Chia-Ming Uang. July 1999.

**PEER 2000/03** *Framing Earthquake Retrofitting Decisions: The Case of Hillside Homes in Los Angeles.* Detlof von Winterfeldt, Nels Roselund, and Alicia Kitsuse. March 2000.

**PEER 2000/02** *U.S.-Japan Workshop on the Effects of Near-Field Earthquake Shaking.* Andrew Whittaker, ed. July 2000.

**PEER 2000/01** *Further Studies on Seismic Interaction in Interconnected Electrical Substation Equipment.* Armen Der Kiureghian, Kee-Jeung Hong, and Jerome L. Sackman. November 1999.

**PEER 1999/14** *Seismic Evaluation and Retrofit of 230-kV Porcelain Transformer Bushings*. Amir S. Gilani, Andrew S. Whittaker, Gregory L. Fenves, and Eric Fujisaki. December 1999.

**PEER 1999/13** *Building Vulnerability Studies: Modeling and Evaluation of Tilt-up and Steel Reinforced Concrete Buildings.* John W. Wallace, Jonathan P. Stewart, and Andrew S. Whittaker, editors. December 1999.

**PEER 1999/12** *Rehabilitation of Nonductile RC Frame Building Using Encasement Plates and Energy-Dissipating Devices.* Mehrdad Sasani, Vitelmo V. Bertero, James C. Anderson. December 1999.

**PEER 1999/11** *Performance Evaluation Database for Concrete Bridge Components and Systems under Simulated Seismic Loads.* Yael D. Hose and Frieder Seible. November 1999.

**PEER 1999/10** *U.S.-Japan Workshop on Performance-Based Earthquake Engineering Methodology for Reinforced Concrete Building Structures.* December 1999.

**PEER 1999/09** *Performance Improvement of Long Period Building Structures Subjected to Severe Pulse-Type Ground Motions*. James C. Anderson, Vitelmo V. Bertero, and Raul Bertero. October 1999.

**PEER 1999/08** *Envelopes for Seismic Response Vectors.* Charles Menun and Armen Der Kiureghian. July 1999.

**PEER 1999/07** *Documentation of Strengths and Weaknesses of Current Computer Analysis Methods for Seismic Performance of Reinforced Concrete Members.* William F. Cofer. November 1999.

**PEER 1999/06** *Rocking Response and Overturning of Anchored Equipment under Seismic Excitations.* Nicos Makris and Jian Zhang. November 1999.

**PEER 1999/05** *Seismic Evaluation of 550 kV Porcelain Transformer Bushings.* Amir S. Gilani, Andrew S. Whittaker, Gregory L. Fenves, and Eric Fujisaki. October 1999.

**PEER 1999/04** *Adoption and Enforcement of Earthquake Risk-Reduction Measures.* Peter J. May, Raymond J. Burby, T. Jens Feeley, and Robert Wood.

**PEER 1999/03** *Task 3 Characterization of Site Response General Site Categories*. Adrian Rodriguez-Marek, Jonathan D. Bray, and Norman Abrahamson. February 1999.

**PEER 1999/02** *Capacity-Demand-Diagram Methods for Estimating Seismic Deformation of Inelastic Structures: SDF Systems*. Anil K. Chopra and Rakesh Goel. April 1999.

**PEER 1999/01** *Interaction in Interconnected Electrical Substation Equipment Subjected to Earthquake Ground Motions.* Armen Der Kiureghian, Jerome L. Sackman, and Kee-Jeung Hong. February 1999.

**PEER 1998/08** *Behavior and Failure Analysis of a Multiple-Frame Highway Bridge in the 1994 Northridge Earthquake.* Gregory L. Fenves and Michael Ellery. December 1998.

**PEER 1998/07** *Empirical Evaluation of Inertial Soil-Structure Interaction Effects.* Jonathan P. Stewart, Raymond B. Seed, and Gregory L. Fenves. November 1998.

**PEER 1998/06** *Effect of Damping Mechanisms on the Response of Seismic Isolated Structures.* Nicos Makris and Shih-Po Chang. November 1998.

**PEER 1998/05** *Rocking Response and Overturning of Equipment under Horizontal Pulse-Type Motions.* Nicos Makris and Yiannis Roussos. October 1998.

**PEER 1998/04** *Pacific Earthquake Engineering Research Invitational Workshop Proceedings, May 14–15, 1998: Defining the Links between Planning, Policy Analysis, Economics and Earthquake Engineering.* Mary Comerio and Peter Gordon. September 1998.

**PEER 1998/03** *Repair/Upgrade Procedures for Welded Beam to Column Connections.* James C. Anderson and Xiaojing Duan. May 1998.

**PEER 1998/02** *Seismic Evaluation of 196 kV Porcelain Transformer Bushings.* Amir S. Gilani, Juan W. Chavez, Gregory L. Fenves, and Andrew S. Whittaker. May 1998.

**PEER 1998/01** *Seismic Performance of Well-Confined Concrete Bridge Columns.* Dawn E. Lehman and Jack P. Moehle. December 2000.